Detection of *Mycobacterium avium* subsp. *paratuberculosis* (MAP) in Sheep Milk Samples by a Novel Biotechnological Approach

A Dissertation Presented by

Dr. Sepideh Hosseiniporgham

Supervised by

Prof. Leonardo Antonio Sechi (Coordinator)

Submitted to the Graduate School of the University of Sassari in partial fulfillment of the requirements for the degree of

Doctor of Philosophy in Life Sciences and Biotechnologies

Cycle XXXIII (Spring 2018- Summer 2021)

Department of Biomedical Sciences

Foreword

This work has been conducted under the supervision of Professor Leonardo Antonio Sechi, the coordinator of the PhD programs in the filed of Life Sciences and Biotechnologies and full professor of the University of Sassari, in Italy. A Programma Operativo Nazionale (PON) of MIUR has funded the PhD project (Cycle XXXIII), since 1st March 2018 to 31st July 2021.

Preface

This thesis is the achievement of my three years studies at doctoral degree of the University of Sassari. It focuses on three main areas including 1) the detection *of Mycobacterium avium* subsp. *paratuberculosis* (MAP) in milk and blood samples via commercial molecular (qPCR) and immunological techniques (ELISA), carried out at the University of Sassari; 2) development of an in-house ELISA assay for detection of antibodies directed against MAP in milk and serum samples, performed at the University of Sassari in a collaboration with Professor Franck Biet and his colleagues in INRAE and Institute of Pasteur in France; 3) optimization of a conventional and novel phage based approaches of, respectively, peptide-mediated magnetic separation phage assay (PMS-phage) and phage-bead qPCR (PBQ) evaluating the viability of MAP in milk and blood samples, performed at the Institute of Zooprofilattico in Sassari, Italy. Accordingly, the following dissertation is arranged based on two papers that were published in the peer-reviewed Journal, *Microorganism* and *Vaccines*, and one manuscript that have already been submitted in other peer-reviewed journal of *Scientific Report* in *Nature* and will be published soon.

Author’s Declaration

The research project entitled “Detection of *Mycobacterium avium* subsp. *paratuberculosis* (MAP) in sheep milk samples by a novel biotechnological approach” has been carried out by Dr. Sepideh Hosseiniporgham under the supervision of Professor Leonardo Antonio Sechi, the coordinator of the PhD program in Life Sciences and Biotechnologies at Biomedical Science Department of the University of Sassari. Due to the fact of COVID-19 pandemic, the part of the project that should have been done abroad was carried out in the Institute of Zooprofilattico located in Sassari, Italy.

Hereby, the undersigned “Dr. Sepideh Hosseiniporgham”, declares that this dissertation is an original report on her doctoral researches at the University of Sassari, it has been written by her and has not been submitted or presented, in whole or in part, for the award of any other academic degree or diploma elsewhere.

Signature of the PhD candidate — Stamp of the Institution

Dr. Sepideh Hosseinporgham — Date:

University of Sassari — Reg. No.:

I certify that I have read this dissertation and that, in my opinion, it is fully adequate in scope and quality as a dissertation for the degree of Doctor of Philosophy.

Signature of the Supervisor — Stamp of the Institution

Prof. Leonardo Antonio Sechi — Date:

University of Sassari — Reg. No.:

Dr. Sepideh Hosseiniporgham: The Detection of *Mycobacterium avium* subsp. *paratuberculosis* by a novel Biotechnological approach- PhD thesis in Life Science and Biotechnologies- University of Sassari, Italy

This dissertation is dedicated to:

My beloved mother "Mrs. Najibeh Kazemzadeh Moghaddam" and dear father "Mr. Ahmad Hosseiniporgham" who dedicated their whole life to me and my siblings nurturing us how to be patient against difficulties and tackle the obstacles; my kind sister "Sama Hosseiniporgham", my best friend, who has always been there for me; my dear brother "Shahab Hosseiniporgham" and sister-in-law "Behnaz Khalaj" who did not let my parents feel my absence at home during the period of my PhD. I love you all and I am proud of you till my last breath.

Acknowledgments

I would like to express my sincere gratitude and appreciation to Prof. Leonardo Antonio Sechi, who trusted me and granted me the opportunity of worldwide collaboration under his supervision and endless support in his laboratory. It has been an honor to work with such a knowledgeable scientist. The collaboration with Prof. Sechi was a delightful experience, filled with so many opportunities and challenges that made me a more critical thinker, independent, problem solver, and a stronger person. I hope we can carry on our collaboration on new scientific areas in the near future.

I would like to extend my appreciation for all the supports that I received from the Institute of Zooprofilattico and my colleagues and friends including Dr. Angela Ruiu, Dr. Stefano Lollai, Dr. Ilaria Dupre, Lucio Rebechesu, and Pierangela Pintore.

I was honored to have a wonderful collaboration with Prof. Franck Biet and his colleagues in INRAE and Institute of Pasteur in France. I do appreciate all support and assistance that I received from Prof. Biet and looking forward to continue our collaboration in the near future.

My best gratitute to LAIT Company, Prof. Stefano Rocca and Tizina Cubeddu at Veterinary Department of the University of Sassari that provided me with sheep milk samples.

I would like to thank Prof. Salvatore Rubino and Prof. Pier Luigi Fiori who are the “Director of Microbiology and Virology Specialization School” and “Director of Department of Biomedical Sciences” at the University of Sassari respectively.

At the end I would like to express my deepest appreciation towards my dear academic family in the University of Sassari, colleagues, and friends including Dr. Antonella Santona, Dr. Domenico Delogu, Senior Edmondo Manca, Dr. Giuseppe Delogu, Dr. Giovanni Sini, Pieranna Nurra, and many other friends who have made my course of study and life in Italy a wonderful and memorable time.

Abstract

Paratuberculosis or Johne's disease (JD) is an incurable gastrointestinal condition in ruminants that is promoted by *Mycobacterium avium* subsp. *paratuberculosis* (MAP), a fastidious acid-fast bacterium. The pathogen could withstand heat and pasteurization, remain intact in the dairy products, and be transferred to consumers. This highlight that MAP could be a zoonotic pathogen having the ability to involve humans in some autoimmune conditions such as Crohn's disease. However, the pathogenicity of MAP could be controlled through implementing competent pasteurization policies along with application of speedy and well-organized detective methods.

In this thesis, we evaluated the functionality of a few in-house developed/ optimized and commercial diagnostic techniques to detect MAP and antibodies directed against it in unpasteurized milk samples.

To estimate whether or not the studied animals disperse MAP (dead or viable cells) in milk samples or the environment, qPCR IS*900* along with ELISA analysis were carried out on two sources of milk samples (bulk tank milk (BTM) and individual milk) and the specificity and sensitivity of both methods were evaluated under different binary gold standard reference models (0,1). Accordingly, a higher proportion of MAP DNA and antibodies against it were detected in BTMs rather than individual milk samples. This is probably due to the fact that BTMs are a mix of several individual milk samples that might be randomly taken from positive or negative animals. In addition, we discovered that milk could be an alternative sample to serum for antibody screening when we have no access to the animal's blood, in which a considerable correlation between antibody titer in milk and serum was found at individual level. Also, bulk tank milk analyses (qPCR and ELISA) demonstrated that MAP

positivity follows a seasonal pattern, in which more cases were milk qPCR-positive and milk ELISA-positive in spring and summer respectively.

At the next step, in order to improve the capture antigen efficiency in an in-house milk ELISA test (H-MELISA), we innovatively used MAP-derived surface-exposed lipopeptids of L3P (specific in sheep) to target the antibodies directed against MAP in sheep milk samples comparing with H-MELISA via other MAP lipopeptide of L5P (specific in cow). The result of this analysis depicted that H-MELISA L3P/L5P could enhance the discovery of positive milk samples from specimens that were potentially negative by commercial ELISA test. Interestingly, the overall positivity rates of H-MELISA via L3P and L5P varied by the source of milk samples, in which at bulk tank milk (BTM) level, the majority of positive cases reacted more against L5P, whereas a predominant number of milk samples were more responsive against L3P at individual level. To clarify whether or not the positivity status of milk samples in H-MELISA L3P/L5P could predict the type of MAP strains (S/C) at BTMs and individual milk samples, strain typing was carried out on DNAs extracted from some of the H-MELISA L3P/L5P positive or negative sheep milk samples using PCR IS*1311*-restriction enzyme analysis. The strain typing confirmed the presence of all three MAP strains (S/C/Bison) among Sardinian milk samples. However, as it was expected from the overall rate of H-MELISA L3P/L5P positivity, C-type and S-type MAP strains happened with higher incidence among BTMs and individual milk respectively. Further examination on the H-MELISA L3P/L5P positivity pattern of each C/S type MAP sample revealed that some samples had a reverse reactivity against both L3P and L5P. These results could be the consequence of either cross-reactivity between L3P and L5P due to the similarity in the structures of the two epitopes or simply a within-herd mixed infection with MAP strains of C and S types.

Eventually, the viability of MAP in unpasteurized goat and sheep milk samples were verified by a conventional (PMS-phage) and novel phage-bead qPCR (PBQ) assays that worked, respectively, with and without the intervention of MAP-specific complementary peptides (aMptD and aMp3). Although, both methods comparably functioned on unpasteurized milk samples that contained no viable MAP, PBQ was privileged PMS-phage assay due to lower LOD (PBQ LOD was 10 MAP cells in 10 mL compared to 100 MAP cells/ 10 mL in PMS-phage assay), rapidity, higher sensitivity, and lack of need for "intervention of other mycobacterial species such as *M. smegmatis* that was commonly used in PMS-phage assay in lawn making step" and "consequent FAS treatment".

List of Abbrevations

MAP	*Mycobacterium avium* subsp. *paratuberculosis*
JD	Johne's Disease
BTM	Bulk Tank Milk
qPCR	Quantitative Polymerase Chain Reaction
MqPCR	Milk quantitative Polymerase Reaction
MELISA	Milk Enzyme-Linked Immunosorbent assay
SELISA	Serum Enzyme-Linked Immunosorbent assay
FPCR	Fecal Polymerase Chain Reaction
S/P%	Sample to Positivity Ratio
OD	Optical Density
H-MELISA	Homemade Milk Enzyme-Linked Immunosorbent assay
CMELISA	Commercial Milk Enzyme-Linked Immunosorbent assay
L3P	Lipotripeptide
L5P	Lipopentapeptide
REA	Restriction Enzyme Analysis
IS*900*	Insertion Sequence *900*
IS*1311*	Insertion Sequence *1311*
PBQ	Peptide-Bead qPCR
PMS	Peptide-Mediated Magnetic Separation
OADC	Oleic Albumin Dextrose Catalase
MB	Middlebrook
SP	Specificity
SN	Sensitivity

Table of Contents

Foreword 2

Preface 3

Author's Declaration 4

This dissertation is dedicated to: 5

Acknowledgments 6

Abstract 7

List of Abbrevations 10

List of Figures 14

List of Tables 16

Chapter I: Introduction 18
- 1.1 History of Johne's Disease 18
- 1.2.1 Taxonomic and Phylogenic Analysis of Mycobacteria 20
- 1.3 *Mycobacterium avium* subsp. *paratuberculosis* (MAP) 21
  - 1.3.1 Strain Types of MAP 22
  - 1.3.2 Mechanisms of MAP Infection in JD 24
- 1.4 MAP Epidemiology 34
  - 1.4.1 Paratuberculosis Host Ranges 34
  - 1.4.2 Geographical Distribution of Paratuberculosis 35
- 1.5 Symptom Manifestation of JD 37
  - 1.5.1 Clinical Symptoms of JD 38
  - 1.5.2 Pathological and Anatomical modifications 38
  - 1.5.3 Risk Factors in JD 40
- 1.6 MAP Infection and Dissemination 40
  - 1.6.1 Prenatal MAP Infection 40
  - 1.6.2 Postnatal Infection 41
  - 1.6.3 Adult Animal Infection 42
- 1.7 Zoonotic Nature of MAP and Its Association with Crohn's Disease in Human 42
  - 1.7.1 Transmission of MAP to Human via Milk and Dairy Products 43
  - 1.7.2 Transmission of MAP via Water Sources and Insects 44
- 1.8 Control of JD by Implementing Preventive Strategies 44
  - 1.8.1 Test and Cull methodology 45
  - 1.8.2 Vaccination 46
- 1.9 The Common MAP Diagnostic Assays 49
  - 1.9.1 Detection of the Immune Response 49
  - 1.9.2 Detection of MAP 53

Chapter II: Aim of the study 61

Chapter III: Materials and methods 62
- 3.1. Bacterial Strains 62
- 3.2. Phage Strains 62
- 3.3. Sample Collection 63
- 3.4. Milk Culture 63
- 3.5. DNA extraction from colonies, milk, and lysed plaques 64

3.6. qPCR IS*900* analysis on DNAs extracted from milk, colonies, and lysed plaques.......66
3.7. Restriction Enzyme Analysis (REA) on IS*1311*-targeted PCR Products and Strain Typing (S- or C-class)..........67
3.8. Separation of serum from blood samples and preparation of milk samples for ELISA analysis..........68
3.9. Commercial Milk and Serum ELISA 68
3.10. In-house milk ELISA (H-MELISA) on BTMs and individual milk samples (MIF) using L3P and L5P epitopes 68
3.11. Preparation of peptides-mediated magnetic beads using two MAP-complementary peptides of aMp3 and aMptD 69
3.12. Optimization of peptide-mediated magnetic separation (PMS) Phage Assay on artificially MAP-contaminated milk samples and validation of the method on natural unpasteurized milk samples 70
3.13. Preparation of phage D29-beads..........71
3.14. Optimization of phage beads on artificially MAP-contaminated milk samples and evaluating their functionality on unpasteurized milk samples..........72

Chapter IV: Results 73

4.1. Detection of *Mycobacterium avium* subsp. *paratuberculosis* (MAP) in Sheep Milk73

4.1.1. Statistical Analysis..........73
4.1.2. BTM qPCR 73
4.1.3. BTM ELISA..........75
4.1.4. MIF MqPCR and MELISA..........79
4.1.5. Discussion..........84

4.2. A Comparative Study on the Efficiency of Two *Mycobacterium avuim* subsp. *paratuberculosis* (MAP)-Derived Lipopeptides of L3P and L5P as Capture Antigen Molecules in an In-House Milk ELISA Test..........90

4.2.1. Statistical Analysis..........90
4.2.2. Homemade milk ELISA with L3P and L5P epitopes on BTMs..........93
4.2.3. Homemade ELISA with L3P and L5P epitopes on Milk samples from MAP-Infected Flock (MIF)..........94
4.2.4. Relationship between the type of MAP strain (S or C) and reactivity against L3P/L5P in the in-house milk ELISA (H-MELISA)..........95
4.2.5. Discussion..........99

4.3. Detection of MAP Viability in Sheep and Goat Milk Samples Via A Novel and Conventional Phage Assay 108

4.3.1. Statistical Analysis..........108
4.3.2. Optimization of peptide-mediated magnetic separation (PMS) phage assay using two different sources of Mycobacteriophage D29..........108
4.3.2.1. Reproducibility assessment and Optimization of PMS-phage assay on 14 sheep milk samples via Laval D29 111
4.3.2.2. Reproducibility assessment and Optimization of PMS-phage assay on 16 bovine milk samples via Actiphage D29 112
4.3.3. PMS-phage assay on unpasteurized sheep milk samples in comparison with milk qPCR IS*900* and milk/serum ELISA 114
4.3.4. Optimization of Phage-Bead qPCR (PBQ) in MAP-spiked PBS and known negative milk..........115

4.3.5. PBQ on unpasteurized milk samples from goat and sheep flocks in comparison with milk qPCR, milk ELISA, and serum ELISA 115
4.3.6. PBQ and PMS-phage assay on milk samples taken from sheep animals in two instances of sampling in comparison with other MAP diagnostic assays of milk qPCR, milk ELISA, and serum ELISA 118
4.3.7. Discussion 119

Chapter V: Conclusion 124

References 127

The list of published papers, submitted manuscript, and presented posters during the PhD studies 151

List of Figures

Figure 1. Cell wall structure of mycobacterial species 20
Figure 2. Phylogenic classification of mycobacteria 21
Figure 3. Phylogeny tree of MAP strains based on whole genome SNPs 24
Figure 4. Procedures of digesting MAP in gasterointestinal tract 26
Figure 5. Impeding phagolysosomal maturation via MAP 29
Figure 6. Global distribution of JD depicting the involved continents 36
Figure 7. The life cycle of lytic bacteriophages 60
Figure 8. Receiver operating characteristic (ROC) curve and area under the curve (AUC) analyses on the MqPCR dataset under the condition that the reference models were adjusted based on MqPCR and MELISA (A) and MELISA (B), respectively 74
Figure 9. The placement of MqPCR-positive BTMs in three different seasons 74
Figure 10. Threshold cycle (TC) changes of BTMs over MqPCR analysis on 14 sheep herds in a longitudinal study (two instances of sampling) 75
Figure 11. MELISA sample-to-positive ratio (S/P%) of 16 BTMs before and after fractionating milk samples 76
Figure 12. Receiver operating characteristic (ROC) curve and area under the curve (AUC) analyses on MELISA dataset when MqPCR and MELISA (A) and MqPCR (B) were considered as the reference models 77
Figure 13. Distribution of MELISA-positive BTMs in three different seasons. 77
Figure 14. Changes in the MELISA sample-to-positive ratio (S/P%) in a longitudinal study. 78
Figure 15. The distribution of 73 BTM samples classified into four binary groups based on the positive/negative status in the MqPCR and MELISA tests 78
Figure 16. Scatterplots of the distribution of 128 milk samples (MIF) in two categories of healthy controls (HCs) and MAP-infected cases tested by MqPCR (A) and MELISA (B). 81
Figure 17. Receiver operating characteristic (ROC) curve analysis and corresponding area under the curve (AUC) analysis of MELISA (A,C,E) and MqPCR (B,D,F) datasets 82
Figure 18. Distribution of 128 MIF milk samples categorized into fifteen quaternary groups based on their positive/negative status in MqPCR, MELISA, SELISA, and FPCR tests 83
Figure 19. Distribution of 128 MIF milk samples classified into 24 binary groups based on the positive/negative status in MqPCR, MELISA, SELISA, and FPCR 84
Figure 20. Pearson correlation test between two in-house MELISAs using two MAP-derived lipopeptides of L3P and L5P 94
Figure 21. Pearson correlation test between two in-house MELISAs using two MAP-derived lipopeptides of L3P and L5P 95
Figure 22. Restriction enzyme analysis (REA) on IS*1311*-positive PCR products obtained from sheep milk samples 97
Figure 23. Procedures of peptide-mediated magnetic separation (PMS) phage assay with intervention of two MAP-complementary peptides of aMp3 and aMptD on MAP-spiked milk samples 109
Figure 24. A schematic view of lysed plaques (3-4 nm) corresponding to MAP concentrations of 10^4 (A) and 10^2 (B) cfu/mL in an artificially contaminated milk sample. 110
Figure 25. PMS-phage assay on 14 sheep milk samples. 111

Figure 26. Venn comparison analysis between peptide mediated magnetic separation phage assay (PMS-phage) dataset and each MAP diagnostic assay of milk qPCR (A), milk ELISA (B), and serum ELISA (C). 115
Figure 27. Schematic views of MAP clumps that are visible with naked eyes captured by phage beads in a MAP-positive goat milk sample. 117
Figure 28. Venn comparison analysis between phage bead qPCR (PBQ) dataset and each MAP diagnostic assay of milk qPCR (A), milk ELISA (B), and serum ELISA (C). 117
Figure 29. Receiver operating characteristic (ROC) curve analysis and corresponding area under the curve (AUC) analysis on PBQ dataset when milk qPCR (A), milk ELISA (B), serum ELISA (C) were binary reference models. 118
Figure 30. Comparison among the results of three diagnostic assays of milk qPCR, milk ELISA, serum ELISA at the first and second rounds of sampling.. 119

List of Tables

Table 1. Non-domestic hosts of Paratuberculosis 35
Table 2. The geographical herd-level distribution of JD; Section 1 36
Table 3. The geographical animal-level distribution of JD; Section 2 37
Table 4. Number of unpasteurized milk and blood samples and their animal sources 63
Table 5. Primers and their sequences used in qPCR analysis 66
Table 6. The sequences of primer set used for amplification of target sequence IS1311 67
Table 7. MAP epitopes used as coating antigen in H-MELISA analyses and their sequences 69
Table 8. Capture peptides used for coating Dynabeads® MyOne ™ Tosylactivated and their sequences 70
Table 9. The placement of BTMs from 14 sheep herds (28 BTMs) in four classes based on MqPCR status (positive/negative) in a longitudinal study 75
Table 10. Comparison between MELISA sample-to-positive ratio (S/P%) of 16 BTMs before and after fractionating milk samples 76
Table 11. MELISA status (positive/negative) of BTMs from 14 sheep herds in a longitudinal study 78
Table 12. Distribution of 73 BTMs based on the positivity/negativity status in MqPCR and MELISA tests and corresponding *p*-values 79
Table 13. Distribution of 128 MIF milk samples in fifteen quaternary groups based on positive/negative status in MqPCR, MELISA, SELISA, and FPCR tests 83
Table 14. Chi-square analysis and the distribution of 128 MIF milk samples classified into 24 binary groups based on the positive/negative status in MqPCR, MELISA, SELISA, and FPCR and corresponding *p*-values 84
Table 15. Distribution of 47 bulk tank milk (BTM) samples based on their positivity/negativity status in H-MELISA L3P, H-MELISA L5P, commercial ELISA (CMELISA), and milk qPCR IS900 (MqPCR). 91
Table 16. Distribution of 81 individual milk samples from a MAP-infected flock (MIF) of sheep based on their positivity/negativity status in H-MELISA L3P, H-MELISA L5P, commercial ELISA (CMELISA), milk qPCR IS900 (MqPCR), serum ELISA (SELISA), and fecal PCR (FPCR). 92
Table 17. Distribution of bulk tank milk (BTM) and individual (MIF) milk samples into two categories of healthy and MAP-positive. 93
Table 18. Distribution of 23 IS*1311*-positive samples in BTM and MIF categories based on the type of MAP strain (S/C/Bison) and corresponding RE fragments on gel-electrophoresis. 97
Table 19. Distribution of 15 BTMs and 8 individual milk (MIF) samples based on the types of MAP in strain typing analysis and H-MELISA L3P/L5P positivity/negativity. 99
Table 20. Optimization of PMS-phage assay via mycobacteriophage D29 from the University of Laval on aliquots of PBS and a known negative bovine milk sample contaminated with different concentrations of MAP comparing the number of lysed plaques appeared on MB 7H10 agar. 110
Table 21. Optimization of PMS-phage assay on MAP-spiked PBS and milk samples representing the number of lysed plaques developed on MB 7H10 and the positivity status of DNA extracted from lysed plaques via PCR IS*900* analysis 110
Table 22. Comparison among the results of HPA and three other tests of MELISA, SELISA and MqPCR 112

Table 23. The comparison between the results of plaque qPCR IS*900* and milk ELISA on 16 bovine milk samples 113
Table 24. Threshold cycles corresponding different concentrations of MAP in MAP-spiked PBS and a known negative milk sample 115

Chapter I: Introduction

1.1 History of Johne's Disease

Johne's Disease (JD) is a long-standing gastrointestinal problem that entangles cattle and herds imposing serious economic concerns to the dairy industry in each society [1,2]. This disease is originated by *Mycobacterium avium* subsp. *paratuberculosis* (MAP) [2]. H.A. Johne and L. Frothingham reported the first case of JD in Germany in 1894 (or 1895) as a "peculiar case of tuberculosis" in a cow. The post-mortem analysis revealed that this cow suffered from sever chronic enteritis represented by the thickness and corrugation of mucus layer throughout the intestine [3–6]. In 1906, Bang claimed that the disease is different from tuberculosis, so he renamed it to Johne's Disease or Pesudotuberculosis [6]. However, MAP was not fully recognized as the causative agent of the disease until 1910 when F. W. Trowt carried out the Koch's postulate cultivating MAP in an in-vivo condition inducing the disease to a model animal (cattle) through infecting them by the bacterium [5–8].

1.2 General Structure of Mycobacteria

Mycobacteria are a group of prokaryotes that have a distinctive cell envelope. That is partially due to the presence of particular lipid and carbohydrate like lipoarabinomannan and mycolic acids [9]. This cell envelope is a double cell membrane enriched with lipid that consists almost 60% of mycobacterium dry weight compared to only 20% lipid components in cell envelope of gram-negative bacteria [10,11]. Cell envelope is stratified into three domains including [12] (figure 1): Domain I, Capsule (C): that consists of high proportion of proteins and lower amount of carbohydrates and lipids. This layer comprises various glycolipids that are fixed in a saccharidic matrix around the mycobacterium. The type of glycolipid is varied by the species of mycobacteria including lipooligosaccharides, phenolic

glycolipids and glycopeptidolipids (GLPs). The difference in lipid of mycobacterial species might highlight the role of phylogenic divergences resulted by mutation in the gens located in the GLP locus [9]. For example: some studies suggested that GLP is present in the cell envelope of both rapid and slow growing mycobacterial species such as *M. chelonae*, *M. scrofulaceum*, *M. abscessus* (rapid) and *M. avium* subsp. *avium* (slow) [13,14]. As a result of mutation in one of eight genes that comprise GLP locus, *M. abscessus* has lost its capability in production of GLPs and this might be associated with the rugged colony morphology in the bacterium [14]. Domain II, Outer Membrane (OM): It is a tripartite membrane that is covalently bound to arabinogalactan-peptidoglycan complex. So that, the inner leaflet of lipid bilayer in OM consists of long chain mycolic acids that covalently linked to the parietal backbone of arabinogalactan (via ester) [15]. Regarding the structure of outer leaflet of OM, there are various debates. While, some studies support the presence of mycolates, phospholipids and lipoglycans (peptidoglycan) in this layer [16], other works believe that diacylglycerols and triacylglycerols are the fundamental components of outer leaflet in OM [15]. Domain III, Inner Membrane (IM): there are also diverse opinions on the components of IM. Some studies claim on the similarity between the structure of IM and other bacterial membranes [15], whereas others believe that IM has a particular lipid, diacyl phosphatidylinositol dimannoside, that plays an important role in low fluidity of the IM that is associated with the drug resistance due to decelerating the drug stream [16].

The hydrophobic characteristic of cell wall in mycobacterial species cause the bacteria form clumps when growing in liquid media. In fact, lipid components in mycobacterial cell wall make the mycobacteria resistant to acid and alkaline in the environment following a reduction in permeability of them to basic dyes [17].

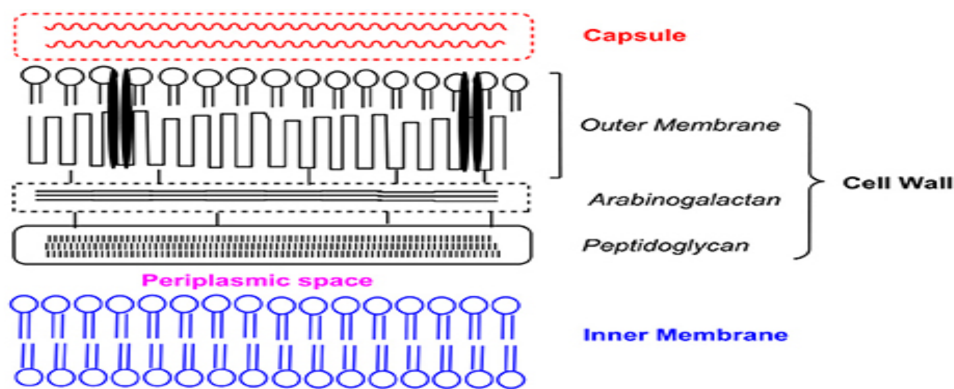

Figure 1. Cell wall structure of mycobacterial species [10]

1.2.1 Taxonomic and Phylogenic Analysis of Mycobacteria

Mycobacteria are classified into three groups (Figure 2) of *Mycobacterium tuberculosis complex* (TB group, causative agent of tuberculosis), *Non-tuberculosis Mycobacteria* (NTB), *Mycobacterium leprae* (causative agent of Leprosy). The pathogenic species of TB group are phenotypically diverse, however they have very similar genetic characteristics and because of that they are categorized in the same group [17]. *Mycobacterium tuberculosis* is one of the most important and pathogenic species that belonged to TB group and triggers tuberculosis in humans. *Mycobacterium bovis* is another species that can potentially result in tuberculosis in both human and cattle, whereas *Mycobacterium africanum* rarely leads to the human tuberculosis [17]. NTB group is those opportunistic mycobacteria that involves in different pathogenicity in immunosuppressive individuals [17]. Some members of this group include *M. avium*, *M. intracellulare complex*, *M. kansasii*, *M. marinum*, *M. fortuitum*, *M. chelonae complex*, *M. abscessus* and *M. scrofulaceum* [18]. *Mycobacterium leprae* is classified as the last group that can lead to leprosy in human. The recent mycobacterium is an obligate parasite and uncultivable in the in-vitro condition [19].

In another classification based on the characteristic of rapidity in growth, mycobacteria are stratified into two groups of fast ad slow growing. The fast growing mycobacteria, i.e. *M. chelonae, M abscessus* and *M. fortuitum* and etc., can develop colonies on solid media almost

after seven days [18,20–22], whereas the slow growers, i.g. *M. avium* and *M. intracellulare,* need more incubation time between 8 to 12 weeks [18,22–25].

Interestingly, M. avium is subdivided into three subspecies of *M. avium* subsp. *avium*, M. avium subsp. paratuberculosis (MAP) and *M. avium* subsp. *silvaticum.* MAP is distinguished from two other subspecies (*M. avium* subsp. *avium* and *M. avium* subsp. *silvaticum*) phenotypically and genotypically by its mycobactin-growth-dependent characteristic [26] and 15-18 copy numbers of Insertion Sequence *900* (IS*900*) respectively [5,27,28].

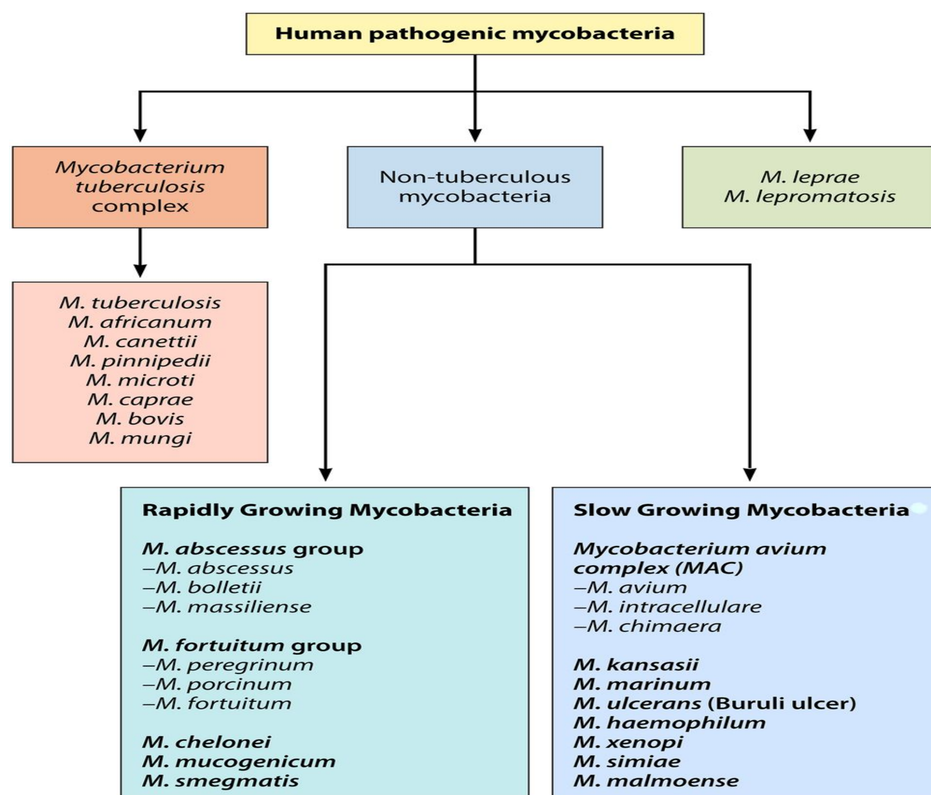

Figure 2. Phylogenic classification of mycobacteria [29]

1.3 *Mycobacterium avium* subsp. *paratuberculosis* (MAP)

MAP is a rod-shape, acid fast, obligate aerobic, non-spore forming, non-motile pathogen that belongs to mycobacteriaceae family. This fastidious mycobacterium has a lengthy generation time (more than 24 hours) that elongates the isolation of bacterium to 7-16 weeks and its growth in in-vitro condition [30–32] depends on the presence of additives like organic source

of iron (Mycobactin J). This iron can be chelated by intracellular exochelin and exchanged with membrane-associated mycobactins [6,33]. However, MAP can keep its survival under diverse conditions like in -14 ºC at least one year, in bovine feces and black soil up to one year, in pond and river water around nine months and 160 days respectively [3]. MAP is resistant to chemical and heat treatments and can survive the pasteurization. The viability of MAP during pasteurization depends on some factors such as the concentration of MAP cells (greater than 10^1 cfu/ml) and considerable D-value (Decimal Reduction Value) for all MAP strains (71-72 Cº/12-14 sec) that is greater than D-value of other bacteria like Listeria (71.7°C/5 sec), Coxiella sp (62°C/30 min) and *M. bovis* (71.5°C/14 sec) [34–36]. MAP has tendency to form clumps and it might play a role in decreasing log reduction in pasteurization [37–39]. This heat-resistance characteristic raises the global concerns over the possibility of transferring this pathogen to humankinds through consumption of dairy products contaminated with MAP.

1.3.1 Strain Types of MAP

Assessment of genetic diversities plays a key role in development of new diagnostic and treatment approaches [37]. MAP genotyping is a demanding process, since MAP is a monomorphic pathogen as same as some other human pathogens like *M. tuberculosis* and *M. leprae* [40,41]. MAP strains have been categorized into different groups based on various hypotheses. In one hypothesis; depending on the type of host ruminant, MAP is classified into two major strain groups of Sheep (S) and Cattle (C) strains (Figure 3) [1,40–42]. S and C types MAP strains have different genetic constructions along with various observable characteristics such as color of colony, chemical process of iron, the patterns that they follow to inactivate the repressors responsible for the production of cytokines and initiate their expression [1]. Sheep animals are vulnerable to both S- and C- type MAP strains, in contrast

cattle is resistant to S type [43]. However, wide strain typing analysis revealed that the association between the type of MAP strains and host species could not inevitably assign a MAP strain to just a specific species of animal, in which a strain that is more likely to be detected in sheep, it might happen in bovine as well and vise versa [40].

All MAP strains grow slowly and have complicated growth requirements, however these characteristics are more distinctive in S type MAP strain [1,44].

In other hypothesis, type I and type II, were assigned as type S and C respectively (Figure 3) [40–42,45]. Recently, strain-typing analysis unveiled another strains of MAP that was named type III. This strain was presumably an evolutionary intermediate that is placed between type S (I) and type C (II). Type B or Bison is another proposed strain group. This strain was firstly found in bison in Montana (USA). The results of molecular analysis showed that type B has similar characteristic to type C (predominant strain in cattle). However, further analysis showed that this strain differs from type C through uncommon growth needs of the isolates and different disease manifestation in clinical stage. Moreover, genotyping analysis on bison type isolates collected from the USA and India disclosed that even these variants differed from each other due to a unique TG deletion at base pair positions 64 and 65 of Insertion sequence IS*1311* at locus 2 that happened in Indian bison type [40,45,46].

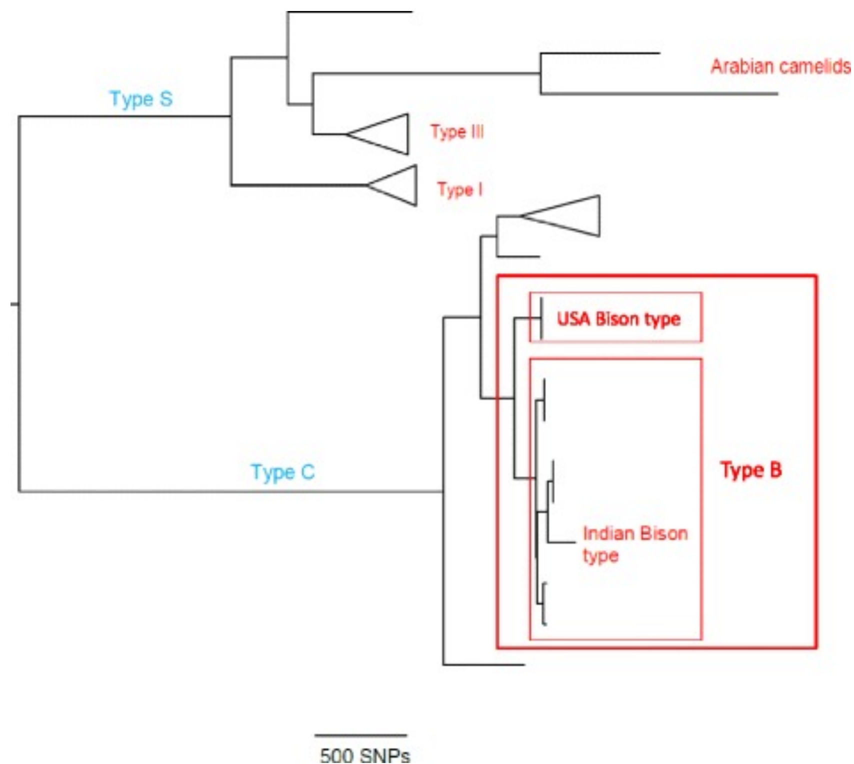

Figure 3. Phylogeny tree of MAP strains based on whole genome SNPs [46,47]

1.3.2 Mechanisms of MAP Infection in JD

JD usually infects the ruminants through the settlement of the bacterium in macrophages located in the lamina propria layer of the small intestine leading to lymph nudes, granulomatous inflammation, and death of JD cases [48]. JD cases have a fragile immune system that makes them vulnerable to other diseases such as lameness, mastitis and pneumonia [2]. MAP follows two stages of infection in susceptible ruminant hosts including I) Pervading the gastrointestinal tract and II) persistence in macrophages. MAP receives various host defenses in each step of infection that needs to be suppressed or attenuated in order to allow MAP promoting the infection [49].

1.3.2.1 Stage I: Pervading the gastrointestinal tract

Researches on experimental animal models suggest that MAP initiates the infection through the invasion of oral mucosa in the tonsil (Figure 4) [49,50]. Then, MAP keeps on its way to

the lymph nodes located in abdominal tissues and ileum via blood circulation [49,51]. As a result of MAP transmitting the infection to jejunal region of the newborn animals, strong mucosal responses are developed [49,52,53]. In neonatal period, the mucosal immune responses are mostly focalized in specific regions [49,54,55]. Studies suggest that newborn calves are more vulnerable to MAP infection rather than adults, because innate and adaptive immune systems have some imperfections in younger animals [56,57]. Theoretically, MAP invasion initiates through both Microfold (M) cells located in the Peyer's patches and transformed epithelial cells [49,54,55]. Fibronectin Attachment Protein (FAP) is one of the MAP-cell-wall proteins, that is activated immediately after crossing the ruminant digestive system [49,58]. The luminal surface of M cells in intestine contains plenty of β1 fibronectin receptor that could be connected to FAP [49,59]. There might be other fibronectin-independent ways that could conduct MAP to epithelial cells in intestine, however the importance of these alternative routs has not discovered yet [49,55]. The shortest time that MAP needs to invade the first host cells is around 30 min [49,60]. Later, these host would transfer the MAP from the lumen in intestine to submucosa that takes between minutes to hours [49,60].

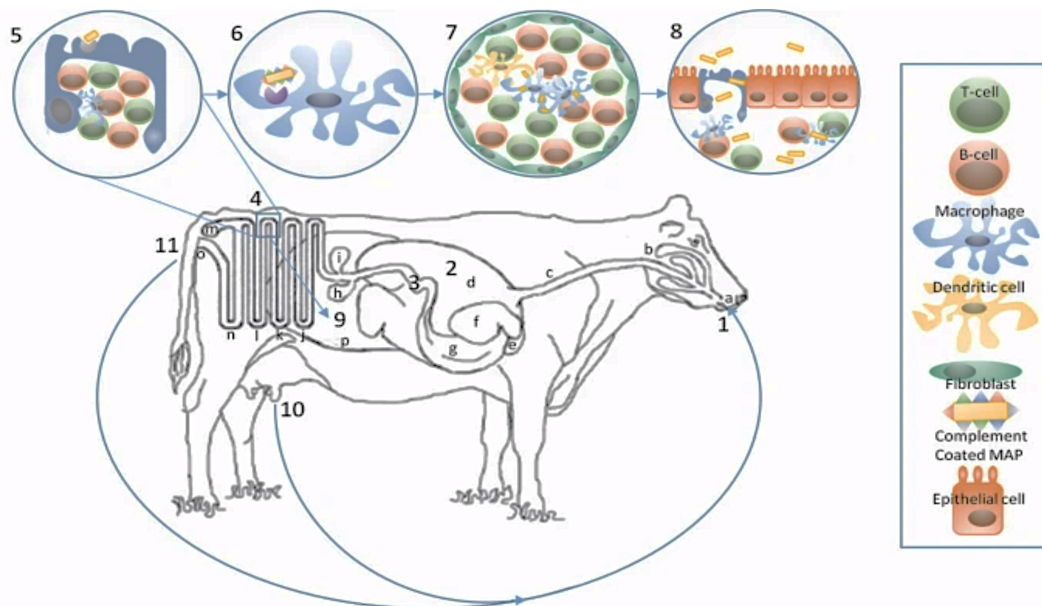

Figure 4. Procedures of digesting MAP in gasterointestinal tract including 1) ingesting MAP and its movment to the GI tract along with absobtion by tonsillar crypts and translocation of MAP to the ileum, 2) activating the FAP in bacterium and opsonization of the bacterium via fibronectin in order to get to the lower GI tract, 3) moveing to the ileum, 4) phagocytozing MAP by M cells located at Peyer's patches and activation of the fibronectin receptors placed at this area due to the bacterum's fibronectin, 5) Absorbing the complement coated MAP cells by complement receptors located at intra-epithelial macrophages, 6) and 7) formation of granulomas by infected macrophages forstering a latent infection, 8) transmitting MAP to unborn calf, 9) and 10) infecting newborns via milk or feces that was disperesed into the environment by MAP-shedder animals. (a) Mouth, (b) Salivary Glands, (c) Esophagus, (d) Rumen, (e) Reticulum, (f) Omasum, (g) Abomasum, (h) Gallbladder, (i) Pancreas, (j) Duodenum, (k) Jejunum, (l) Ileum, (m) Cecum, (n) Large Intestine, (o) Anus, and (p) Uterus [49].

1.3.2.2 Stage II: Persistence in macrophages

MAP in macrophages could survive in host's body putting some strategies into action that could guarantee its existence against the host-immune defenses:

1.3.2.2.1 MAP invasion of the macrophages

At this step, potential MAP cells that could cross the intestinal epithelial barriers, start invading macrophages located under cuticle layers that are represented by several recipient molecules for absorbing mycobacteria such as complement receptors (CR1, CR3 and CR4), the immunoglobulin receptors (FcR), mannose, and scavenger receptors. The survival of

MAP in intracellular condition is associated to the routes that MAP chooses to enter into macrophage via, in which this rout via specific receptor-mediated mechanism can induce particular immune responses following a specific pattern of cytokine secretion [49,61]. So that, macrophage activities might be limited by some routs such as uptake via complement receptors. The studies on bovine belonged to both healthy and JD categories showed that the opsonization of MAP with serum facilitates the uptake of MAP via complement receptor into bovine macrophages remarkably [49,62,63]. This represents that when MAP selects to access macrophages via complement receptors, it follows a specific strategy to evade critical host defenses.

1.3.2.2.2 Blocking phagolysosome fusion

MAP applies different strategies to set up a persistent infection and guarantees its survival inside phagosomes either by impeding the fusion of lysosome into phagosome disrupting the phagolysosome formation and hindering the subsequent hydrolysis and oxidation reactions, or by inhibiting phagosome acidification (Figure 5) [64–66]. In addition, the destruction of the infected phagosomes depends on the active involvement of the internalized pathogens [65,66]. Different studies show that viable MAPs, not dead, are able to block the endosomal maturation and that is supported by the modification of the patterns of endosomal markers [66]. Accordingly, only viable MAP could inhibit the acidification of phagosomes. One of the destructive mechanisms that imped the phagsome-lysosome fusion along with the phagosome maturation is through the interaction of MAP with phagosomal membranes [67].The studies suggest that mycobacterial lipids can defect the structural and functional profiles of the phagosome membranes [67]. For example: sulfolipid damages the phagosome fusion and lipid phosphatase SapM influences the functional characteristics of phagosome membrane [68,69]. Phosphatidilinositol 3 Phosphatase (PI3P) is a phagosome membrane-trafficking

lipid that regulates the acquirement of lysosomal constituents. The studies reveal that PI3P in host cells infected with live mycobacteria was continuously removed by hydrolysis activity of SapM [49,65].

Acidification of phagosome in maturation step depends on hydrolytic enzymes existed in lysosome vacuoles that these enzymes have the most optimum catabolic activity in the acidic pH [70]. The acidification of vacuoles depends on the activity of an integral proton pump protein (H^+-ATPase or V-ATPase) utilizing ATP in order to pump proton into the vacuoles. Those phagosomes that are infected with pathogenic mycobacteria have higher pH than non-infected ones, specifically the MAP-infected phagosomes even showed higher acidity than the other phagosomes infected with other mycobacteria [70]. Interestingly, the V-ATPase in MAP infected phagosomes is expressed in higher quantities [71,72] than phagosomes infected with non-pathogenic mycobacteria [73]. On the other hand, MAP produces a protein effector molecule that is named Protein tyrosine phosphatase (PtpA) that binds to a specific subunit of macrophaghe V-ATPase that is associated with the luminal acidification and probably coordinates with phagosome-lysosome fusion through the interaction with the macrophage class C vacuolar protein sorting complex [74]. PtpA mediates the dephosphorylation of VPS33B, removes V-ATPase and impedes the acidification [74]. Some host proteins could induce the development of endosomes for instance ATPase N-ethylmaleimide- sensitive factor (NSF), soluble NSF attachment proteins (SNAPs), and vesicle and target membrane SNAP receptors (SNARES) [75,76]. In which, Rab-GTPase regulates the procedures of maturation. For example, Rab5 and Rab7 assists the fusion of, respectively, early endosomes and mature pahagosomes with endosome and lysosome respectively [49,77]. In contrast, MAP could hamper the maturation of endosomes into functional mycobacteriocidal compartments through hindering the activity of Rab5 and early

endosomal autoantigen 1 (EEA1) towards phagosomes engulfed pathogenic mycobacteria [78]. In addition, MAP can inhibit the secretion of the tryptophan aspartate-containing coat protein (TACO) that is responsible for fusion of phagosome with the lysosome [79]. Affecting the cell signaling is another strategy that mycobacteria use to defect endosome maturation [80]. For example: the interaction between EEA1 and LAMP-3 with late endosomes could be hindered via mitogen activated protein kinase (MAPK)-p38 signaling. However the inactivation of MAPK-p38 signaling can act reversely and triggers the phagosomal acidification and enhances late endocytice markers [49,80].

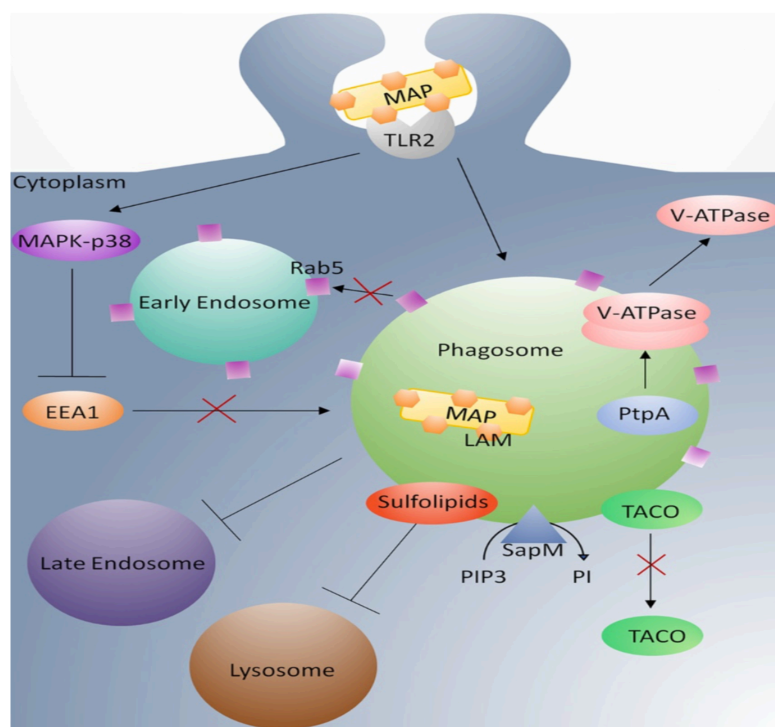

Figure 5. Impeding phagolysosomal maturation via MAP [49].

1.3.2.2.3 Blocking macrophage responsiveness

Toll-Like Receptors (TLRs) are a sub-class of Pattern Recognition Receptors (PRRs) that play an important role in innate immune responses through regulating nonspecific defenses against potential harmful pathogens along with cytokine responses and other TLR-mediated cellular processes that are essential for mycobacterial pathogenesis such as the maturation of

phagosomes [49,54,81]. Active expression of TLR against MAP can protect the host against infection. Whereas, mutation in TLR can enhance the sensitivity of the individuals to mycobacterial-dependent infections and reduce the TLR-mediated responses in MAP infected hosts. Each TLR induces various immune responses, for example: TLR9 induces the critical defenses against MAP, whereas TLR1 and TLR2 promote the responses that halt the immune defenses against MAP [81–84]. TLR2 has polymorphism with TLR1 and TLR6, in which it could bind to various receptor-specific pathogen associated molecular patterns (PAMPs), this characteristic can predispose individuals to MAP [82,85]. So, TLR2 recognizes the MAP-cell wall lipoprotein receptor and bind to it [86]. Mannosylated liparabinomannan (Man- LAM) as a mediator plays an important role in activation of TLR2 and subsequently commence of signaling through MAPK-p38 pathway and this influence the expression of IL-10. Accordingly, increasing the expression of IL-10 discourages the expression of other genes like pro-inflammatory cytokines, chemokines, IL-12, and major histocompatibility factor class-II. This is why MAP suppresses the antimicrobial responses against infected microphages through increasing the expression of IL-10 and activation of Man-LAM-induced TLR2-MAPK-p38 signaling pathway [87]. The studies show that anti-TLR2 antibodies could offset the devastating impacts of internalized MAP on the involved macrophages. This is followed by increasing the acidification and maturation of phagosomes and ends to the killing of MAP [87]. However, the level of IL-10 is not affected by anti-TLR2 treatment showing that anti-TLR2 independently modifies the acidification and maturation of phagosomes through other mechanisms like hampering EEA1 [49,87,88].

1.3.2.2.4 Interferon Gamma Signaling

IFNγ is one of the key cytokines that regulates the host immune defense against various intracellular pathogens (mycobacteria) [49,89]. IFNγ is produced as the most primary

responses to MAP infection that keeps active throughout a persistent infection. Of bactericidal responses that are induced by IFNγ signaling pathway, the following defenses are notable: reactive oxygen and nitrogen intermediates, production of cytokines and promotion of phagosome maturation. IFNγ binds to specific receptors in order to activate Janus family Kinase Signal Transducer and Activator of Transcription (JAK-STAT) pathway [90]. The researches show that hosts with inadequate amount of IFNγ or IFNγ receptor chain mutations are more vulnerable to intracellular-pathogen related infections, as the importance of IFNγ in the pathogenicity of Johne's Disease (JD) has been recorded in few studies [91,92]. In the subclinical stage of JD, the concentration of IFNγ sees a significant rise at ileal and cecal lymph nodes [93]. In an in-vitro study on PBMCs (from both infected and healthy cases) that were induced by MAP antigens, higher level of IFNγ was produced among infected isolates [49,94].

1.3.2.2.5 Superoxide dismutase

Active Oxygen Intermediate (ROI) such as superoxide anion, hydrogen peroxide and hydroxyl free radicals, can induce the elimination of pathogens such as mycobacteria via mature phagolysomes [49,67]. However, some studies recorded that the production of ROI such as superoxide anion by monocytes has been impeded in response to MAP infection or the stimulation of MAP-infected monocytes by IFN-γ [95]. MAP can neutralize superoxide radicals and generally the production of ROI through the secretion of superoxide dismutase and inhibition of IFNγ simulated signaling respectively [96,97]. However, MAP-inhibited TLR9 cannot suppress the production of ROI [49,98].

1.3.2.2.6 Nitric Oxide

Reactive Nitric intermediates (RNIs) are another components that found in phagolysosome

environment and have antibacterial profiles against pathogens [49,99]. Mycobacteria such as *M. tuberculosis*, MAP and *M. leprae* are susceptible to IFNγ-induced RNIs [99–101]. However, studies on mouse macrophages showed that the production of RNIs might be defected by some chemicals leading to an increase in the survival of *M. tuberculosis* in macrophages [99]. In addition, the amount of chemically produced nitric oxides could influence their destructiveness significantly [102]. While studies on bovine monocytes show that the level of IFN-γ-induced RNIs increases immediately after MAP infection, the yielded nitric oxide is inadequate to promote the bacterial demolition [102]. In fact, phagosomes infected by mycobacteria cannot get access to enough nitric oxide synthase necessary for killing the mycobacteria [49,103].

1.3.2.2.7 Apoptosis

Apoptosis is a programmed cell death that is different from necrosis [49,104,105]. The intracellular destruction of Mycobacteria-infected macrophages could be induced through apoptosis [105]. In which, MAP infected macrophages that experienced apoptosis could be phagocytosed by other healthy macrophages [105]. While, this could impede the growth of MAP, it facilitates the transmission of MAP into the other healthy macrophages keeping them far away from immune inspection suppressing the inflammatory responses [106]. As cell lysis of MAP-infected macrophages results in liberation of chemotactic stimulants existed in the intracellular spaces. These stimulants could promote the acute phase of inflammation that is associated with tissue destruction, whereas apoptosis suppresses the recent inflammatory reactions [106]. Apoptosis enables MAP to replicate in new spaces and set up a consistent infection getting concealed from the host immune defenses [106]. Studies show that MAP not only could encourage apoptosis, but also could suppress it. The settlement of live mycobacteria in macrophages can promote apoptosis, whereas the heat-killed MAP cells can

mediate apoptosis insignificantly [107]. Interestingly, the death of macrophages is promoted by apoptosis in higher levels of MOI (multiplicity of infection), in which caspase-dependent apoptosis is activated in MOI higher than 10, whereas caspase and nitric oxide independent apoptosis and necrosis are initiated in MOI higher than 50. This proves that mitochondrial destructions results in apoptosis of infected macrophages [108]. The other hypothesis believes that MAP impedes apoptosis of the infected macrophages to be concealed from immune system and buy more time for replication [109]. Of MAP inhibitory strategies, minimizing the expression of caspase 3/7 and 8 genes that leads to a reduction in the activity of caspase "3/7, 8 and 9" [110] and increasing the release of induced-macrophage IL-10 through reducing the expression of TNFα, and enhancing the release of TNFR2 that leads to TNFα neutralization [49,64] are more noticeable. In addition, Man-LAM (mannosylated arabinoomannan: a major lipoglycan belonging to the slow growing mycobacterial cell wall) can inhibit apoptosis through lowering the level of released cytosolic calcium. In a normal condition, the presence of calcium ions in cytosol can promote the penetrability of mitochondrial membrane [64]. BAD is a pro-apoptotic protein that regulates apoptosis through binding to its antagonist (anti-apoptotic proteins) such as Bcl-2 [111,112]. However, Man-LAM promotes the phosphorylation of BAD protein and keeps it away from binding to anti-apoptotic receptors [49,113]. As result of that, the presence of unbound anti-apoptotic proteins like free Bcl-2 inhibits the release of cytochrome C (cytochrome C mediate the allosteric activation of apoptosis-protease activating factor 1) from mitochondria membrane [49,114].

1.3.2.2.8 IL-10

IL-10 is an anti-inflammatory cytokine that is manufactured by monocytes, macrophages, B-cells and T-cells (lymphocytes) [49,110]. IL-10 can minimize the host inflammatory

responses through different strategies including impeding Th1-type responses, suppressing the production of pro-inflammatory cytokines, and concealing the mycobacteria infected the macrophages and dendritic cells from the host immune responses. The mentioned strategies can enhance the viability of MAP within macrophages [49,110,113]. In contrast, studies reported that negating IL-10 that yielded by MAP-infected macrophages could activate the expression of some inflammatory genes including TNFα, IL-12, IL-8, MHC-II and that would be followed by the acidification of phagosomes, macrophages apoptosis and production of nitric oxide [49,110].

1.4 MAP Epidemiology

The rising incidence of JD has been reported in different areas of the world. JD has a remarkable incidence in the presence of sufficient rainfall, ground water, and humidity and even in tropical area [7,115,116].

1.4.1 Paratuberculosis Host Ranges

The principle carriers of JD are ruminants including bovine and sheep, etc. However, evidence show that JD has a wide range of hosts such as horses, pigs, mice, hamster, cat and other wild species of animals (Table) might be infected and involved with the disease. Some species of claw-hoofed animals are susceptible to both S (Sheep) and C (Cattle) strains of MAP [48,115,117–119], The studies show that experimentally infected pigs featured the disease with granulomatous enteritis and lymphadenitis, whereas pigs that were kept with the infected cattle had the evidence of mesenteric lymph nodes enlargement that might be indicated with tuberculosis like lesions [115,120–122]. The disease has also been reported among macaque monkeys [115,123]. Among non-ruminant hosts, a strong association was found between infected rabbits and a cattle with the history of disease [124,125] and also

MAP was cultivated from the tissues of foxes and stoats [115,126].

Table 1. Non-domestic hosts of Paratuberculosis [115]

Species	Country
Fallow deer (*Dama dama*)	Czech Republic Germany USA
Axis deer (*Axis axis*)	USA
Tule elk (*Cervus elaphus nannodes*)	USA
European red deer (*Cervus elaphus*)	Czech Republic Scotland Ireland New Zealand
White-tailed deer (*Odocoileus virginianus*)	USA
Roe deer (*Capreolus capreolus*)	Czech Republic
Sika deer (*Cervus nippon*)	USA
Elk (*Cervus elaphus*)	USA Canada
Moose (*Alces alces*)	USA
Pudu (*Pudu pudu*)	Belgium
Antelope kudu (*Tragelaphus strepsiceros*)	Czech Republic
Feral goats (unspecified)	New Zealand
Pygmy goat (*Capra hircus*)	Germany
Rocky Mountain goat (*Oreamnos americanus*)	USA
Capricorn (*Ibex ibex*)	Germany
Capricorn (*Capra cylindrycornis*)	Czech Republic
Moufflon (*Ovis musimon*)	Czech Republic USA Germany
Aoudads (*Ammotragus lervia*)	USA
Bighorn sheep (*Ovis canadensis*)	USA
Cameroon sheep	Germany
Jimela topi (*Damaliscus lunatus jimela*)	USA
Sicilian ass	USA
Pygmy ass (*Equus asinus* form. *dom.*)	The Netherlands
Alpaca (*Lama pacos*)	Australia
Bactrian camel (*Camelus bacterianus*)	USA
Rabbit (*Oryctolagus cuniculus*)	UK
Fox (*Vulpes vulpes*)	UK
Stoat (*Mustela erminea*)	UK
Stumptail macaques (*Macaca arctoides*)	USA

1.4.2 Geographical Distribution of Paratuberculosis

The cases of JD have been reported in different countries throughout the world. This is mainly due to a long latency period of the disease manifestation in the infected animals in addition to the presence of asymptomatic MAP-shedders that could potentially and silently disseminate the disease everywhere. Since, the infected animals might be undetectable at the first stages of the disease, livestock marketing and transportation of MAP-carriers from one region to another region or from one country to another country could contribute in the global outbreak of JD [127–129]. According to the latest studies, the geographical incidences of JD are as follows (Figure 6): Africa (53%), India (23.3%), Europe (20%), South America (18.3%), North America (16.9%) and Australia (6.8%) (Fig.). The Table 2 and Table 3 represent the geographical distribution of JD in the level of herd and individual respectively.

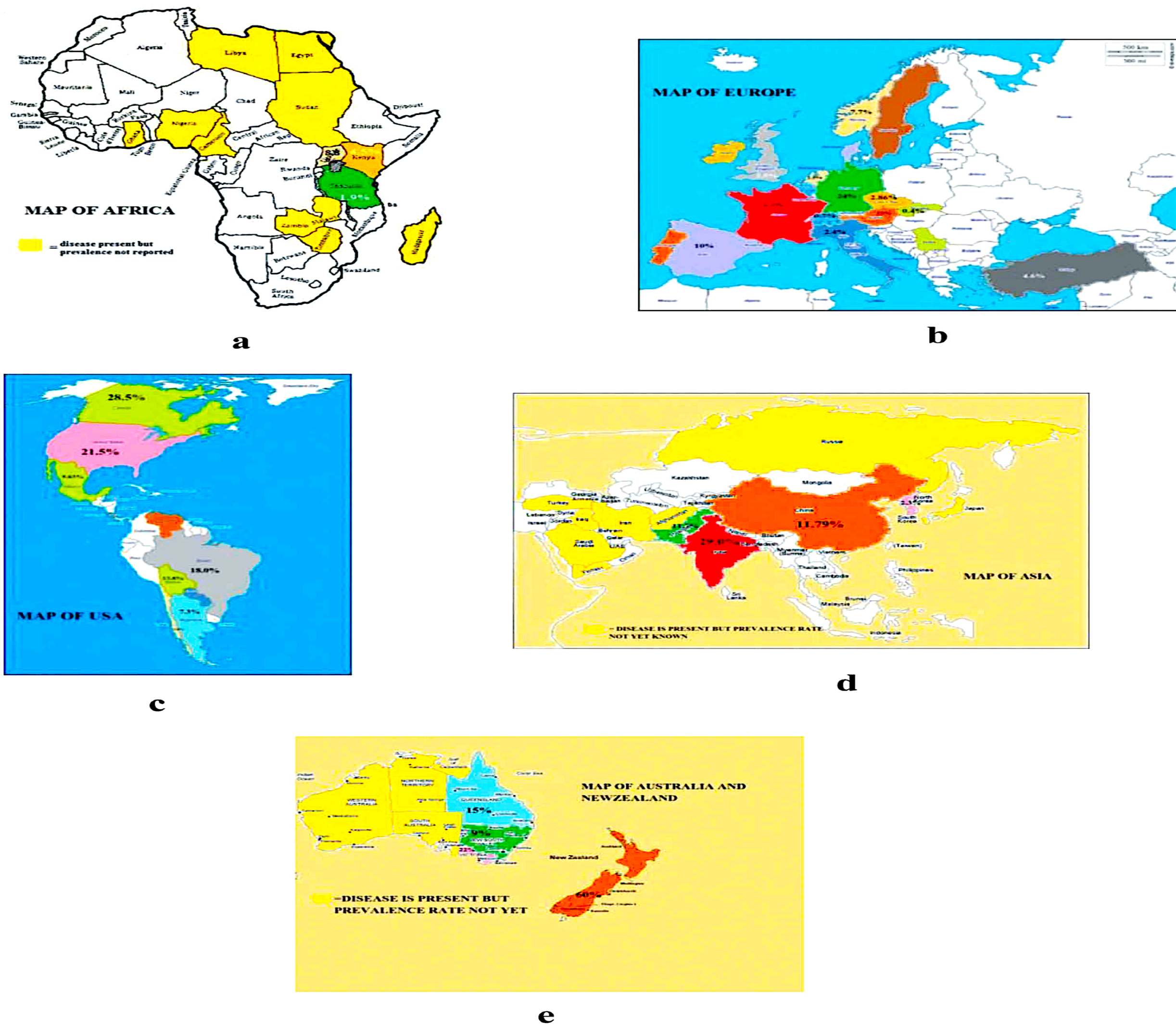

Figure 6. Global distribution of JD depicting the involved continents including Africa (a) Europe (b), North and South America (c), Asia (d) and Australia (e)

Table 2. The geographical herd-level distribution of JD; Section 1 [127]

Country/region	Study period	Test	Age group	No. of animals	Test positive animals	Prevalence (%)
			Europe			
Belgium	1997–1998	HerdChek, IDEXX	> 2 years	458	82	18
France/Yonne	1998–1999	Pourquier ELISA	All	155	105	68
Germany/Bavaria	2005	ELISA, Svanovir		493	207	42
Italy/Latium	-	HerdChek, IDEXX		369	155	42
Italy/Veneto	2000–2001	HerdChek, IDEXX	> 12 months	419	272	65
Italy/Verona province	1997–1998	Tissue culture + histopathology		73	5	7
Norway	2002	Faecal culture		200	20	10
Slovenia	2000–2001	Pourquier ELISA	> 2 years	302	35	12
Sweden	2000–2001	Faecal culture		200	0	0.0
Switzerland	1993–1994	Parachek ELISA	Dairy	113	9	8
The Netherlands	1998	HerdChek, IDEXX	Dairy ≥ 3 years	371	200	54
Turkey		ELISA	> 2 years	545	206	38
Denmark	1998	Milk ELISA	-	900	497	55
AFRICA						
Kenya	1973	CFT	Cattle	200	9	4.5
Egypt	2005	Culture and IS900 PCR	Cattle	2150	75	3.5
AMERICA (SOUTH AND NORTH)						
Brazil/Paráiba	-	ELISA	Cattle	36	21	58.3
Brazil/Espírito Santo	-	ELISA	Cattle	23	20	87
Brazil/Sao Pablo	-	ELISA	Dutch breed cattle	20	19	95
Brazil/Goiás	1998	ELISA	Dairy cattle	17	17	100
Mexico, Hidalgo	203–2004	ELISA	Dairy cattle herds	29	28	96.5
Costa rica	1990	ELISA	Dairy cattle herds	364	68	18.7
Brazil/Rio de Janeiro	-	ELISA	Dairy cattle	45	37	82
Brazil/Pernambuco	-	ELISA	Dairy cattle herds	19	9	47.4
Chile/Region VIII: Bío Bío	-	Culture of Environment samples and PCR	Dairy cattle herds	14	6	42.9
Chile/Region X: Los Lagos	-	ELISA	Dairy cattle herds	20	19	95
Venezuela/Monagas	-	Skin test MAP PPD	Dual purpose herds	8	7	87.5
Venezuela/Monagas	-	ELISA	Dual purpose herds	8	8	100
Puerto Rico	2004	ELISA	Dairy cattle herds	28	23	82
North America	1997	ELISA	Beef cattle herds	380	30	7.9
Texas	-	ELISA	Beef cattle herds	115	50	43.8
ASIA AND AUSTRALIA						
China	-	ELISA	Cattle	113	23	20.35
New Zealand	1998	ELISA	Herd prevalence	-	-	60
State of Victoria	1998	ELISA	Herd prevalence	1748	1968	88.8
New South Wales	1998	ELISA	Herd prevalence	163	1968	8.2
South east Australia	1998	ELISA	Herd prevalence	20	1968	1.0
Tasmania	1998	ELISA	Herd prevalence	37	1968	1.8

Table 3. The geographical animal-level distribution of JD; Section 2 [127]

Country/region	Study period	Test	Age group	No. of animals	Test positive animals	Prevalenc (%)
			Europe			
Austria	-	ELISA	Cull cattle > 2 years	756	144	19.0
Belgium	1997–1998	HerdChek, IDEXX	France > 2 years	13,150	116	0.9
France/Yonne	1998–1999	Pourquier ELISA	All	8,793	292	3.3
Germany/Bavaria	2005	ELISA, Svanovir		2,748	662	24
Italy/Latium	-	HerdChek, IDEXX		19,627	472	2.4
Italy/Veneto	2000–2001	HerdChek, IDEXX	> 12 months	27,135	949	3.5
Italy/Verona province	1997–1998	Tissue culture + histopathology		73	5	6.8
Norway	1996–1997	HerdChek, IDEXX		9,456	728	7.7
Slovenia	2000–2001	Pourquier ELISA	> 2 years	9,388	41	0.4
Sweden	2000–2001	Faecal culture		4,000	0	0.0
Switzerland	1993–1994	Parachek ELISA	Dairy	1663	12	0.7
The Netherlands	1998	HerdChek, IDEXX	Dairy ≥3 years	15,745	400	2.5
Turkey		ELISA	> 2 years	8,873	409	4.6
United Kingdom/South west England	1994	PCR	Cull cattle	1,297	46	3.5
AFRICA						
Libya	1986	Histological examination and ZN staining	Cattle	300	60	20
Uganda	2011	ELISA	Cattle	943	35	3.7
Zambia	1984	ELISA	Antelopes	373	20	5.36
Zambia	1989	CFT	Ovines	50	16	32
AMERICA (SOUTH AND NORTH)						
Argentina/Buenos Aires	1992	ELISA	Beef cattle	2530	350	13.8
Brazil/Pará	-	Beef cattle	ELISA	514	182	35.4
Brazil/Espírito Santo	-	Dairy cattle	ELISA	1450	165	11.4
Brazil/Sao Paulo	-	Dairy cattle	ELISA (Idexx)	403	153	37.9
Argentina/Corrientes	2001	Dairy cattle	Milk culture and faecal culture	123	0	0.0
Argentina/Corrientes	2001	Dairy cattle	ELISA (Parachek)	79	6	7.6
Argentina/Corrientes	2001	Dairy cattle	ELISA (PPA-3) strain 18	123	12	99.8
Argentina/Corrientes	2001	Dairy cattle	Skin test bovine PPD (Instituto de Sanidad Ganadera)	123	4	3.3
Argentina/Corrientes	2001	Dairy cattle	Skin test avian-PPD (DILAB/ SENASA)	123	9	7.3
Brazil/Paraíba	-	Dairy cattle	ELISA	486	49	10.1
Brazil/Goiás	1998	Dairy cattle	ELISA	166	100	60.24
Mexico, Hidalgo	2003–2004	Dairy cattle	ELISA	1639	148	9.0.3
Costa rica	-	Dairy cattle	ELISA	654	78	11.9
Brazil/Rio de Janeiro	-	Dairy cattle	ELISA (Parachek)	1004	181	18
Brazil/Pernambuco	-	Dairy cattle	ELISA (Pourquier – IDEXX)	408	11	2.7
Chile/Region VIII: Bío Bío	-	Dairy cattle	ELISA (Pourquier)	596	38	6.4
Chile/Region X: Los Lagos	-	Dairy cattle	ELISA (Pourquier)	872	111	12.8
Venezuela/Monagas	-	ELISA	Mature dual purpose cattle	240	173	72.1
Venezuela/Monagas	-	Skin test MAP PPD (National Veterinary Services Laboratories)	Mature dual purpose cattle	240	10	4.2
Puerto Rico	2004–2005	ELISA	Dairy cattle	2053	117	5.7
ASIA						
Northern India	2004–2005	ELISA	Dairy cattle	1425	414	29
Uttar Pradesh	2004–2005	ELISA	Cattle and buffaloes	601	192	31.9
Punjab	2004–2005	ELISA	Cattle and buffaloes	372	87	23.3
Pakistan	2011	ELISA	Cattle and buffaloes	134	15	11.19
China	-	ELISA	Cattle	3674	433	11.79
Korea	2012–2013	ELISA	Korean cattle	2,606	60	2.3%

1.5 Symptom Manifestation of JD

The progress of Paratuberculosis in the infected animals follows a four-phase procedure including silent, sub-clinical, clinical and advanced. Although, the infection begins in neonates [130,131], the signs of the disease appears around 2 to 10 years. Accordingly, silent stage (I) begins in animals bellow 1 year old and the infected animals do not show any

symptoms at this phase in which the presence of MAP is not detectable[132]. JD is a contagious disease that could be transmitted from one case to Paratuberculosis-free animals via MAP that was shedded into the environment or existed in the reproductive system of the infected female animals [2,133] In subclinical stage (II), the infected animals still do not show the signs of the disease but the organism might be detectable in shedders. The infected animals start manifesting the symptoms like diarrhea and weight lose (in spite of having good nutrition) in clinical stage (III) and the presence of antibodies against MAP could be tracked by serological tests. In advanced stage (IV), the infected animals that progressed the disease to this phase get weak and emaciated day by day and shed a large number of MAP into feces that leads to the granulomatous in lymph nude and small intestine and death of the infected animals [133]

1.5.1 Clinical Symptoms of JD

Although, the early age groups (≤ 4 months) of the domestic ruminants are more sensible to JD, symptom manifestation initiates after a long incubation period (≥ 2 years) compared to the wild ruminants (that commonly affected by milk) that develop the signs of MAP infection within 8 to 12 months after the first exposure [115,116].

1.5.2 Pathological and Anatomical modifications

The clinical stage of JD is represented by lymph nudes and lesions that are restricted to the dorsal part of gastrointestinal tract (GI) in cattle. By the progression of the disease to the advanced stage, the other parts of GI may be involved in the disease. That may associated with disseminating the lesions in the area between the rectum to duodenum, increasing the thickness of intestine wall up to three to four times of normal condition and appearing the grooves in mucosa [134]. Furthermore, the edges of ileocecal valve along with redness at

primary stage of JD, and subsequent oedema and increasing the thickness and grooms. No ulcer or gap happens in the mucosal surface at this stage. However, a moderate enlargement along with oedema, central necrosis and mineralisation can be seen in mesenteric and even ileocecal lymph nodes (the two recent events occur in all species but it is prominent in deer) [135]. The changes may also occur in the jejunum and ileum, in which serosal lymphatic vessels get enlarged and form a beaded appearance [115].

1.5.2.1 Cattle

Increasing the thickness and corrugation of the ileum are the consequences of granulomatous infiltration in cattle [112]. Granulomatous lesions consist of macrophages that phagocytized MAP [59,136] and other mycobacteria [137]. In which, the content of these macrophages is infiltrated into intestinal lamina propria [137,138]. Some studies show that lesions in cattle with JD are not associated with caseous necrosis, calcification and fibrosis [139].

1.5.2.2 Sheep

Sheep with JD does not develop sever lesions and the mucosal thickness and corrugations of are almost normal [139]. In some cases, cross species transmission of MAP strains between ovine and caprine results in dispersed color modification of areas of the intestine into orange or yellow [139,140].

1.5.2.3 Goat

In goats, the colonization of MAP in association with calcification can be seen in different areas of the intestine including mucosa, submucosa, serosa, lymphatics and regional lymph nudes [139]. However, a study reported that a low concentration of mycobacteria was

detected in granulomatous-dependent lesions in the subclinical stage of JD [141].

1.5.3 Risk Factors in JD

Some factors can affect the progress of JD in the infected animals including a simultaneous infection of the host with parasite-virus-bacteria and stress during transportation of animals [115,142]. Additionally, pH alteration of the soil could influence or even exacerbate the clinical symptoms in the infected animals. Rearing cattle in an alkaline rich soil, especially limestone zones, can increase the incidence of JD among the animals, however it has minor impact on the clinical manifestation of the disease. In contrast, an American study depicted that the rate of infection was significant among the cattle reared in acidic soils [115,143]. Of clinical symptoms, the following signs are more frequent among the animals in cattle: incurable chronic and intermittent diarrhea, throat and abdominal abscesses, roughening hair coat [144], thinness and all of these may lead to the death of the infected animals [145,146].

1.6 MAP Infection and Dissemination

The presence of MAP infected animals along with optimum conditions that encourage the survival of MAP in farms could ease the circle of disease transmission to Paratuberculosis-free animals remarkably. This is due to the capability of the infected animals in shedding plenty of MAP into the environment. Shedding MAP via feces is the most common way of conveying MAP among cattle and depending on the extent and severity of the disease in cattle, the infection may occur in different platforms of pasturage or pens (fenced area in the farm) [115,147].

1.6.1 Prenatal MAP Infection

The newborn lambs or calves might be primarily be infected by MAP via the oral rout. However, some studies reported that MAP potentially could be transmitted to fetus in womb

before birth [148], as MAP has been isolated from the reproductive tissue, uterine mucosa and fetuses tissue of cows [149–151].

1.6.2 Postnatal Infection

Calves are the most vulnerable groups among herd animals that can easily be infected through sucking teats contaminated by feces, ingestion of MAP-exposed colostrum, milk, feed and water and grazing in contaminated pastures [7]. This is highly due to lack of efficient hygiene practices that can control disease and separate the healthy calves from MAP-shedders (via feces, milk, colostrum) [115].

1.6.2.1 Infection via Feces

In MAP-infected animals, the large portion of MAP is discharged into feces, since most lesions and lymph nodes tend to be form in the lower areas of the small intestine. The concentration of MAP that is shedded into feces exceeded to 10^8 colony forming units (CFU) at the advance stage of the JD and this plays an important role in spreading the bacterium into the environment [115].

1.6.2.2 Infection via Milk and Colostrum

Milk and colostrum are classified as the potent sources that can convey MAP into newborn calves, as some studies reported a noticeable amount of MAP in milk samples from clinically developed symptoms cattle (35%) as well as symptomless cases by 11.6% [152,153]. MAP has been isolated from the milk (22.2%) and colostrum (8.3%) of cows in a heavy MAP infected herd. In addition, the evidence showed that animals that discharge MAP in profuse quantities through fecal routs, they probably releae MAP in colostrum as well [154].

1.6.2.3 Infection via Afterbirth (Placenta Explosion)

MAP has been isolated from the endometrium (innermost lining layer of the uterus) of MAP infected animals. This explains the possible risk of transmitting the pathogen from MAP-infected cows to newborns during parturition and afterbirth [151,155,156]

1.6.2.4 Infection Via Semen

MAP could potentially be conveyed into intrauterine space via semen infecting the new zygote and consequently fetus. This has been confirmed by the results of some studies on reproductive organs and semen of MAP-infected bulls diagnosed with acid-fact bacilli in their isolates [115,157,158].

1.6.3 Adult Animal Infection

Newborn calves could be infected with traces of MAP, however adults could even withstand considerable dose of the microorganism [147,148,159]. Accordingly, MAP-infected adults could have one of the two following destinies: 1) to develop the symptoms and step further to the clinical stages of JD or 2) to stay silent and being as a reservoirs of the microorganism while they express a minor sensibility to Johnin (MAP-extracted antigen used in JD skin test) [160].

1.7 Zoonotic Nature of MAP and Its Association with Crohn's Disease in Human

The evidence of MAP has been reported in human cases that suffered from gastrointestinal problems such as Crohn's Disease (CD) developing features similar to JD [161–164]. Dalziel firstly reported this association in 1913 [165] and Crohn and his colleagues were explained it later in 1932 [166,167]. In 1980, MAP was isolated from patients with CD for the first time and this shed the light on this hypothesis that MAP may be the causative agent of CD. In fact,

the microorganism was firstly identified as an uncategorized mycobacterial species different from MAP, but further molecular analysis (DNA-DNA hybridization) on the isolated strains revealed that the bacterium was MAP [168–171]. CD is an idiopathic (cause of the disease is unknown) condition that causes a long-standing inflammation in gastrointestinal tracts [115,144] The disease is symptomized by frequent fatigue, abdominal pains, chronic weight loss, diarrhea, granulomatous ileocolitis [115] followed by remissions and relapses [144]. In addition, the ailment usually initiates at the ages between 16 to 25 and lasts up to the end of life. Some factors can foster the risk of the disease including genetic predisposition, impaired immune system and environmental features such as the interactions to intestinal microorganisms [144]. Although, the evidence of MAP may be found in both samples from CD patients and healthy controls, MAP has frequently been found in samples from CD cases via culture, molecular, and serological assessments [144]. Some studies hypothesized that MAP is more likely to be transferred to human hosts who live in farms or have a direct contact with infected domesticated animals. However, no convincible association has been reported among the aforementioned factors and the incidence of CD in humans. In fact, the diverse environment and food sources could only increase the risk of exposure of individuals with MAP contaminated sources. However, this possibility that MAP might trigger CD as well as JD should not be ignored [144].

1.7.1 Transmission of MAP to Human via Milk and Dairy Products

MAP is an obligate intracellular pathogen that can be concealed from host immune responses through being engulfed in macrophages (a type of white blood cell) and scatter throughout the body after crossing the mucosal barriers in the small intestine [7]. In which, milk and mammary glands of the symptomatic and symptomless animals could not be excluded from the presence of MAP [153,154,172–174]. Since, milk has white blood cells as other body

fluids (such as blood), MAP can find a way to the milk stream in MAP infected animals and proliferate inside the white blood cells [114X]. On the other hand, MAP in milk and colostrum could tolerate high temperature and survive the pasteurization [175–180] convey to the pasteurized dairy products and consequently may encounter the consumers of these products with a serious risk [181].

1.7.2 Transmission of MAP via Water Sources and Insects

The MAP-infected animals shed MAP via their waste (i.e., feces, semen) into the environment and subsequently contaminate waters (ground and flowing waters). This may enhance the risk of transmitting this bacterium to humankinds and other host species [182]. As in a study, a remarkable association was seen between the prevalence of Crohn's disease in individuals from Cardiff (a city of South Wales) and the level of MAP contamination caused by sheep and cattle grazing on pastures located in hilly areas of the city [183]. Additionally, MAP has been isolated from different species of diptera (Scatophaga spp., Lucilia caesar, Calliphora vicina) that fed on the wastes of MAP-infected animals in grazing filed or sucked the fluids extracted from gastrointestinal tracts of slaughtered cases [184]. This highlights the possibility of transmitting MAP to humankinds by other routs, because the infected insects might seat on, touch, or suck every edible products such as fruits/ vegetables/ and contaminate them[115].

1.8 Control of JD by Implementing Preventive Strategies

Paratuberculosis is a chronic contagious disease that potentially involves the health status of ruminants in each cattle or herd. These characteristics in addition to the long subclinical period of the JD that retard the symptom manifestation, face the control of JD with serious concerns [185,186]. In order to reduce the risk of possible larger outbreaks, some prevention

measures should be taken into the account before any attempts could not do the trick. Of these measures the followings are considerable: estimating the rate of prevalence, detection of the infected herds, controlling the disease among the infected animals by separating the infected cases, defining the potential level of each herd in introducing the disease, rearing the young animals in aseptic condition, slaughtering the cases at clinical stage of JD, culling the positive tested animals at subclinical stage, minimizing the risk of disseminating MAP via fecal MAP- shedders into the pastures and water sources by fencing the grazing areas and water ways [187], and feeding the new born calves by milk or colostrum from Paratuberculosis-free sources [188–190]. Although, culling the subclinical and clinical MAP-infected cases is the best practical approach suppressing the disease, this strategy is not fully implementable in developing countries due to economic causes. However, the preventive approaches should put a high priority on culling and separating the animals that extremely discharge MAP via feces following with monitoring the resistant cases that have not developed symptoms or been diagnosed with MAP by necropsy analysis [48,189,191].

1.8.1 Test and Cull methodology

The implementation of some preventive strategies such as impeding the imports of animals with unknown history to other herd or cattle, adding or replacing animals from Paratuberculosis-free herds [188]; separating the new calves and lambs born from JD-positive parents; biannual and annual monitoring of lambs (sheep) or baby goats [192] and calves (cattle and buffaloes) [188,193] born from infected animals; slaughtering the female off-springs with positive serological (e.g. ELISA) or culture based tests, and eventual yearly testing of mature animals and immediate elimination of symptomless/ sub-clinical/ clinical MAP shedders [189].

1.8.2 Vaccination

One of the most practical and economical JD-preventive approaches is vaccination. This method along with diagnostic tests and cull strategies could reduce the incidence of clinical cases in each herd significantly [189,190,194,195]. However, many countries are not reluctant to include the vaccination in their JD-controlling programs excluding seven territories that have routine vaccination programs against Paratuberculosis. That is due to the fact that these vaccines are not DIVA (they can not induce the immunological protection of the host and differentiate the infected from the vaccinated animals) and interfere with serological analysis against Paratuberculosis and tuberculosis [189,196,197]. They may also interfere with skin test such as tuberculin used for the diagnosis of tuberculosis. However, DIVA vaccines have recently been developed and validated on animals. Australia has lessened the rate of Paratuberculosis through vaccination from >35% to <1% over the last 35 years, whereas Danish, Swedish and Norwegian governments totally replaced the vaccination with stamping out strategies. In the USA, a mutant vaccine is used against Patauberculosis in bovine cattle [189]. In India, native vulnerable breeds of domestic livestock are immunized through vaccination by native strain enhancing the productivity of these animals remarkably [190,198]. In addition, an in-house ELISA based on the application of two capture-antigen molecules of entire-MAP protoplasmic antigens and recombinant secretory proteins has recently been developed in India facilitating the discrimination of non-enumerated MAP-infected and vaccinated animals [199]. In fact, the presence of these undifferentiated animals may face the JD-screening programs with difficulties [189,199]. Interestingly, several subunit (e.g. immunogenic secretory proteins) or vectored dependent vaccines have been introduced that they need to undergo more verification in order to get approved and validated, since some of them could not induce higher levels of immunity against MAP as live attenuated or

killed MAP vaccines [195,200,201]. Moreover, vaccines that are made of live microorganism (MAP) reduced Paratuberculosis at the clinical stage, however they could not completely put an end to the MAP infection due to trading activates (selling or replacement) on the vaccinated animals [189]. As a big drawback, the vaccinated animals with the live microorganism (MAP) could indirectly transfer the infection to humans through the consumption of products (such as dairy, meat etc.) made by these animals [202]. In fact, the vaccines containing the killed MAP are more cost effective drawing the interest of some developing countries. However, a few numbers of killed vaccines could get approved against Paratuberculosis internationally [198,203,204]. Herein, the characteristics of standard vaccines along with a list of under developing target-specific vaccines against JD:

1) The characteristics of standard JD vaccines

- Could not hurt the animals dermally
- Reduce the level of cross reactivity resulted from the near species (e.g. between Paratuberculosis and tuberculosis) in serological diagnosis
- Could discriminate the naturally infected and vaccinated animals from each others
- Minimize the discharge of MAP via waste matter in the infected animals

2) The under developing target-specific vaccines against Paratuberculosis of domestic livestock

- Weekend but alive MAP cell
- Vaccines that undergone genetic modification steps such as deletion, haphazard mutation, and insertion
- Killed cell wall deficient (CWD) of entire MAP cell
- Vector-based vaccine: use of *M. bovis BCG* as vector to express MAP proteins
- MAP protein subunits vaccine: the lowest component of these vaccines are proteins that resulted by the rearrangement of MAP DNAs encoding the following proteins Hsp70, 74F, Ag85AA, g85BAg, 85C, SOD
- DNA vaccine: plasmid DNA encoding a crude mix of MAP proteins

In addition, the results of JD control program through vaccination based on 146 vaccines introduced in different countries revealed that these vaccines played a significant role in decreasing the incidence of Paratuberculossis in the national level [189,190].

1.8.2.1 Monitoring Parameters in Vaccination

According to the Johne's disease Integrated Program (JDIP), the animals that got vaccine shots should frequently be monitored in the following aspects [189,205]:

1.8.2.1.1 Herd Profile

Animals should be classified based on the ages (bellow 12 months, between 12 and 18 months and months, and matureness) and sex (males and female) in each herd and the vaccinated cases above 3 months years old should be monitored frequently, regardless to their sex, physical condition, and stage of JD (sub-clinical, clinical, and advanced) [189].

1.8.2.1.2 Herd's Paratuberculosis History

The state of Paratuberculosis in each herd is defined based on a combination of various factors such as JD history, death rate, severity of disease, necropsical analysis, farm observation and the rate of slaughter caused by JD [189].

1.8.2.1.3 Assessment of Animals prior Vaccination

Animals that are subjected to vaccination should be assessed by screening analyses (molecular (e.g. PCR IS*900*), immunological (ELISA), microscopic, and culture based) on their feces, blood, serum, and milk twice a year (monthly intervals) [189].

1.8.2.1.4 Monitoring Analysis after Vaccination

The vaccinated cases should be followed up within 0 to 360 days after vaccination taking into the account the parameters including health status (rates of disease and death etc.), weight and heath of reproductive system (the weight of body at the time of birth, the after birth weight, the functionality of reproductive system, etc.), physical condition (diarrhea, weakness, etc.), immunological parameters (the titers of specific antibodies in blood) and status of shedding MAP. If the vaccinated animals die during the observation period, they should be tested by necropsy analysis. In which, the presence or absence of thickness and microscopic tears related to Paratuberculosis would be checked in tissues taken from abdominal organs specifically lymph nudes intestinal mucosa [189].

1.9 The Common MAP Diagnostic Assays

MAP-infected animals initiate shedding MAP into the environment, even prior manifestation of clinical and advanced-related stages symptoms (2-6 years after infection). To manage MAP carriers impeding them not to spread the infection to Paratuberculosis-free cases, practical and definitive detective methods are required. Some of the most common diagnostic methods are described as follows [115]:

1.9.1 Detection of the Immune Response

Immune responses are induced in the MAP infected animals in various stages of JD, however by developing the disease to the clinical stage different cellular and humoral responses could be tracked in Paratuberculosis cases [115].

1.9.1.1 Cell Mediated Immunity (CMI)

There are different methods in order to assess CMI in MAP-suspected cases such as dermal

or skin testing (ST) or intradermal test [206] and interferon-gamma (INF-γ) production assay [207].

1.9.1.1.1 Skin Testing (ST)

ST is a common skin assay that is based on the delayed hypersensitivity (DHR) reactions and it has a long history in bovine tuberculosis diagnostic studies. This test is similar to tuberculin assay injecting the *M. avium* subsp. *paratuberculosis*'s extract into the intradermal layer of skin. Soon after 24 to 72 hours, MAP status (positivity/negativity) could be evaluated based on the skin irritation or thickness changes, in which the thicknesses more than 4 mm corresponded to the MAP positivity. However, ST is not an efficient technique in MAP screening programs, neither it has enough specificity (due to cross-reactivity with close mycobacterial species such as *M. bovis*) nor it can predict the status of JD in the infected cases [7,116,208,209]. In fact, ST has a moderate sensitivity and significant specificity of 54% and 79% respectively [210].

1.9.1.1.2 Interferon-gama (INF-γ) detection

Lymphocytes are a type of white blood cells that produce INF-γ in response to antigens exposure [115]. INF-γ is a key role cytokine that mediates the antibody reactivity in immunocytes and target tissues [211]. The MAP-infected animals would be equipped with specific circulating cells that flow through the blood stream in order to discover the MAP antigens and discharge remarkable amount of INF-γ at the target zone. The principle of Interferon-gama (INF-γ) assay is similar to skin test (ST), however it is carried out as two different in-vitro tests including bioassay [207] and sandwich enzyme immunoassay (EIA) [212]. While, EIA is preferentially used for INF-γ screening analysis against MAP, than bioassay, in some studies on young animals [213,214], the results revealed that EIA lacks

specificity due to probable chance of cross reactivity with other mycobacteria and inaccurate perception of the results [115].

1.9.1.2 Humoral Immune Response (HIR)

At the primary stages of Paratuberculosis, MAP stimulates the cell-mediated reactions that lead to focalizing the infection in the intestinal walls. However, no humural immunity (antibody reactivity) could be evaluated at these stages. By progressing the disease, antibody reactivity initiates (10-17 months after infection) and antibodies directed against MAP in the blood circle of infected animals could be tracked by serological tests such as Agar Gel Immunodiffusion (AGID), Enzyme-Linked Immunosurbent Assay (ELISA) and Complement Fixation Test (CFT).

1.9.1.2.1 Agar Gel Immunodiffusion (AGID)

AGID is a complementary serological assay that were firstly (1990s) executed as on MAP-infected animals above 18 months. In which, AGID-positive animals were further analyzed by fecal culture prior culling [218]. Studies on MAP infected cattle showed that AGID test has higher specificity (90%) at clinical and advanced stages, since the titers of antibodies against MAP increase significantly at these phases. However, the sensitivity of the assay drops by 30% before the symptom manifestation [210]. This depicts that AGID lacks enough sensitivity rather than ELISA and CFT [215].

1.9.1.2.2 Complement Fixation Test (CFT)

CFT is a serological assay that measure the antibodies targeted against MAP in the serum of infected animals. The principle of this method is based on the reactivity between antibody (IgM and IgG subclasses 1, 2, and 3) and antigen detecting the complement reactivity. CFT is

not a preferred method in detection of true JD-positive cases, since it has lower sensitivity and specificity than AGID and ELISA, and produces many false positive and negative results. In addition, the antigens that are used in the assay may be differed due to the diversity in antigens composition resulted by various antigen preparation steps applied in different countries [115,215].

1.9.1.2.3 Enzyme-Linked Immunosurbent Assay (ELISA)

The titers of antibodies directed against MAP in sera and milk of MAP-infected animals are commonly screened by Enzyme-Linked Immunosurbent Assay (ELISA) [216–218], since the assay is rapid, simple and economic rapidity [219–221]. However, the titers of antibodies against MAP in serum and milk of animals at primary stages of JD are that much low that induce an insignificant sensitivity to ELISA analysis (SN = 15%) [115,209,222]. In contrast, the sensitivity of ELISA significantly increases at the clinical stage of JD by 85% [210].

Milk ELISA and serum ELISA with similar functionality (Similar ranges of sensitivity 21.2% and 23.5% respectively; agreement between serum ELISA and milk ELISA: $R^2 = 0.5$, $P < 0.0001$) has been getting more and more popular among farmers, since collecting milk is not laborious and could be considered as an ordinary task in each farm [218]. Up to now, some Paratuberculosis ELISA tests have been introduced and evaluated [223] based on their competency in sensitively quantification of antibodies directed against MAP in milk samples [221]. In addition, commercial ELISA tests could comparably estimate antibody reactivity against MAP in milk as well as serum samples, as significant level of concordance was seen between milk and serum ELISA at sheep individual level [224]. However, commercial milk ELISA tests available for detection of Paratuberculosis always have some imperfections due to lack of sensitivity, in particular, if the milk comes from asymptomatic animals at early stage of JD [219,225] or lack of enough specificity in targeting the antibodies directed against

MAP and minimizing the rate of cross reactivity with close mycobacterial species [219,226]. This may underline the importance of using alternative capture-antigen molecules (as coating antigens) in ELISA that could enhance the sensitivity and specificity of the immunoassay simultaneously. Currently, two lipopeptides have been discovered specific to MAP envelope that differ based on the types of MAP strain, with the C-type and S-type subtype III [9] producing lipopentapeptide (L5P) and lipotripeptide (L3P), respectively [9,227]. These differences are due to the structure of the non-rhibosomal peptide synthetases (NRPS: encodes by mps1 gene) that assemble the non ribosome peptide moiety of the lipopeptides and differs in the number of adenylation modules from three to five in S and C types respectively [9,227]. L5P has been tested successfully in the serum ELISA diagnostic test [9,227,228]. These antigens may improve the functionality of current commercial tests being specific to MAP, readily synthesized chemically as a pure product without batch-to-batch variation and need for the pre-absorption step.

1.9.2 Detection of MAP

The detection of MAP comprises various diagnostic assays that can directly detect MAP (viable or dead) in samples. Some of these methods are as follows:

1.9.2.1 Culture

Culture as a reference test has been applied in MAP-diagnostic studies since 100 years ago estimating the incidence of viable microorganism in various type of samples such as milk, feces, and tissue [44,215]. MAP is a really slow growing bacterium and this characteristic could influence the sensitivity of method culture to minimum (30%-50%), whereas its specificity might soar to 100% [44,216,229,230]. However, the incidence of viable MAP in milk and colostrum is not comparable with specimens such as feces [9]. MAP is a fastidious

mycobacterium that could grow on the media containing the growth factor of mycobactin J (iron-chelated substance) such as Herrold's Egg Yolk Media (HEYM) [231] and modified Löwenstein-Jensen medium. The concentration of MAP in milk could be enhanced through a sample preparation step with chemical decontaminants and antibiotics, however these procedures could narrow the sensitivity of culture [44].

1.9.2.2 Radiometric Culture (BACTEC)

BACTEC is an automated blood culture system that has been improved the detection and recovery of both aerobic and anaerobic organisms from both adult and pediatric patient's specimens. This method was firstly modified to monitor the growth of *Mycobacterium tuberculosis* radioactively [115]. The system was later adapted to diagnose MAP in JD cases [232]. The adapted system characterized by specific culture media (available in the market) that were enriched with some additives that facilitate the growth of fastidious MAP cells in samples [115]. Interestingly, this system advanced in lower limit of detection (LOD) and more rapidity of the detection (7 weeks) than the other available standard culture based methods. In addition, the system would be compatible with various specimens from different species of animals such as sheep [115]. However, BACTEC based detection has a few drawbacks including costly apparatus needed for reading the culture vials and hazardous radioisotope manipulation step required for screening target MAP cells [115,233].

1.9.2.3 Quantitative Polymerase Chain Reaction (qPCR)

The quantification of MAP in milk and various specimens has been put into the practice via quantitative polymerase chain reaction (qPCR) analysis. Although, qPCR is impotent to differentiate the viable MAP cells from non-viable ones, its advanced in many features such as accessibility, replicability, speed, and economic cost. Of MAP targets (F57, IS-MAP02

and hspX) that are frequently used in qPCR analysis, insertion sequence IS*900* is more popular in MAP screening programs, since this target is not only specific to MAP but also sensitive repeated in 12-18 copies in entire MAP DNA [44,234]. As some IS*900*-based qPCR studies reached the Limit of Detection (LOD) of 1 cfu/mL, this might introduce a new perspective in early detection of JD [235,236].

1.9.2.4 Magnetic Separation

Magnetic separation (MS) is the process of magnetically separating target cells or biomolecules from a background consists of inhibitors and non-target molecules in order to purify targets reducing the background signals and facilitate the target manipulation at a condensed level [237]. The capture efficiency in MS might be influenced by the profiles of the beads (composition, size, concentration, and surface adaption) and ligand molecules used for coating the beads [238,239].

However, the nonspecific recovery of mycobacterial species other than MAP may introduce some inefficiency to MS. As some studies depicted that uncoated beads can capture mycobacteria (<10%) other than MAP in a united sample simultaneously [239]. This is possibly due to the tendency of bacteria to form an electrostatic or van der Waals bond with the superficial ions of paramagnetic beads. In addition, some nonspecific recoveries (>10%) triggered by nonspecific paratopes used for coating paramagnetic beads inducing the cross-reactivity between coating ligands and close non-target mycobacterial species [239].

Todays, advent of MS in phage assay, molecular (i.e. PCR), immunological (i.e. antigen detection immunoassay) and culture based analyses, has improved the sensitivity and specificity of diagnostic assays remarkably [238]. As MS in isolation and together with other detective techniques such as PCR and culture, are usually used as diagnostic tools in food and

veterinary microbiology-relevant studies [240] for detection and isolation of pathogenic microorganisms such as *Listeria monocytogenes* [241,242], *Salmonella* spp. [243,244], and *Escherchia coli* O157:H7 [245] in clinical samples.

Magnetic beads usually contain free carboxyl groups that could be bonded with any molecules (such as antibody, peptides, phages, etc.) that have free amine groups. According to the type of ligands (antibody or peptide) used for coating magnetic beads, MS is classified into two classes of immuomagnetic separation (IMS) and peptide-mediated magnetic separation (PMS) [239].

In immunomagnetic separation, a reciprocal reaction is created between specific antibodies (i.e. mono or polyclonal antibodies; as coating ligand) and cell surface epitopes of target bacteria [239]. The first MAP-specific-target IMS technique was developed by Grant et.al., with the aim of assessing the presence of MAP in milk samples applying sheep anti rabbit IgG type M-280 Dynabeads coated by rabbit anti-MAP IgG [246]. IMS enhanced the specificity and sensitivity of MAP-diagnostic studies, although the type of antibody used as coating ligand may narrow the efficiency of IMS [239]. As a MAP-diagnostic study revealed that using monoclonal antibodies of 6G11 and 15D10 as ligands for coating MyOne Tosylactivated Dynabeads enhanced the capture sensitivity significantly [247]. Such sensitivity and specificty were also reported in other study on detectinon of a low quantity of MAP in artificially contaminated milk samples via a monoclonal-based IMS-PCR that worked better than culture [248].

Some other works demonstrated that beads coated with polyclonal antibodies could reduce the specificity of culture-based diagnosis due to inefficient capture of non-target bacteria along with target ones [238].

On the other hand, the application of other confirmative methods such as qPCR IS*900* with IMS improved the limit of detection (LOD) to 10^3 CFU/mL compared to the higher ranges of LOD by 1 to 2 log_{10} units generated by direct PCR IS*900* on milk [249]

PMS could be followed by other techniques such as speedy phage amplification (in just 24 hours) and lengthy culture-based analysis (12-18 weeks) enumerating the number of viable targets in each sample. In addition, PMS can relieve the need for sample decontamination prior culture-based analysis remarkably [250].

Peptide-mediated magnetic separation (PMS) has a similar principle as IMS, however in PMS, antibodies are substituted with MAP specific peptides. aMptD and aMp3 are two MAP-specific complementary peptide that are commonly used as ligands for coating paramagnetic beads in MAP-PMS studies. These peptides (12-mer) were firstly discovered by phage display biopanning of MAP cells (Ph.D.-12 Phage library) and their highly purified versions are produced chemically [251,252]. aMp3- and aMptD-mediated magnetic beads could retrieve MAP in specimens containing 10^4 to 10^3 cfu/mL of the bacterium by 85% to 100% reducing the rate of cross-reactivity with close mycobacterial species to less than 1% [238]. The functionality of peptide mediated magnetic bead separation (PMS), in isolation and integrated with other confirmatory diagnostic methods such as culture, qPCR IS*900* [249], immunoassays (e.g. antigen detection immunoassay), phage assay [238] have been evaluated in few studies [253].

Recently, novel MAP-specific ligands such as biotin-EEA402 were proposed to PMS-based studies that could enhance the MAP-capture efficiency as well as aMptD and aMp3 [247]

1.9.2.5 Phage Amplification Assay

Bacteriophages are viruses that can infect specific bacteria. Fredrick Twort [254] from England was firstly discovered them, however Felix d'Herelle [255], a French Canadian scientist, characterized them precisely and named them as bacteriophages [256]. The results of genetic researches and modern genomics revealed that due to the ability of phages in transmitting and cloning genetic matters inside host bacteria, they play important roles in evolution of the microbial cells and their pathogenicity [256]. Prior the advent of antibiotic era, the bacterial infections were suppressed by phage therapy and soon after the new discovery, phages were replaced with antibiotics in the western areas for a while. However, by drastic increasing the number of antibiotic-resistant cases, the western science community has reviewed the efficiency of phage therapy in treatment of bacterial infection [256]. In addition, bacteriophages were soon harnessed in diagnostic approaches to assess the viability of bacteria in various samples, since current laboratory diagnostic methods such as PCR could not detect the viable bacteria via DNA [239]. Todays, some phage amplification commercial kits such as FASTPlaque TB™ and Actiphage are accessible in the market that can evaluate the MAP-viability in any sample types in the shortest time within 24-48 hours. These kits all have similar principles to visualize viable MAP existed in samples through introducing a lytic mycobacteriophage that could infect the viable cells and bursting the infected cells in a lawn created by *M. smegmatis* (as a fast-growing mycobacteria) [257]. That is followed by counting the number of plaques and molecular analyzing (PCR or qPCR) [258] the DNA recovered from the lysed zone (amplifying MAP-specific target sequence) [257]. Currently, the PMS step prior phage assay enhanced the specificity of detection through concentrating the target bacteria and eliminating inhibitors in various samples (inhibitors may imped reactions in PCR) [250]. In other study PMS-phage assay together with ELISA formed a phage-mediated immunoassay using polyclonal antibodies produced

against D29 to detect released progenies of phage D29 [257]. Interestingly, a modern one-day phage-magnetic separation qPCR (PhMS-qPCR) has been optimized that could detect the viable MAP in milk samples up to the $LOD_{50\%}$ of 10 MAP cells in 50 mL [259].

1.9.2.5.1 Mycobacteriophage D29

Mycobacteriophage D29 is a double-stranded, tailed lytic bacteriophage that belongs to viral order of *Cadovirales*. According to the structure and length of the tail, members of this order are classified into three families of *Myoviridae*, *Podoviridae* and *Siphoviridae.* The Mycobacteriophage D29 belongs to *Siphoviridae* family [260,261]. The results of whole genome sequencing depicts that D29 has a close affinity with L5 (a moderate mycobacteriophage) and a 3.6 kb deletion mutation in the repressor gene that induces the lysogen formation in L5, is removed in D29 [262] D29 was originally isolated from a soil sample in California [263,264] and has various host ranges from fast-growing (i.e. *M. smegmatis* [263] (saprophytic)*, M. chelonae,* and *M. fortuitum* [265]) to pathogenic slow-growing mycobacterial strains such as MAP [265], *M. tuberculosiss* [257], *M. ulcerans*, *M.scrofulaceum* [265], and *M. leprae* [266].

1.9.2.5.1.1 Life Cycle of Lytic Phages

Lytic phages are those viruses that could make hosts replicate their gentic matter releasing their progonies by bursting the host cell wall. Accordingly, their life cycle has a few steps including: 1) diffusion that phage gets in touch with its host cell [256]; 2) adsorption the distal ends of phage tails adhere to the superficial components of host species (i.e. pili, felagella, capsules, proteins, lipopolysaccharides (LPSs), and teichoic acids [267]) and adsorption happens [256] (Figure 7A); 3) injection: the phage that could firmly attach to the surface injects its DNA (located inside the capsid) into the host cell [256] (Figure 7A), 4)

replication: phage then takes the control of host replication system and makes it replicate the phage DNA through the destruction of host genome and reuse of its nucleotides [256](Figiure 7B and 7C), 5) completion of the phage structure: the phage body-parts are simultaneously produced by the host (Figure 7D), 6) assembeling: soon after placing the phage DNA inside the capsid, phage assembly occurs (Figure 7E and 7F and 7G), 7) bursting and continuing the infection: the host cell is lysed and the progenies are released and the infection continues [256] (Figure 7H).

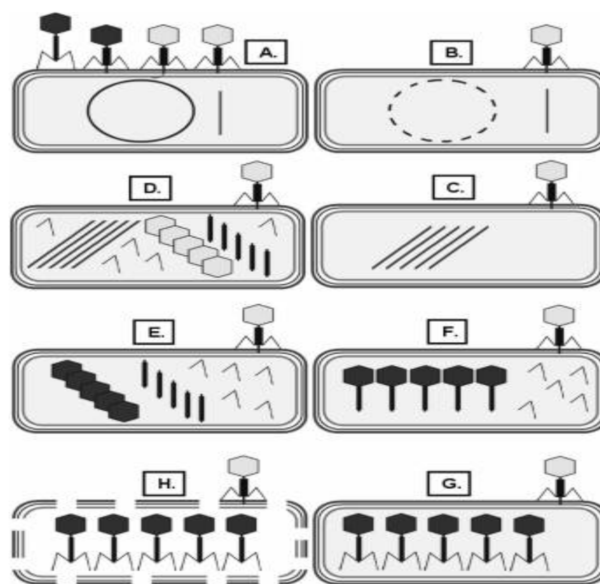

Figure 7. The life cycle of lytic bacteriophages. A) Phage adsorps the host molecule and inject its DNA; B) Phage breaks down the host DNA to reutilize the nucleotides in its DNA replication; C) Phage starts replicating its DNA; D) phage makes various parts of its structure and empty heads appears (proheads); E) Phage DNA is embedded into capsid; F) and G) Phage assemble different parts of its body; H) Host's cell wall is broken down and the newly propagated phages release from cells. The time for bursting the host cells varies but it might take at least 10 min [256]

Chapter II: Aim of the study

The footprints of MAP have been discovered in some animal and human relevant diseases. Due to the fact that the acid-fast bacterium has complicated growth requirement and could rarely be detected alive in all types of samples such as milk by conventional culture-based methods, alternative strategies are needed to speed up the identification of the restricting the chain of transmission to healthy animals and even human communities. Accordingly, this thesis has been assigned based on the three following objectives:

1) Detection of MAP and antibodies directed against it in BTMs and individual milk samples through, respectively, milk qPCR IS900 and milk ELISA analyses estimating the specificity and sensitivity of the methods using various gold standard reference models.
2) Development of an in-house milk ELISA (H-MELISA) test in order to estimate the presence of antibodies directed against two MAP surface-exposed lipopeptides of L3P and L5P and discovering the association between L3P/L5P positivity and the type of MAP strain (S/C) by PCR IS*1311* restriction enzyme analysis.
3) Speedy recovery of MAP and assessment of its viability in goat and sheep milk samples via a conventional and novel phage based analyses that work with (PMS-phage assay) and without (phage-bead qPCR) the intervention of MAP specific complementary peptides of aMp3 and aMptD.

Chapter III: Materials and methods

3.1. Bacterial Strains

Mycobacterium avium subsp. *paratuberculosis* (MAP) strain CR131 (ATCC 19698) and *Mycobacterium avium* subsp. *paratuberculosis* strain 1515 (ATCC 43015) were used as definite controls throughout the study [224]. *Mycobacterium smegmatis* strain MC^{2}155 (ATCC 700084) was also used as a negative mycobateial species to make a lawn for visualization of lysed plaques in peptide mediated phage assay. Mycobacterial species represented an optimum growth at 37 ºC and in a medium containing Middlebrook 7H9 broth (Sigma- Aldrich, Milan, Italy), 10% Oleic Albumin Dextrose Catalase (OADC; Sigma-Aldrich, Milan, Italy) [224]. To accelerate the growth rate of MAP, Mycobactin J (2 mg; Allied Monitor, Fayette, MO, USA) as an iron-chelated growth factor was just added into MAP culture.

3.2. Phage Strains

The efficiency of two mycobacteriophage D29 strains in detection of viable MAP was assessed in peptide-mediated magnetic separation (PMS) phage assay. One of them was purchased from the University of Laval in Canada and another came with a commercial phage assay kit named Actiphage (Actiphage, UK, England). Laval D29 produced lysed plaque that were almost 1 mm, whereas D29 Actiphage plaques were characterized with distinctive circles that sized between 3-4 mm. However, since Laval D29 did not fulfill the considered prerequisites in PMS-phage assay, D29 from Actiphage kit was selected to be used throughout this study. To reach the working concentration of 10^9 pfu/mL, the phage was propagated as described before [259] and stored at 4 ºC until use.

3.3. Sample Collection

A total of 301 milk samples were collected and dedicated to the following studies (Table 4). Hands and tits were sanitized before collecting milk samples followed by preserving the specimens at 4 ºC during transportation. The aliquots that were subjected to phage assay stored at 4 ºC overnight to be tested a day after. Blood samples were also drained from jugular veins, dispensed into sodium heparin vacutainer tubes (Becton Dickinson (BD), Milan, Italy), transferred to the diagnostic laboratory at RT, and underwent the process of serum separation.

Table 4. Number of unpasteurized milk and blood samples and their animal sources

Number of Samples/ Times of Sampling	Type of Sample	Date of Sampling
73 (14 out of these 73 samples were checked twice)	Bulk Tank Milk (BTM)	23.07.2018 to 25.07.2019
16/ Once	Individual milk samples from asymptomatic bovines (for optimization of PMS-phage assay via Actiphage D29)	18.02.2020
14/ Once	Individual milk samples from a MAP-infected flock (MIF) of sheep (for optimization of PMS-phage assay via Laval mycobacteriophage D29)	07.07.2020
128/ Once	Individual milk samples collected from a MAP infected flock (MIF) of sheep	10.04.2019 to 23.09.2019
20 / Once	Individual milk and blood samples from asymptomatic goats	10.05.2021
8/ Once	Individual milk and blood samples from asymptomatic sheep	12.04.2021 to 26.04.2021
21/ Twice	Individual milk and blood samples from asymptomatic sheep	12.04.2021 to 31.05.2021

3.4. Milk Culture

MAP viability in milk samples was assessed through a modified culture analysis. Briefly, 25 to 30 mL of the samples (depending on the provided volumes) was centrifuged at 5300× g and 4 °C for 30 min. Then, the whey part was discarded; both cream and pellet [32] fractions resuspended in 25 to 30 mL hexadecylepyridinium chloride (HPC; 0.75%), agitated properly and incubated at RT for 4 hours [32]. Treatment with HPC, a chemical decontaminant, could enhance the recovery of MAP from cream fraction [268] and reduce the chance of growing

microorganisms other than mycobacteria on the media [269]. The samples were again centrifuged at 5300 × g and 4° C for 30 min. After that, supernatant was removed and pellet was resuspended in 1 mL 1× phosphate-buffered saline (PBS; pH = 7.5). Subsequently, aliquots of suspensions (200 µL) were spread on Middlebrook (MB; Sigma-Aldrich, Milan, Italy) 7H10 containing 10% Oleic Albumin Dextrose Catalase (OADC; Sigma-Aldrich, Milan, Italy) and Mycobactin J (2 mg/L; Allied Monitor, Fayette, MO, USA) following an incubation at 37 ºC for 6 to 12 weeks. The plates were observed frequently and Ziehl-Neelsen (ZN) stain was used to detect acid-fast bacilli [269]. Later, DNA was extracted from ZN-positive colonies and used as templates for qPCR IS*900* and PCR IS*1311* analyses.

3.5. DNA extraction from colonies, milk, and lysed plaques

Milk samples that were cultured on MB 7H10 were observed frequently and the positive Ziehl-Neelsen (ZN)-positive single colonies underwent further molecular inspection. In which, colonies were harvested, suspended in 1 mL 1× PBS (pH = 7.4), and centrifuged at 5300× g at 4 °C for 30 min. Then, supernatant was decanted and DNA was extracted from pellets using RTP Mycobacteria kit [224] (Stratec kit, Stratec Molecular GmbH, Berlin, Germany) according to the manufacture instruction for the extraction of DNA from sputum samples (Protocol 1).

DNA was extracted from 5 mL aliquots of each milk sample. Samples were allowed to reach the room temperature (RT) before the experiment and diluted in 25 mL 1× PBS (pH = 7.4). The, they were centrifuged at 5300× g rpm and 4 ºC for 30 min [224]. Then, the whey phase was decanted; the cream and pellet portions were recovered, resuspended in 6 mL of hexadecylpyridinium chloride (HPC: Sigma-Aldrich, Milan, Italy; 0.75% w/v), mixed thoroughly by vortex, and incubated at RT for 1 h. Then, samples were centrifuged at 5300×

g at 15 ºC for 20 min and followed by supernatant removal step. Later, pellets were resuspended in 1 mL 1× PBS (pH = 7.4), uniformed by ribolyzer using glass beads (Sigma-Aldrich, Milan, Italy; diameter of 3 mm) for 4 cycles of 45 s at 4 m/s [224]. The homogenization step was aimed to liberate MAP cells from somatic cells [174,270]. Then, this suspension was centrifuged at 10,000× g rpm and 4 ◦C for 15 min, and DNA was extracted from the pellet using Norgen Kit (Norgen Biotek Corp., Thorold, ON, Canada) or RTP Mycobacteria kit (Stratec kit, Stratec Molecular GmbH, Berlin, Germany) [224]. DNAs extracted from milk samples using RTP Mycobacteria DNA extraction kit subjecting to several modifications as follows: 1× PBS (pH = 7.4) was substituted for NAC buffer; incubation times at 95 ◦C (15 min) and 65 ◦C (10 min) were increased to 30 and 20 min, respectively; and the column centrifugation steps were extended by 2 min based on the density of samples [224]. Due to the reason that Stratec Molecular GmbH stopped manufacturing the RTP kit, DNAs were extracted from some milk samples using Norgen Kit according to the factory instruction for unknown or gram positive bacteria

Regarding the lysed plaques developed in peptide-mediated magnetic separation (PMS) phage assay, DNA was extracted from the plaques using freeze-squeeze method [271]. In which, plaques developed on MB 7H10 agar were excised (1-10) and were placed on a 200 µL-filter tip fitted in a 1.5 mL microcentrifuge tube. Then, tubes were stored at -80 ºC for 5 min and immediately centrifuged at highest speed (16000 ×g) for 3 min. The filtrate was transferred into a new microcentrifuge tube and stored at -28 ºC to be analyzed by qPCR analysis [271].

3.6. qPCR IS*900* analysis on DNAs extracted from milk, colonies, and lysed plaques

Depending on the aims of studies presented in this thesis, the quantification of target sequence IS*900* was carried out through qPCR analysis via Syber or TaqMan-probe using different sets of primers.

In non-probe based qPCR analysis via Syber, the primer set of AV1 and AV2 (Sigma-Aldrich, Milan, Italy) was selected to amplify the insertion sequence 900 in samples. The master mix contained 10 µL ×10 SYBR Select Master Mix, 0.2 µM of each of the primers AV1 and AV2, and water up to finial level of 20 µL. Subsequently, 20-100 ng of DNA was added to each reaction [224]. The amplification was done under the following circumstance: initial denaturation at 95 ºC for 3 min, followed by 50 cycles of denaturation at 95 ◦C for 40 s, annealing at 68 ºC for 40 s, and extension at 72 ºC for 40 s, with a final extension at 72 ºC for 5 min [224].

TaqMan-probe was used for amplification of DNA extracted from phage assay, to which reactions contained 10 µL ×2 master mix (QuantiFast Probe PCR Kits, Milan, Italy), 0.3 µM of each primer of IS*900*-F and IS*900*-R (Sigma-Aldrich, Milan, Italy; Table 5), 0.15 µM IS*900* TaqMan prob (labeled with FAM; Table 5), 0.2 µL exogenous DNA as internal amplification control 0.5× (IAC), 1 µL mixed primer and probe for IAC 0.5× (labeled with VIC), and PCR grade water up to the final quantity of 20 µL. Later, DNA template was added to each reaction at the concentration of 20–100 ng [224]. Positive (*Mycobacterium avium* subsp. *paratuberculosis* strain CR131) and negative controls (water and Master Mix) were assigned in all qPCR analyses. Accordingly, the amplification was performed under the following condition: initial denaturation at 95 ºC for 15 min, followed by 50 cycles of denaturation at 95 ºC for 15 s and annealing at 60 ºC for 1 min.

Table 5. Primers and their sequences used in qPCR analysis

Primers and Probe	Sequences
IS*900*-F (AV1)	5'-ATGTGGTTGCTGTGTTGGATGG- 3'[224]
IS*900*-R (AV2)	5'-CCGCCGCAATCAACTCCAG- 3'[224]
IS*900*-F	5' -CCGGTAAGGCCGACCATTA- 3'[272]
IS*900*-R	5' -ACCCGCTGCGAGAGCA- 3'[272]
IS*900* Probe	6FAM-CATGGTTATTAACGACGACGCGCAGC- TAMRA[272]
P90	5' -GAAGGGTGTTCGGGGCCGTCGCTTAGG- 3'[259]
P91	5' -GGCGTTGAGGTCGATCGCCCACGTGAC- 3' [259]

3.7. Restriction Enzyme Analysis (REA) on IS*1311*-targeted PCR Products and Strain Typing (S- or C-class)

Insertion sequence IS*1311* was targeted in seven colonies and fifty-three milk DNAs (including 34 BTMs and 19 MIF milk DNAs) that were IS*900*-positive and amplified by conventional PCR using primer set of IS*1311*-F and IS*1311*-R. The reaction mixture consisted of 0.2 µM of each primer (Table 6), 200 µM of each dATP, dCTP, dGTP, and dTTP, 1× PCR buffer, 1.5 mM $MgCl_2$, 3 µL of DNA template, and PCR grade water up to the final quantity of 20 µL [273]. The PCR condition was as follows: initial denaturation at 94 °C for 3 min, followed by 35 cycles of denaturation at 94 °C for 30 S, annealing at 60 °C for 30 S, and extension at 72 °C for 1 min, with a final extension at 72 °C for 10 min [274]. Eventually, IS*1311*-positive products (608-bp bands on gel-electrophoresis (2%)) were subjected to restriction enzyme analysis using hinf-1. Briefly, 10-13 µL of amplicon (depending on the strength of bands in visualization step) was added into a master mix including 2 µL Restriction Buffer 10× (RB), 0.2 µL Bovine Serum Albumin (BSA), 0.5 µL Restriction Enzyme (RE) and water up to the final concentration of 20 µL. This was followed by incubation of samples at 37 ºC for 2 h and visualization by gel-electrophoresis (3%).

Table 6. The sequences of primer set used for amplification of target sequence IS1311

Primers	Sequences
IS*1311*-F (M56)	5' -GCGTGAGGCTCTGTGGTGAA- 3' [273]
IS*1311*-R (M119)	5' -ATGACGACCGCTTGGGAGAC- 3'[273]

3.8. Separation of serum from blood samples and preparation of milk samples for ELISA analysis

After receiving blood samples in diagnostic laboratory, samples were incubated at RT for 1 hour to be settled down. Then, they were centrifuged at 2500 rpm and 4 ºC for 15 min; serum was separated from blood cells and stored at –28 ºC [275].

To remove inhibitors such as lipids (cream) and somatic cells (pellet), milk samples were centrifuged at 10,000× g and 4 °C for 2 min, and then the whey phase, the liquid between the cream and pellet, was aspirated into a new Eppendorf tube (1.5 mL) and stored at −28 °C [224].

3.9. Commercial Milk and Serum ELISA

Antibodies induced against MAP in milk and serum samples were evaluated by an indirect commercial ELISA kit (IDEXX Laboratories, Westbrook, ME, USA) according to the factory instruction [224].

3.10. In-house milk ELISA (H-MELISA) on BTMs and individual milk samples (MIF) using L3P and L5P epitopes

Capture antigens of L3P and L5P were synthesized manually on a solid phase using Fmoc chemistry as described before [9,276]. In brief, MAP-specific lipopeptides, L3P and L5P (Table 7) were reconstituted in Ethanol 99.8% (Sigma-Aldrich, Milan, Italy), diluted in 0.05 M carbonate-bicarbonate buffer (Sigma-Aldrich; pH: 9.5) at a final concentration of 10 µg/mL, and 50 µL of them was used for coating each well of 96-well plates. Then, plates were stored at room temperature (RT) overnight to be air-dried completely. At the next step, plates were coated with 100 µL PBS/0.5% (w/v) gelatin (produced from cold water fish skin; Sigma-Aldrich, Milan, Italy) and stored at 37 ºC for 1 hour. Later, plates were washed 5

times with 200 µL PBS-Tween (PBST; 0.05%) and charged with 100 µL of diluted milk samples diluted in PBS (1:2). Then, samples were homogenized using an orbital shaker (50 rpm/5 min)[224] and incubated at 37 ºC for 90 min. In addition, positive and negative controls that came with IDEXX kit were included in the analysis. Arachidic acid as the second negative control was also applied in order to resemble and monitor the reactivity of lipid moiety of the lipopeptides (L3P/L5P) in response to lipid structures in milk samples. The controls were diluted in PBS-Tween (0.05%) at the final concentration of 1:20 diluted. Later on, plates were washed 5 times with 200 µL PBS-Tween (0.05%), charged with 100 µL Anti sheep IgG H&L (HRP) (1:150000, abcam6900), and incubated at 37 ºC for 1 h. After that plates were washed 5 times with PBS-Tween 0.05%, 100 µl substrate containing TMB (3,3', 5,5'-tetramethylbenzidine; abcam 171522) was added to each well, and in plates were incubated at RT for 13 min consequently. At the end, the reaction was stopped by adding 100 µL of stop solution containing 5% Methanesulphonic acid (abcam 171529) and ODs were measured at 450 nm (SpectraMAX Plus384).

Table 7. MAP epitopes used as coating antigen in H-MELISA analyses and their sequences

Peptide	Sequence
Lipotripeptide (L3P)	CH_3-$(CH_2)_{18}$-CONH-D-Phe-L-NMe-Val-L-Ala-OCH_3 [276]
Lipopentapeptide (L5P)	CH_3-$(CH_2)_{18}$-CONH-D-Phe-L-NMe-Val-L-Ile-L-Phe-L-Ala-OCH_3 [276]

3.11. Preparation of peptides-mediated magnetic beads using two MAP-complementary peptides of aMp3 and aMptD

Dynabeads® MyOne ™ Tosylactivated (Thermo Fisher, Life Technologies, Milan, Italy, Code 65501) were separately coated with MAP-complementary peptides of aMp3 and aMptD according to the manufacture's instruction as described before [277]. Briefly, 250 µL of the beads were washed twice with Sodium Borate 0.1 M (as coating buffer; pH = 9.5), and resuspended (100 µL) in the same buffer. The aMp3 or aMptD peptides (Table 8) were added

(0.25 μg/mL [278]) to the retrieved beads and the suspension equilibrated with coating buffer up to the final volume of 895 μL mixing properly. Later, ammonium sulfate 3M (415 μL) was added to the mix and vortexed thoroughly, and the suspension was incubated at 37 ºC overnight rotating (10-20 rpm) continually. A day after, the coated beads were washed twice with 1 mL 1× PBS following the resuspension of retrieved beads in 500 μL 1× PBS (without blocking buffer). The already prepared capture beads were stored at 4 ºC until use.

Table 8. Capture peptides used for coating Dynabeads® MyOne ™ Tosylactivated and their sequences

Peptide Name	Sequence
aMp3	NYVIHDVPRHPA [251]
aMptD	GHNHHHQHHRPQ [252]

3.12. Optimization of peptide-mediated magnetic separation (PMS) Phage Assay on artificially MAP-contaminated milk samples and validation of the method on natural unpasteurized milk samples

Aliquots of a known-MAP-negative commercial bovine milk sample (9 mL) were spiked with different dilutions of MAP stain CR131 (1 mL; the optical density of stock was adjusted at 0.2 corresponding the concentration of 10^7 cfu/mL), agitated by vortex, and incubated at 37 ºC for 30 min. Then, samples were centrifuged at 2500× g and 4 ºC for 15 min, cream and whey phases were carefully decanted, pellet was resuspended in 1 mL Middlebrook 7H9 broth and sonicated at 37 KHz and 10° C for 4 min. Negative and positive controls were included from the initial step as before. Then, samples were transferred into eppendorfs (2 mL) and 5 μL of each peptide-mediated beads (with aMptD or aMp3) were added to each sample. Later, samples were agitated for 30 min by rotator (Stuart) at RT and placed on a magnetic rack for 10 min. Subsequently, liquid was aspirated and MAP-captured beads were washed three times with PBS-Tween 20 (0.05%) while each recovering step took 2 min. The retrieved beads were resuspended in 1 mL MB 7H9 (contained 10% OADC and 2 mM

$CaCl_2$), transferred into flip-top vials, and incubated at 37 ºC overnight (18 h). A day after, captured MAP cells were infected by mycobacteriophage D29 at final concentration of 10^8 cfu/mL (100 µL) and samples were incubated at 37 ºC for another 2 hours. Later, exogenous phages that could not take part in the infection step were inactivated adding 100 µL ferrous ammonium sulfate (100 mM) to each sample following a continues rotation step at RT for 10 min. Consequently, FAS was neutralized adding 5 mL MB 7H9 (contained 10% OADC and 2 mM $CaCl_2$) and samples were incubated at 37 ºC for 90 min. To visualize the infected cells characterized by lysed plaques that surrounded by a lawn, 1 mL *M. smegmatis* at concentration of 10^8 cfu/mL (OD = 0.7-1) was added to each sample. Eventually, the suspensions were cultured in petri dishes with 5 mL 55 ºC-MB 7H10 agar, solidified at RT for 30 min, and incubated at 37 ºC for the next 18 hours.

In regard to unpasteurized sheep milk samples, 10 mL milk aliquots incubated, respectively, at RT/1 hour and 37 ºC/ 30 min, and assayed as described in optimization step.

3.13. Preparation of phage D29-beads

Mycobacteriophage D29 was used as ligand for coating magnetic beads as descried by Foddai and Grant [259] in their recent publication. Briefly, 10 mg Dynabeads® MyOne ™ Tosylactivated (Thermo Fisher, code 65501, Milan, Italy) were transferred into eppendorf (2 mL), washed two times with 1mL sodium carbonate decahydrate buffer at concentration of 0.1 M and pH = 9.5 (VWR, Milan, Italy) as binding buffer, and magnetically recovered. Then, beads were resuspended at the same binding buffer, exposed to mycobacteriophage D29 (Actiphage, UK, England) at the concentration of 10^8 pfu/mL, and incubated at 37 ºC overnight rotating (10-20 rpm) continually. A day after, beads were recovered magnetically, washed two times with the binding buffer, and resuspended in Middle Brook 7H9 medium supplemented with 10% OADC and 2mM $CaCl_2$. At the end, the phage-bead suspension was

stored at 4 ºC and only fifteen minutes prior inoculation transferred into the room temperature in order to be equilibrated with this temperature.

3.14. Optimization of phage beads on artificially MAP-contaminated milk samples and evaluating their functionality on unpasteurized milk samples

MAP suspension (strain CR131) at stationary phase was de-clumped using sonicator at 37 KHz and 10° C for 4 min and its concentration was adjusted at optical density of 0.8 (10^8 cfu/mL) at 600 nm. Then, this stuck was serially diluted in 8 folds, and 1 mL of dilutions containing 10^4 to 10^1 cfu/mL were used for spiking a known negative commercial bovine milk sample (9 mL). Artificially contaminated milk samples were mixed thoroughly, incubated at 37 ºC for 30 min, and centrifuged at 2500 ×g and 4º C for 15 min consequently. To monitor the functionality of the assay and any carryover contaminations respectively, positive (MAP) and negative controls (PBS) were included from the beginning of each analysis. Later, supernatant containing cream and whey were decanted, and pellet was resuspended in 1 mL MB 7H9 (supplemented with 10% OADC and 2mM $CaCl_2$). At the next step, phage beads (15 µL) were added to each sample and incubated at 37 ºC while rotating (10-20 rpm) for 30 min. After two washing steps with 1 mL PBST (0.05%), beads were magnetically recovered, resuspended in 50 µL MB 7H9 (supplemented with 10% OADC and 2mM $CaCl_2$), and incubated at 37 ºC without agitation. Then, samples were heated to 55 ºC/2min and centrifuged at 10000 ×g and RT for 1 min. At the end, supernatant containing DNA was aspirated and transferred into new PCR micro tubes and stored at 4 ºC for short time or -20 ºC for longer period. Regarding the unpasteurized milk samples, 10 mL of each sample were incubated at RT and 37º C, respectively, for 1 hour and 30 min and underwent the same procedure as described before in optimization step.

Chapter IV: Results

4.1. Detection of *Mycobacterium avium* subsp. *paratuberculosis* (MAP) in Sheep Milk

4.1.1. Statistical Analysis

To evaluate the sensitivity and specificity of each milk assay (milk qPCR and milk ELISA) receiver operating characteristic (ROC) curve and area under the curve (AUC) were carried out (R software). In the MIF group, serum ELISA and fecal PCR independently and together formed (individuals with at least one positive test were considered positive) were considered as binary reference models [279,280]. Whereas milk ELISA in isolation for milk qPCR data set, milk qPCR in isolation for milk ELISA dataset, and both milk qPCR-milk ELISA as a united model for each of milk qPCR and milk ELISA were considered as gold standard models (herds with only one milk assay (MqPCR or MELISA) considered positive) at BTM level [279]. To understand how much different the diagnostic assays are dependent Chi-square was performed (Graphpad Prism 8) [224].

4.1.2. BTM qPCR

71.62% out of 73 bulk tank milk (BTM) samples contained detectable concentration of MAP DNA via milk qPCR (MqPCR). The positivity ratio ranged between 13 to 38 cycles, corresponding to the DNA concentration of 1.05 × 102 ng/μL > C < 5.25 × 10−6 ng/μL [224]. The sensitivity and specificity of MqPCR was considerable when both milk qPCR and milk ELISA together was the reference model (Approach one: AUC = 0.97, Control vs MAP-infected, cutoff = 6.58, sensitivity: 0.95, specificity: 1, p < 0.0001; Figure 8A) compared to the time milk ELISA (MELISA) in isolation was the gold standard (Approach three: AUC = 0.622, control vs MAP-infected, cutoff = 35.42, sensitivity: 0.5, specificity: 0.79, p = 0.098; Figure 8B) [224]. The pattern of milk qPCR positivity was changed based by season, so that

positivity rate soared in spring (45.21%) and minimized in winter (5.48%) (Figure 9) [224]. In addition, our longitudinal survey on 14 herds with over two instances of sampling (BTM) showed that 21.43% of samples were firstly MqPCR-negative, but then became positive; 28.57% and 7.14% were MqPCR-positive and -negative, respectively, over two times sampling. In contrast, some samples primarily were MqPCR-positive (42.86%) but became negative at the second time (Figure 10, Table 9) [224]. The mentioned result confirmed that some infected animals discharge MAP intermittently [224].

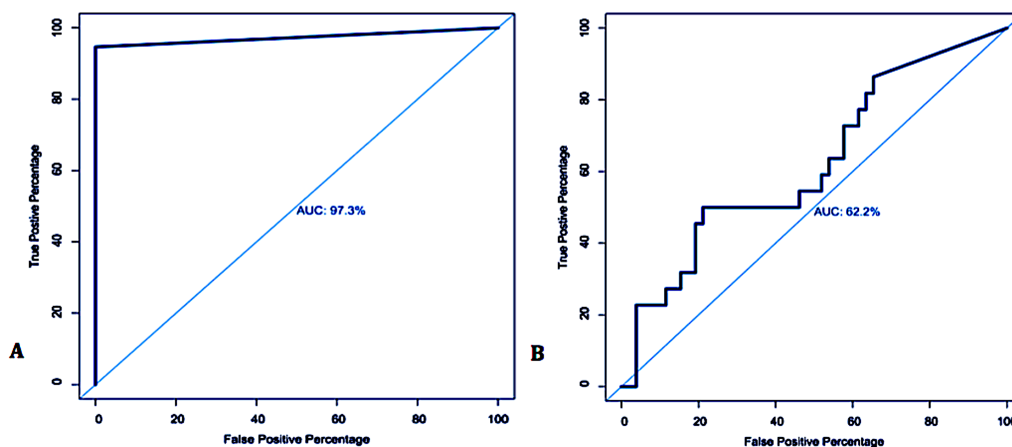

Figure 8. Receiver operating characteristic (ROC) curve and area under the curve (AUC) analyses on the MqPCR dataset under the condition that the reference models were adjusted based on MqPCR and MELISA (**A**) and MELISA (**B**), respectively [224].

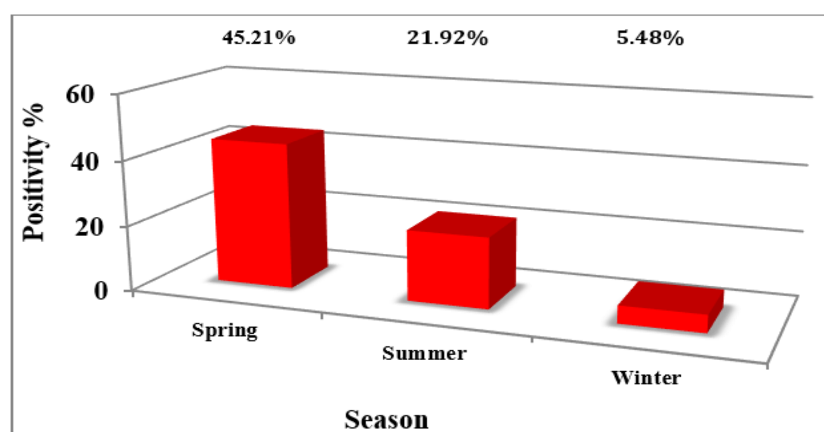

Figure 9. The placement of MqPCR-positive BTMs in three different seasons: spring (45.21%), summer (21.92%), and winter (5.48%) [224].

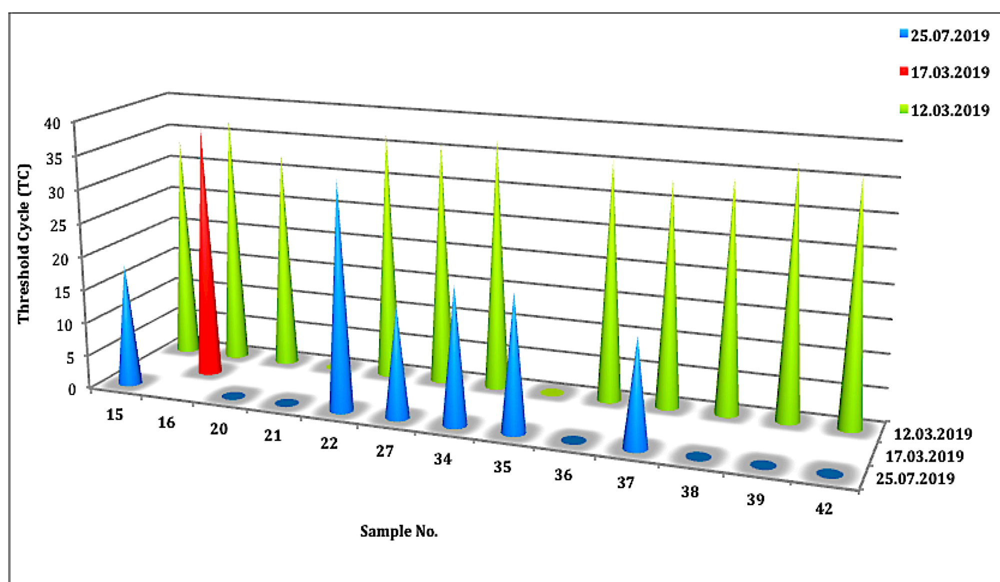

Figure 10. Threshold cycle (TC) changes of BTMs over MqPCR analysis on 14 sheep herds in a longitudinal study (two instances of sampling). [224].

Table 9. The placement of BTMs from 14 sheep herds (28 BTMs) in four classes based on MqPCR status (positive/negative) in a longitudinal study [224].

Samples	TC%
MqPCR was first negative, then positive	21.43%
MqPCR was positive in both rounds of sampling	28.57%
MqPCR was negative in both rounds of sampling	7.14%
MqPCR was first positive, then negative	42.86%

4.1.3. BTM ELISA

ELISA on 15 whole and fractionated BTMs depicted that by eliminating the portions of milk samples that contain inhibitors (cream and pellet), sample-to-positive ratios (S/P%) enhance by 0.3 to 15 degrees (Mean~7) (Figure 11, Table 10) [224].

Among 73 BTMs were tested by MELISA, only 29.7% had significant concentrations of antibodies against MAP. MELISA had a moderate sensitivity and remarkable specifity when both MqPCR and MELISA was binary reference model (AUC = 0.73, control vs MAP-infected, cutoff = 13.94, sensitivity: 0.59, specificity: 0.89, p = 0.00035; Figure 12A). In addition, MqPCR induced higher specificity rather than sensitivity to MELISA (AUC = 0.656, control vs MAP-infected, cutoff = 33.03, sensitivity: 0.34, specificity: 0.95, p = 0.037; Figure 12B). The comparison among MELISA results of these 73 BTMs in different season

depicted that the highest MELISA-positive cases happened in summer (17.81%), whereas the winter had the least positive cases (2.74%) (Figure 13) [224]. Over two time sampling of 14 herds 14.28% and 57.14% were MELISA-positive and -negative, respectively, in both assessments. Some samples detected negative by MELISA (28.57%) at first, but became positive later (Figure 14, Table 11). The result of this analysis confirmed that the antibody levels changed by season from 1.3% to 60.4% in S/P% soaring in summer.

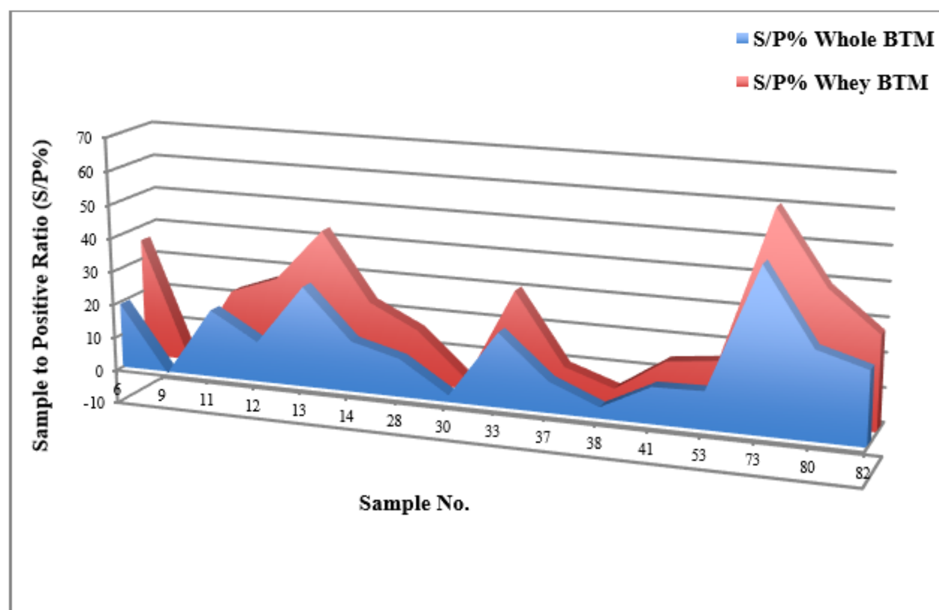

Figure 11. MELISA sample-to-positive ratio (S/P%) of 16 BTMs before and after fractionating milk samples [224].

Table 10. Comparison between MELISA sample-to-positive ratio (S/P%) of 16 BTMs before and after fractionating milk samples [224].

Sample No.	Whole BTM S/P%	Whey BTM S/P%
6	19.33609959	35.64315353
9 *	−0.497925311	−0.082987552
11	20.08298755	22.44813278
12	11.90871369	27.63485477
13	29.70954357	43.15352697
14	14.97925311	22.98755187
28	11.24481328	15.97510373
30	2.033195021	2.780082988
33	21.82572614	30.45643154
37	9.211618257	9.543568465
38	3.278008299	4.647302905
41	10.66390041	14.10788382
53	11.0373444	15.72614108
73	47.71784232	60.24896266

80	25.6846473	39.04564315
82	21.45228216	27.38589212

* Sample 9 was a known negative commercial BTM.

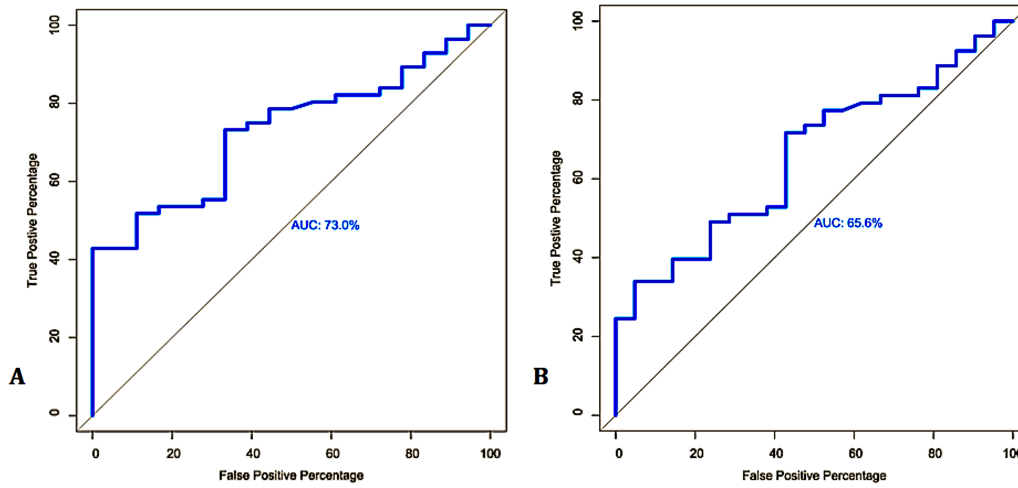

Figure 12. Receiver operating characteristic (ROC) curve and area under the curve (AUC) analyses on MELISA dataset when MqPCR and MELISA (**A**) and MqPCR (**B**) were considered as the reference models [224].

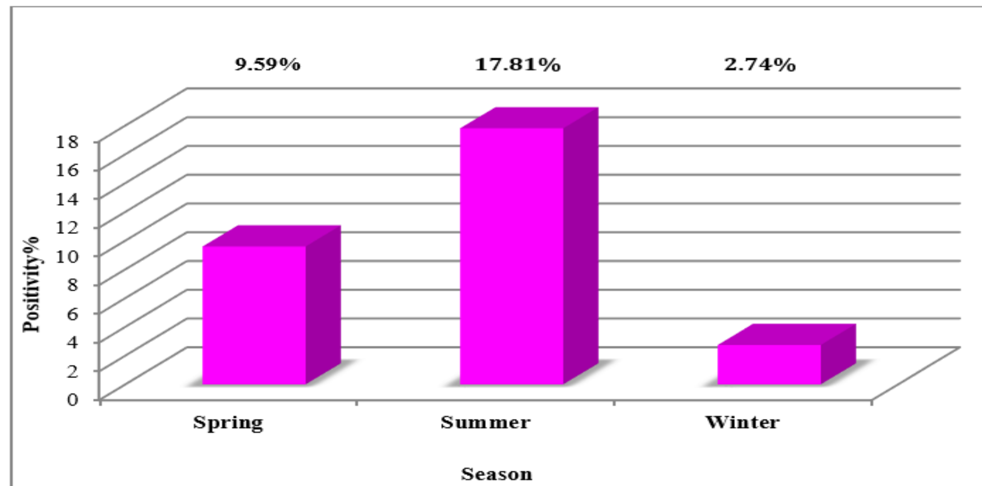

Figure 13. Distribution of MELISA-positive BTMs in three different seasons: spring (9.59%), summer (17.81%), and winter (2.74%) [224].

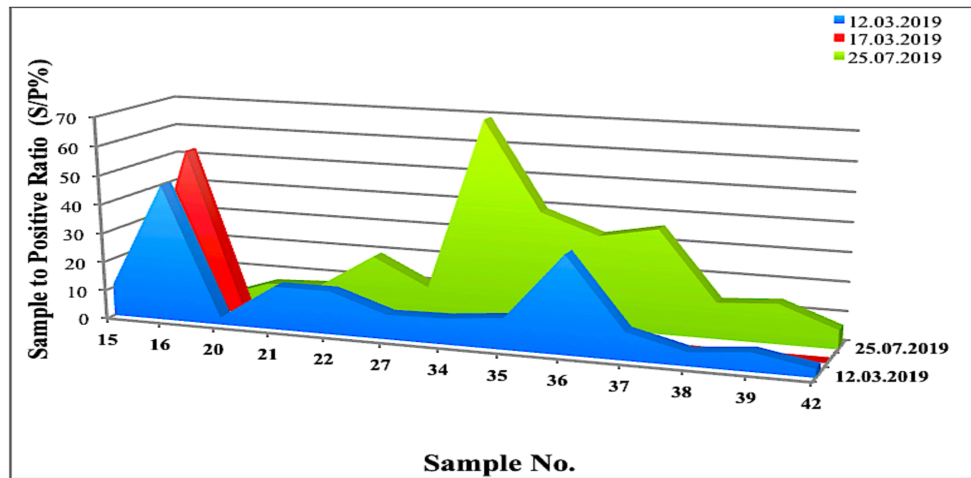

Figure 14. Changes in the MELISA sample-to-positive ratio (S/P%) in a longitudinal study (28 BTMs from 14 sheep herds) [224].

Table 11. MELISA status (positive/negative) of BTMs from 14 sheep herds in a longitudinal study [224].

Samples	Results (%)
MELISA was first negative, then positive	28.57%
MELISA was positive in both rounds of sampling	14.28%
MELISA was negative in both rounds of sampling	57.14%

The Chi-square test showed a significant correlation between MqPCR and MELISA: X^2 (1, n = 73) = 2.99, $p < 0.1$ (26.03% positive (Pos) (MqPCR and MELISA), 46.6% Pos (MqPCR) and negative (Neg) (MELISA), 23.3% Neg (MqPCR and MELISA) and 4.11% Neg (MqPCR) and Pos (MELISA) (Figure 15, Table 12).

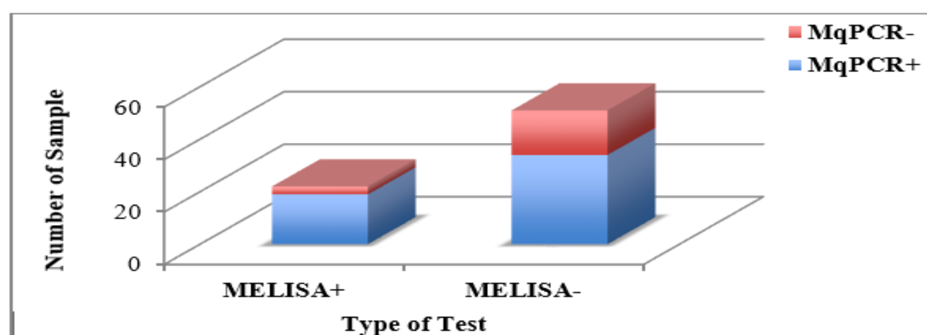

Figure 15. The distribution of 73 BTM samples classified into four binary groups based on the positive/negative status in the MqPCR and MELISA tests. Pos (MqPCR) and Neg (MELISA) constituted the main proportion of samples (46.58%), followed by 26.03% Pos (MqPCR and MELISA), 23.3% Neg (MqPCR and MELISA), and 4.11% Neg (MqPCR) and Pos (MELISA). Pos: positive; Neg: negative [224].

Table 12. Distribution of 73 BTMs based on the positivity/negativity status in MqPCR and MELISA tests and corresponding *p*-values [224].

	MELISA+	MELISA−
MqPCR+	19	34
MqPCR−	3	17
p-value ($p < 0.1$) *	0.083	
p-value ($p < 0.05$)	Insignificant (IS)	

* Since the dependency was insignificant at $p < 0.05$, the statistical significance was adjusted for $p < 0.1$.

4.1.4. MIF MqPCR and MELISA

Of the 128 MAP-infected flock milk samples, 19.53% and 80.47% were detected as being MqPCR-positive and -negative, respectively. The positivity ratio ranged between 16 and 46 cycles (TC), corresponding to a DNA concentration of 1.05×10^2 ng/µL > C < 5.25×10^{-6} ng/µL (Figure 16A). MELISA also produced positivity (21.09%) and negativity (78.91%) rates close to those of MqPCR, whereas the MELISA S/P% ranged from 31.93% to 157.11% (Figure 16B). ROC curve analysis was carried out by comparing the sensitivity (SN) and specificity (SP) of MqPCR and MELISA in various cutoffs based on three different binary reference models. When both SELISA and FPCR were used as the reference model, MELISA was more sensitive and specific (MELISA; AUC = 0.77, control vs MAP-infected, cutoff = 26.72, sensitivity: 0.61, specificity: 0.95, $p < 0.0001$; Figure 17A) than MqPCR (MqPCR; AUC = 0.61, control vs MAP-infected, cutoff = 8.03, sensitivity: 0.4, specificity: 0.87, $p = 0.047$; Figure 17B). MELISA also showed the highest sensitivity and specificity when the binary reference model was based on SELISA only (MELISA; AUC = 0.87, control vs MAP-infected, cutoff = 26.72, sensitivity: 0.75, specificity: 0.94, $p < 0.0001$; Figure 17C) compared to MqPCR (MqPCR; AUC = 0.6, control vs MAP-infected, cutoff = 24.325, sensitivity: 0.36, specificity: 0.86, $p = 0.1$; Figure 17D). However, when the reference model was based on FPCR, the specificity of MELISA slightly dropped by 0.12 (MELISA; AUC = 0.62, control vs MAP-infected, cutoff = 8.20, sensitivity: 0.67, specificity: 0.72, $p = 0.129$;

Figure 17E) compared to MqPCR (MqPCR; AUC = 0.66, control vs MAP-infected, cutoff = 8.03, sensitivity: 0.47, specificity: 0.84, $p = 0.044$; Figure 17F).

According to the positive/negative status of samples from the four tests of MELISA, MqPCR, SELISA, and FPCR, the animals were stratified into 15 quaternary groups. A dominant number of samples (58%) were detected as being negative by all tests (MqPCR, MELISA, SELISA, and FPCR), compared to only 2% that were positive by all tests (Figure 18, Table 13). In another classification, the studied animals were classified into 24 binary groups based on the MAP status (positivity/negativity) of samples analyzed by each binary test of MqPCR and MELISA, MELISA and SELISA, MqPCR and FPCR, MELISA and FPCR, and SELISA and FPCR. Accordingly, Chi-square analysis was performed on each binary group. The proportion of samples in each category was as follows: 74.22% Neg (MqPCR and FPCR), 73.44% Neg (MELISA and SELISA), 72.66% Neg (MELISA and FPCR), 71.88% Neg (SELISA and FPCR), 67.19% Neg (MqPCR and MELISA), 66.41% Neg (MqPCR and SELISA), 7.8% Pos (MqPCR and MELISA), 13.3% Neg (MqPCR) and Pos (MELISA), 11.72% Pos (MqPCR) and Neg (MELISA), 16.4% Pos (MELISA and SELISA), 5.5% Neg (MELISA) and Pos (SELISA), 4.7% Pos (MELISA) and Neg (SELISA), 5.5% Pos (MqPCR and FPCR), 6.3% Neg (MqPCR) and Pos (FPCR), 14.06% Pos (MqPCR) and Neg (FPCR), 5.5% Pos (MELISA and FPCR), 6.3% Neg (MELISA) and Pos (FPCR), 15.6% Pos (MELISA) and Neg (FPCR), 5.5% Pos (SELISA and FPCR), 6.3% Neg (SELISA) and Pos (FPCR), and 16.41% Pos (SELISA) and Neg (FPCR). MELISA and SELISA were recognized as the most dependent tests (Chi-square: X^2 $(1, n = 128) = 62.57$, $p < 0.0001$). However, the dependency gradually decreased between the following test groups: MqPCR and FPCR ($p = 0.0048$), MqPCR and MELISA ($p = 0.0098$), MELISA and FPCR ($p =$

0.0098), SELISA and FPCR (p = 0.0134), and MqPCR and SELISA (p = 0.0145) (Figure 19, Table 14).

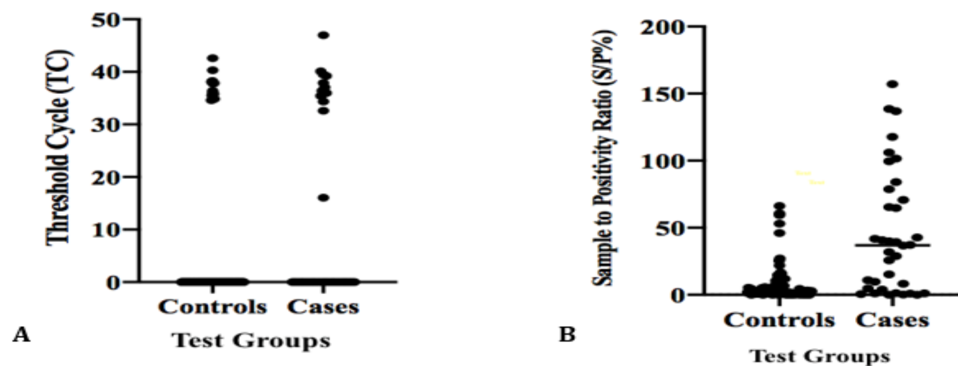

Figure 16. Scatterplots of the distribution of 128 milk samples (MIF) in two categories of healthy controls (HCs) and MAP-infected cases tested by MqPCR (**A**) and MELISA (**B**). HCs were adjusted based on the results of both SELISA and FPCR tests. The threshold cycle corresponding to MqPCR positivity was determined as being between 16 and 46 cycles (**A**), whereas the S/P% corresponding to MELISA positivity was between 31.93% and 157.11% (**B**) [224].

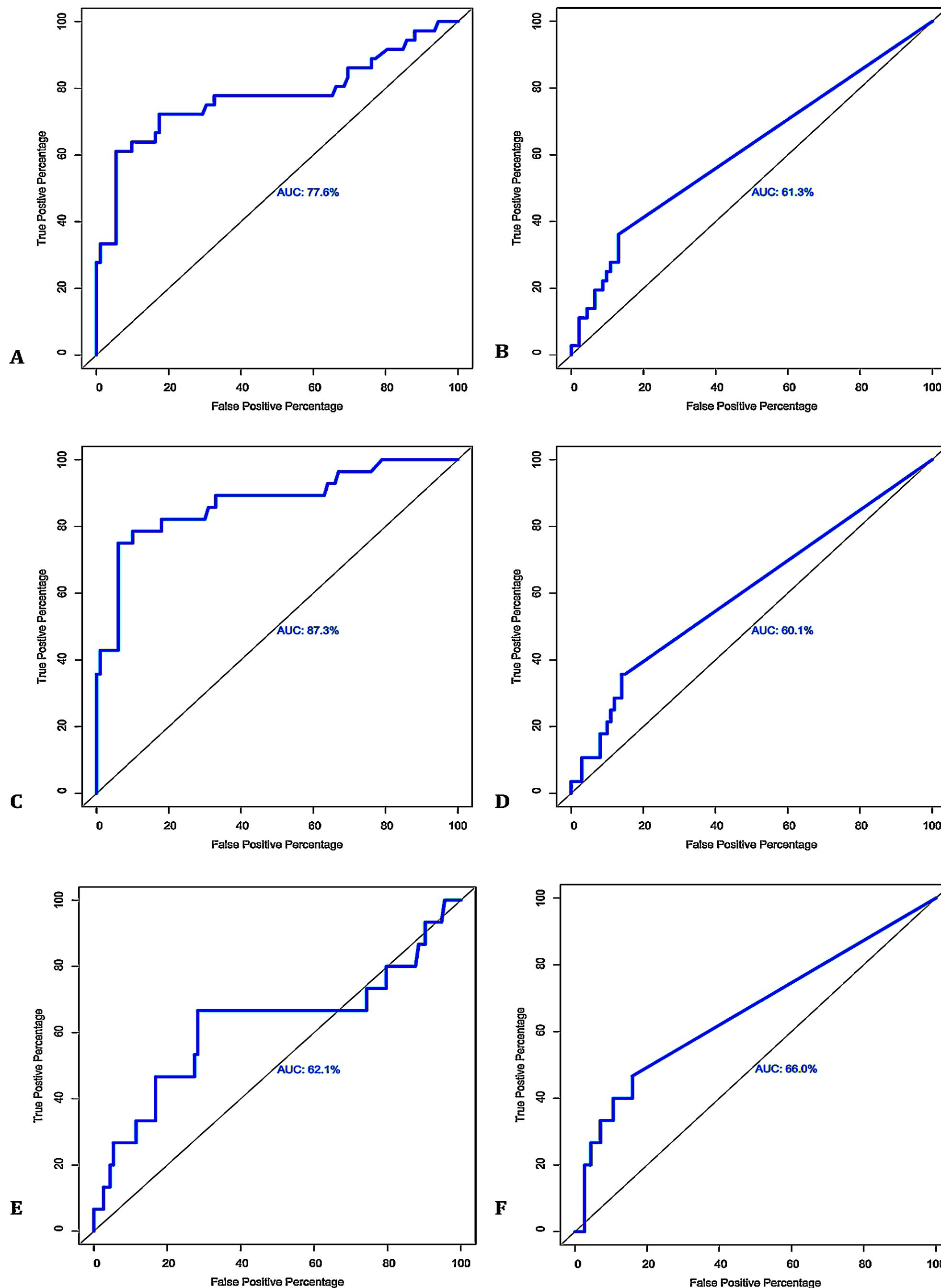

Figure 17. Receiver operating characteristic (ROC) curve analysis and corresponding area under the curve (AUC) analysis of MELISA (**A**,**C**,**E**) and MqPCR (**B**,**D**,**F**) datasets. The sensitivity and specificity of the MELISA and MqPCR tests in the detection of MAP in 128 MIF milk samples were evaluated based on three different gold standards of SELISA and FPCR (**A**,**B**), SELISA (**C**,**D**), and FPCR (E,F) [224].

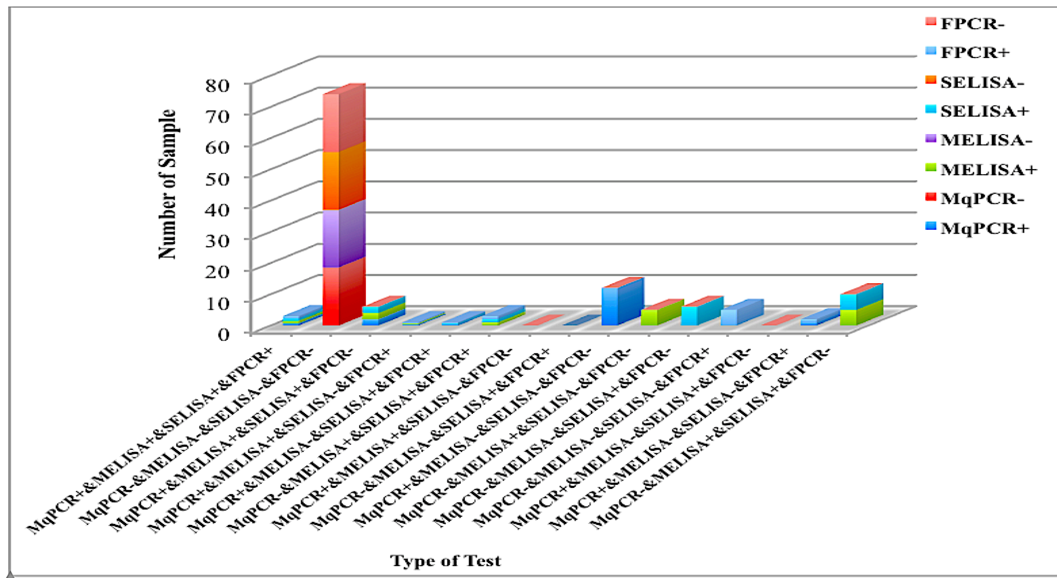

Figure 18. Distribution of 128 MIF milk samples categorized into fifteen quaternary groups based on their positive/negative status in MqPCR, MELISA, SELISA, and FPCR tests [224].

Table 13. Distribution of 128 MIF milk samples in fifteen quaternary groups based on positive/negative status in MqPCR, MELISA, SELISA, and FPCR tests [224].

Type of Tests	Number of Samples
MqPCR+ and MELISA+ and SELISA+ and FPCR+	3
MqPCR– and MELISA– and SELISA– and FPCR−	74
MqPCR+ and MELISA+ and SELISA+ and FPCR−	6
MqPCR+ and MELISA+ and SELISA− and FPCR+	1
MqPCR+ and MELISA− and SELISA+ and FPCR+	1
MqPCR− and MELISA+ and SELISA+ and FPCR+	3
MqPCR+ and MELISA+ and SELISA− and FPCR−	0
MqPCR− and MELISA− and SELISA+ and FPCR+	0
MqPCR+ and MELISA− and SELISA− and FPCR−	12
MqPCR− and MELISA+ and SELISA− and FPCR−	5
MqPCR− and MELISA− and SELISA+ and FPCR−	6
MqPCR− and MELISA− and SELISA− and FPCR+	5
MqPCR+ and MELISA− and SELISA+ and FPCR−	0
MqPCR+ and MELISA− and SELISA− and FPCR+	2
MqPCR− and MELISA+ and SELISA+ and FPCR−	10
Total number of samples	128

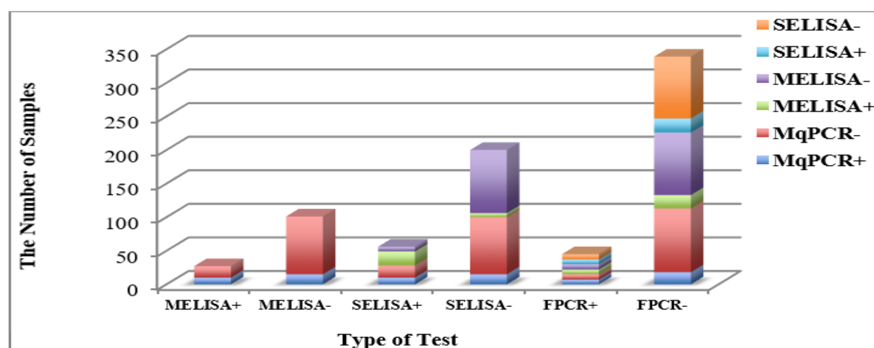

Figure 19. Distribution of 128 MIF milk samples classified into 24 binary groups based on the positive/negative status in MqPCR, MELISA, SELISA, and FPCR. The following categories had the greatest proportions: 74.22% Neg (MqPCR and FPCR), 73.44% Neg (MELISA and SELISA), 72.66% Neg (MELISA and FPCR), 71.88% Neg (SELISA and FPCR), 67.19% Neg (MqPCR and MELISA), and 66.41% Neg (MqPCR and SELISA) [224].

Table 14. Chi-square analysis and the distribution of 128 MIF milk samples classified into 24 binary groups based on the positive/negative status in MqPCR, MELISA, SELISA, and FPCR and corresponding *p*-values [224].

	MELISA+	**MELISA-**	**SELISA+**	**SELISA−**	**FPCR+**	**FPCR−**
MqPCR+	10	15	10	15	7	18
MqPCR−	17	86	18	85	8	95
p-value ($p < 0.05$) *	0.0098		0.0145		0.0048	
MELISA+			21	6	7	20
MELISA−			7	94	8	93
p-value ($p < 0.05$) *			$p < 0.00001$		0.0098	
SELISA+					7	21
SELISA−					8	92
p-value ($p < 0.05$) *					0.0134	

* Statistical significance was adjusted for a p-value of < 0.05.

4.1.5. Discussion

Our findings suggest that milk is a potent sample for screening Paratuberculosis in sheep flocks. However, the sensitivity and specificity of milk tests, i.e., MqPCR and MELISA, might be affected by some factors, such as the type of milk samples (BTM or individual samples), the disease status of animals participating in the survey, and the selected gold standard for statistical analysis [280,281]. Our BTM analyses (MqPCR and MELISA) demonstrated that MAP positivity follows a seasonal pattern, which was proven through a longitudinal study on 14 sheep herds.

Our MIF-relevant studies showed that MELISA and SELISA had the highest levels of concordance among the tests (89.8%). Such agreements were previously recorded by two other studies about the evaluation of the kinetics of antibodies directed against MAP during the lactation period ($R^2 = 0.5358$) [282] and the assessment of the efficiency of a multiplex bead-based immunoassay in the detection of MAP-immunogenic antigens in animals with JD

(R^2 = 0.572 to 0.756) [283].

We compared the efficiency of different gold-standard models to reach the highest sensitivity and specificity in detection of the true incidence rate of MAP in milk samples. We diagnosed that SELISA together with FPCR is one of the best practical reference models in individual-level milk assessments. However, each of them as an independent gold standard favors a specific milk assay (MqPCR or MELISA). The results suggest remarkable sensitivity and specificity of MELISA when the binary reference models were based on SELISA in isolation (SP: 0.94, SN: 0.75; $p < 0.0001$) and in combination with FPCR (SP: 0.95, SN: 0.61; $p < 0.0001$). In comparison, MqPCR had its highest specificity (SP: 0.87; SN: 0.4; $p = 0.047$) and sensitivity (SP: 0.84, SN: 0.47; $p = 0.044$) when the gold standards were based on SELISA + FPCR and FPCR, respectively. However, when FPCR was the standard model, the specificity of MELISA dropped slightly (SP: 0.72, SN: 0.67; $p = 0.129$). Our result is in accordance with another study that was conducted on BTMs from 21 dairy sheep flocks, evaluating the SP and SN of a modified milk ELISA in the detection of antibodies directed against MAP. A recent study that applied each of fecal PCR and serum ELISA as an independent reference test depicted that MELISA introduced a notable SP and SN when the reference test was based on SELISA (SP: 100%, SN: 72.7%) compared to when FPCR was the gold standard (SP: 46.7%, SN: 83.3%) [281]. Interestingly, in another comparative work on the evaluation of the efficiency of a high-yield fecal qPCR (YHDEqPCR) assay in the detection of MAP, the poorest level of agreement was seen between YHDEqPCR and milk ELISA (1%; $p = 0.739$), although the correlation between YHDEqPCR and milk qPCR was also insignificant (36%; $p = 0.591$) [222].

At the herd level (BTM), we developed a binary gold standard from both MqPCR and

MELISA results that remarkably enhanced the sensitivity and specificity of each milk assay, i.e., MqPCR or MELISA. In order to assess whether or not this gold standard favors a specific milk assay, each of MqPCR and MELISA was used as an independent gold standard to evaluate the efficiency of the other diagnostic assay (MELISA or MqPCR). MqPCR offered a significantly greater sensitivity and specificity (SP: 1, SN: 0.95; $p < 0.0001$) than MELISA (SP: 0.89, SN: 0.59; $p = 0.00035$) when both MqPCR and MELISA were the reference models. We reached a similar SP but higher SN in MqPCR analysis than another BTM-MAP-detection study conducted on 21 sheep flocks under the condition that any of serum ELISA, milk ELISA, fecal PCR, and fecal culture was assigned as the gold standard (SP: 100%; SN: 25%) [281].

We found that MqPCR as a reference test induced a remarkable specificity (SP: 0.95, SN: 0.34; $p = 0.037$) to MELISA compared to when MELISA was the reference test and MqPCR was the diagnostic assay (SP: 0.79, SN: 0.5; $p = 0.098$).

Our results revealed that the incidence of MAP and antibodies against it were lower in the MIF level than the herd groups (BTM) [281,284–286]. MqPCR and MELISA results were concordant with each other by 75% and 50% in MIF and BTM levels, respectively. Accordingly, the positivity rates of MqPCR and MELISA were estimated to be 19.53–21.09% in the MIF group and 72.6–30.14% in the BTM group. Thus, 47% of BTM and 11.7% of MIFM cases were detected as being positive by MqPCR without showing a sufficient antibody titer for positivity by MELISA. The significant disagreement ratio (47%) between MqPCR and MELISA in the BTM group was probably due to the high proportion of intermittent MAP shedders in each herd, lack of environmental hygiene practices that inhibit the dissemination of MAP through the environment, the inequity of the animals that

participated in the survey in terms of immune status, stages of disease, age, and genetic predisposition [280,287–289]. Furthermore, MqPCR IS*900* is one of the most sensitive MAP-detection assays and can detect the lowest concentration of MAP in the MAP-shedder animals in the initial stages of JD. As an American survey on the assessment of the sensitivity of various MAP-detection approaches (fecal–milk culture and qPCR) demonstrated that qPCR IS*900* can distinguish MAP-shedder cows via milk, colostrum, and feces more sensitively than the culture-based assays [32].

The results of BTM analyses (MqPCR and MELISA) on 73 samples from 59 herds showed an association between MAP-positivity rhythm and seasonal changes. We found that MqPCR and MELISA positivity have different seasonal patterns, in which the dominant number of positive MqPCR cases (45.21%) occurred in the spring. However, the highest number of MELISA-positive subjects (17.81%) was seen in the summer. This suggests that the number of MAP shedders increases in the spring due to seasonal breeding, possible sexual transmission of MAP, and the presence of animals shedding MAP via feces, which all corresponded to higher percentages of MqPCR-positive cases in the spring. However, humoral immunity due to MAP positivity was notable in the summer (MELISA). As a study on the detection of MAP in reproductive tissue showed that horizontal sex transmission increases the risk of MAP dissemination in infected rams, even though the lesions related to Johne's disease are not developed in the reproductive tissues, MAP can be disseminated to the reproductive tissues [157,158,290–293]. Also, an Italian study on MAP seroprevalence in dairy sheep flocks evidenced that the rate of MAP seropositivity was enhanced in the spring and autumn ($p < 0.071$) [294].

However, our longitudinal study on 14 herds (BTMs) showed that the intensity of MAP-

positivity, corresponding to lower TC values in MqPCR (ranged from 15 to 34 cycles), was more noticeable in the summer. A similar Canadian study on detecting MAP in milk and colostrum detected a higher proportion of MAP shedders in the summer by milk and colostrum qPCR than fecal and milk cultures [32]. Our longitudinal study also determined an increase in the number of positive MELISA cases in the summer. Even though some cases were MELISA-negative both in the spring and summer, the antibody titers against MAP had an upward trend in the summer and changes were remarkable in some cases (S/P% increased by between 1.3% and 60.4%). This finding is in accordance with the results of another study about the association of season of sampling with change of MAP antibody titers in BTM. This study also confirmed that the MAP antibody titer follows a seasonal pattern in milk samples: peaking in the summer and drastically dropping in the winter [217].

Our findings are limited by some factors, such as sample size, lack of communication with the herd's owners regarding the health status of animals that participated in this survey and hygiene practices, and limitations in following up all herds in each season.

Our experiments on the efficiency of different reference standard models suggest that the type of gold-standard test remarkably affects the sensitivity and specificity of both MqPCR and MELISA tests. In MIF study, SELISA in isolation and together with FPCR introduced the best sensitivity and specificity to MqPCR and MELISA tests. Furthermore, MELISA and SELISA results were concordant in 75% of cases ($p < 0.0001$), and this proved that MELISA could be used as a predicting test in the MAP screening programs at the MIF level. Of course, this conclusion directly depends on some factors, such as the age, immune status, stage of disease and so forth of the animals that participated in the survey. Our herd-level studies demonstrated that the results of MqPCR and MELISA together could form a practical binary

reference model (gold standard) under the condition that there is no information on the health status of the herd's animals. The results of both milk assays (MqPCR and MELISA) could represent how much potential each herd has to disseminate MAP through the environment and transmit the disease to other herds. The BTM-level studies depicted that MqPCR is more sensitive and specific ($p < 0.0001$) than MELISA ($p = 0.00035$). However, the agreement between the results of both milk assays was statistically significant when the *p*-value was adjusted to 0.1 ($p = 0.083$); this was equal to 50% concordance. This suggests that a high proportion of animals in each herd were MAP shedders. Our studies on 73 sheep herds indicated that MAP positivity follows a seasonal pattern. The number of positive MqPCR cases (45.21%) peaked in the spring, while the trend of MELISA positivity was notable (17.81%) in the summer. However, the result of the longitudinal study on 14 herds showed that the lower TC values, corresponding to stronger positivity, are most obvious in the summer. This may suggest that a large number of MqPCR-positive cases in the spring could be MAP shedders. The results obtained in this study highlight the risk of the transmission of this pathogenic mycobacterium to the community. A higher exposition to MAP, which causes a persistent infection in its host [295], may lead to trigger not only inflammatory bowel diseases including Crohn's disease [295,296], but also different autoimmune diseases, as it has been previously associated with in several studies [297–306]. This should motivate reflection by legislators and encourage the adoption of the best policies to lower the leakage of this bacterium into communities.

4.2. A Comparative Study on the Efficiency of Two *Mycobacterium avuim* subsp. *paratuberculosis* (MAP)-Derived Lipopeptides of L3P and L5P as Capture Antigen Molecules in an In-House Milk ELISA Test

4.2.1. Statistical Analysis

Statistical analysis was carried out using R software (version 4.0.5). To estimate the best cutoff corresponding positivity, receiver operating characteristic (ROC) curve analysis and area under the curve (AUC) were carried out using various binary reference models (0,1) at the levels of herd and individual respectively. The samples that were used in this study came from animals that were recently tested by other MAP-diagnostic assays such as milk qPCR (MqPCR), commercial milk ELISA (CMELISA), serum ELISA (SELISA), and fecal PCR (FPCR) (Table 15 and 16) [224]. Accordingly, the milk samples were distributed into two groups of negative and MAP-positive controls based on the positivity/negativity status of the studied animals tested by milk qPCR, commercial milk ELISA, serum ELISA, and fecal PCR. In which, the specimens belonged to animals with at least one positive result considered MAP-positive, whereas the healthy milk samples came from animals that had no positivity with none of the mentioned techniques (Table 17). In this study, the binary reference models were proposed based on the result of the MqPCR and CMELISA, in isolation and together, at BTM level. Unfortunately, the access to the animal blood and feces was impossible at BTM level. However, at individual level, collecting blood and feces was as feasible as milk samples, in which the references were adjusted based on the results MqPCR, CMELISA, serum ELISA (SELISA), fecal PCR (FPCR) individually and together. Later, the sensitivity of selected cutoffs in prediction of positive/negative cases was estimated based on the level of concordance that H-MELISA L3P/H-MELISA L5P had with MqPCR/CMELISA at BTM level and MqPCR/CMELISA/SELISA/FPCR at individual level (MIF). In addition,

Pearson correlation analysis was performed and the association level between H-MELISA L3P and H-MELISA L5P data sets at BTM and individual (MIF) levels was computed (the statistical significance was adjusted for a *p*-value of < 0.5).

Table 15. Distribution of 47 bulk tank milk (BTM) samples based on their positivity/negativity status in H-MELISA L3P, H-MELISA L5P, commercial ELISA (CMELISA), and milk qPCR IS900 (MqPCR).

Number of samples (BTMs)	H-MELISA L3P	H-MELISA L5P	Commercial MELISA (CMELISA)	Milk qPCR IS900 (MqPCR)
Sample 2	-	+	+	-
Sample 3	-	-	+	+
Sample 4	-	+	-	-
Sample 5	-	+	+	-
Sample 6	+	-	+	+
Sample 7	-	+	+	+
Sample 8	-	-	+	+
Sample 9	-	-	-	-
Sample 10	-	+	+	+
Sample 12	-	+	-	+
Sample 13	-	+	+	+
Sample 14	-	+	-	+
Sample 16	-	+	+	+
Sample 17	+	+	-	-
Sample 18	-	+	+	+
Sample 19	+	-	+	+
Sample 20	-	+	-	+
Sample 21	-	-	-	-
Sample 22	-	+	-	+
Sample 23	+	+	-	+
Sample 25	+	+	+	+
Sample 28	+	+	-	+
Sample 29	-	+	-	+
Sample 30	+	+	-	+
Sample 31	-	+	-	+
Sample 32	-	+	-	-
Sample 33	+	+	+	+
Sample 35	-	+	-	-
Sample 47	+	+	+	+
Sample 50	-	+	-	-
Sample 51	-	+	-	-
Sample 52	+	+	-	-
Sample 55	-	+	-	-
Sample 72	-	+	-	-
Sample 73	+	-	+	+
Sample 74	+	-	+	+
Sample 75	-	+	+	+
Sample 79	-	-	+	+
Sample 80	-	-	+	+
Sample 81	-	-	-	-
Sample 82	+	-	-	+
Sample 83	-	-	-	-
Sample 84	-	-	+	+
Sample 85	-	-	-	-
Sample 87	-	-	-	-
Sample 89	-	-	-	-
Sample 91	-	+	-	-

Table 16. Distribution of 81 individual milk samples from a MAP-infected flock (MIF) of sheep based on their positivity/negativity status in H-MELISA L3P, H-MELISA L5P, commercial ELISA (CMELISA), milk qPCR IS900 (MqPCR), serum ELISA (SELISA), and fecal PCR (FPCR).

Number of samples (individual milk samples from flock (MIF))	H-MELISA L3P	H-MELISA L5P	Commercial MELISA (CMELISA)	Milk qPCR IS900 (MqPCR)	Serum ELISA (SELISA)	Fecal PCR (FPCR)
3	+	-	-	-	-	-
4	+	-	-	-	-	-
5	+	-	+	+	-	+
6	-	-	+	+	+	+
7	+	-	+	+	+	+
8	+	-	+	-	+	+
9	+	-	-	-	-	-
10	+	-	-	-	-	-
11	+	-	-	-	-	-
12	+	-	-	-	-	-
13	-	-	-	-	-	-
15	+	+	-	-	-	-
16	-	-	-	-	-	-
17	+	-	-	-	-	-
18	-	-	-	-	-	-
19	-	-	-	-	-	-
20	-	-	-	-	-	-
22	+	-	+	-	+	-
23	+	-	-	-	-	-
24	+	-	-	-	-	-
25	+	+	+	-	+	-
27	+	-	-	-	-	-
28	-	-	-	-	-	-
29	+	+	-	-	-	-
33	+	-	-	-	-	-
35	+	-	-	-	-	-
36	+	-	+	-	+	+
37	-	-	-	-	-	-
38	+	+	+	-	+	-
39	-	-	-	-	-	-
41	+	-	-	-	-	-
45	-	-	-	-	-	-
49	-	-	+	-	-	-
50	+	+	-	-	+	-
53	+	+	+	-	+	-
55	-	+	+	-	+	-
56	-	-	-	-	+	-
61	+	-	-	-	-	-
62	+	+	+	+	+	-
64	+	-	-	+	+	+
65	+	+	-	+	-	-
66	+	-	-	-	-	-
67	+	-	-	-	-	-
69	-	-	+	+	+	-
70	+	-	+	-	+	-
72	+	-	+	+	+	+
73	+	-	-	-	-	-
75	-	-	-	+	-	-
76	-	-	-	+	-	-
78	+	+	-	-	-	-
79	+	+	-	-	-	-
80	+	-	-	-	-	-
81	+	+	-	-	-	-
82	+	+	+	-	+	+
83	+	+	-	+	-	-
84	+	+	-	-	-	-
86	+	+	-	+	-	-

88	+	-	-	-	+	-
89	+	-	-	-	-	-
90	+	+	-	-	-	-
91	+	-	-	-	-	-
92	+	-	-	-	-	-
93	-	-	+	+	+	-
94	-	+	+	+	+	-
95	+	+	+	-	+	-
96	-	-	+	-	+	-
97	+	+	-	-	+	-
99	+	-	-	+	-	-
100	+	-	-	+	-	-
101	+	-	-	-	-	-
102	+	-	-	-	-	-
103	-	-	-	-	-	-
104	-	-	-	-	-	-
105	+	+	-	-	-	-
111	-	-	-	-	-	-
112	+	+	+	+	+	-
113	+	+	-	+	-	-
114	-	+	+	+	+	-
119	-	+	+	-	+	-
121	+	+	-	-	-	-
128	-	-	-	-	-	-

Table 17. Distribution of bulk tank milk (BTM) and individual (MIF) milk samples into two categories of healthy and MAP-positive.

Number/ Type of milk sample	Number of negative controls	Number of MAP-positive controls
47/ BTM	17	30
81/ Individual (MIF)	45	36

4.2.2. Homemade milk ELISA with L3P and L5P epitopes on BTMs

ROC curve analysis was carried out and optical densities of 0.8895 and 0.59925 were selected as the cutoffs corresponding L3P and L5P positivity respectively. Among all binary reference models that were applied in cutoff assessments, MqPCR and CMELISA, independently, induced significant specificity to H-MELISA L3P (SP: 94.74%, SN: 39.3%, AUC: 64.8%) and H-MELISA L5P (SP: 70.37%, SN: 50%, AUC: 59.4%) analyses respectively.

Accordingly, 29.78% and 63.83% of 47 BTMs were identified positive producing various titers of antibodies directed against L3P and L5P epitopes respectively. In addition, similar level of concordance was seen between H-MELISA L3P and each MAP diagnostic assays of

MqPCR and C-MELISA by 60%, whereas H-MELISA L5P and each of MqPCR and CMELISA were in agreement by 51.06% and 38.30% respectively.

Interestingly, Pearson correlation test revealed a moderate positive association between antibody reactivity against two MAP-derived lipopeptides of L3P and L5P (*r* (45) = 0.5, p =0.00039; Figure 20) in H-MELISA analysis at BTM level.

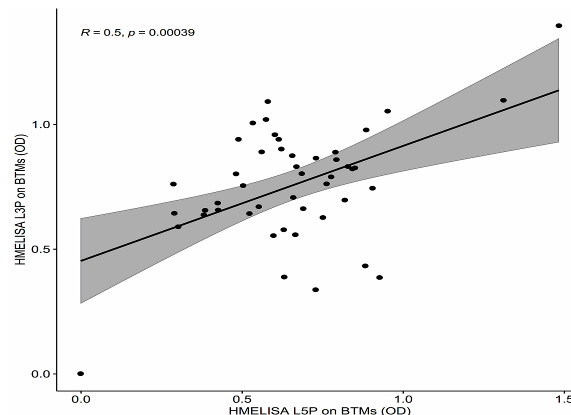

Figure 20. Pearson correlation test between two in-house MELISAs using two MAP-derived lipopeptides of L3P and L5P (*r* (degree of freedom = 45) = 0.5, p =0.00039).

4.2.3. Homemade ELISA with L3P and L5P epitopes on Milk samples from MAP-Infected Flock (MIF)

Cutoffs corresponding H-MELISA L3P and H-MELISA L5P positivity were adjusted at optical densities of, respectively, 0.406 and 0.513 through ROC curve analyses. Regarding the choice of gold standard, H-MELISA L3P acted more specifically (SP: 71.93%, SN: 37.5%%, AUC: 64.2%) with both CMELISA and FPCR together, whereas MqPCR and SELISA as a united gold standard induced higher specificity (SP: 80.43%, SN: 48.6%, AUC: 59%) to H-MELISA L5P. This is in the condition that SELISA conferred a specificity of above 70% to both H-MELISA L3P (SP: 70.9%, SN: 34.61%, AUC: 61.6%) and H-MELISA L5P (SP: 76.36%, SN: 50%, AUC: 54.5%).

In MIF category, antibodies directed against L3P and L5P were detected in 69.14% and 32.09% of cases respectively. A moderate agreement was found between H-MELISA L3P

dataset and each of following MAP diagnostic assays: MqPCR (47%), FPCR (45.7%), CMELISA (42%), and SELISA (42%), whereas this association was more robust in relation to H-MELISA L5P (SELISA (67.9%), CMELISA (66.67%), MqPCR (64.2%), and FPCR (60.49%)).

Additionally, data generated by the two homemade milk ELISA (L3P/L5P) were analyzed by Pearson correlation test. This analysis indicated that a low positive association existed between antibody reactivity against two MAP-derived lipopeptides of L3P and L5P (*r* (79) = 0.37, p =0.00059; Figure 21) at MIF level.

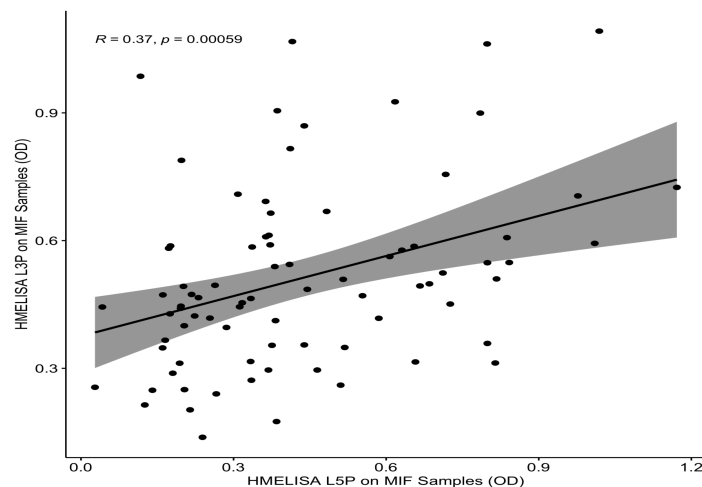

Figure 21. Pearson correlation test between two in-house MELISAs using two MAP-derived lipopeptides of L3P and L5P (*r* (degree of freedom = 79) = 0.37, p =0.00059) on 81 MIF milk samples.

4.2.4. Relationship between the type of MAP strain (S or C) and reactivity against L3P/L5P in the in-house milk ELISA (H-MELISA)

To understand whether or not the positivity status of samples in H-MELISA L3P/L5P could predict the type of MAP strains (S/C) in BTMs or individual (MIF) level milk samples, strain typing was performed on qPCR IS*900*-positive colonies and milk samples using PCR *IS1311*-restriction enzyme (RE) analysis (*hinf*-1). In fact, the amplification of IS*900* target

was important prior strain typing giving us an overview about the presence/lack of MAP in samples, regardless of the type of MAP strains. However, insertion sequence IS*1311* was selected in strain typing since this region has polymorphism within subspecies and this characteristic could be exploited in restriction analysis to discriminate various types of MAP strains (S/C/Bison) from each other.

Seven out of 128 milk samples contained viable ZN-positive colonies that were qPCR IS*900*-positive. However, only one of them was also positive for IS*1311*. Restriction enzyme analysis (REA) of the IS*1311* amplified product from sample 82B demonstrated the colony is C-type MAP, as its band pattern matched the C-type reference strain (Figure 22A). Furthermore, IS*1311* was PCR amplified in 44.12% and 42.11% of IS*900*-positive BTMs and MIFs respectively (23 out of 53 samples). Interestingly, IS*1311* strain typing analysis showed that all three classes of MAP (S, C, and Bison) existed among Sardinian sheep milk samples (Figure 22B). The S and C types produced two similar bands at 323- and 285-bp, however C type patterns could be distinguished by two additional IS*1311* fragments at 218-bp and 67-bp in size. In total, there were four S type strains identified in BTM by this method. An additional six S type strains identified in individual sheep samples as well. Finally, there were eight C type strains in BTM and individual sheep (Figure 22B, Table 18). Furthermore, Bison type was differentiated from the other strains indicating three bands at the lengths of 323-bp, 218-bp, and 67-bp [274,307] (Figure 22B). Consequently, Bison type contributed the lowest quantities in both groups of BTM (18B, 19B, and 29B) and MIF (64V) with 20% and 12.5% respectively (Figure 22B, Table 18).

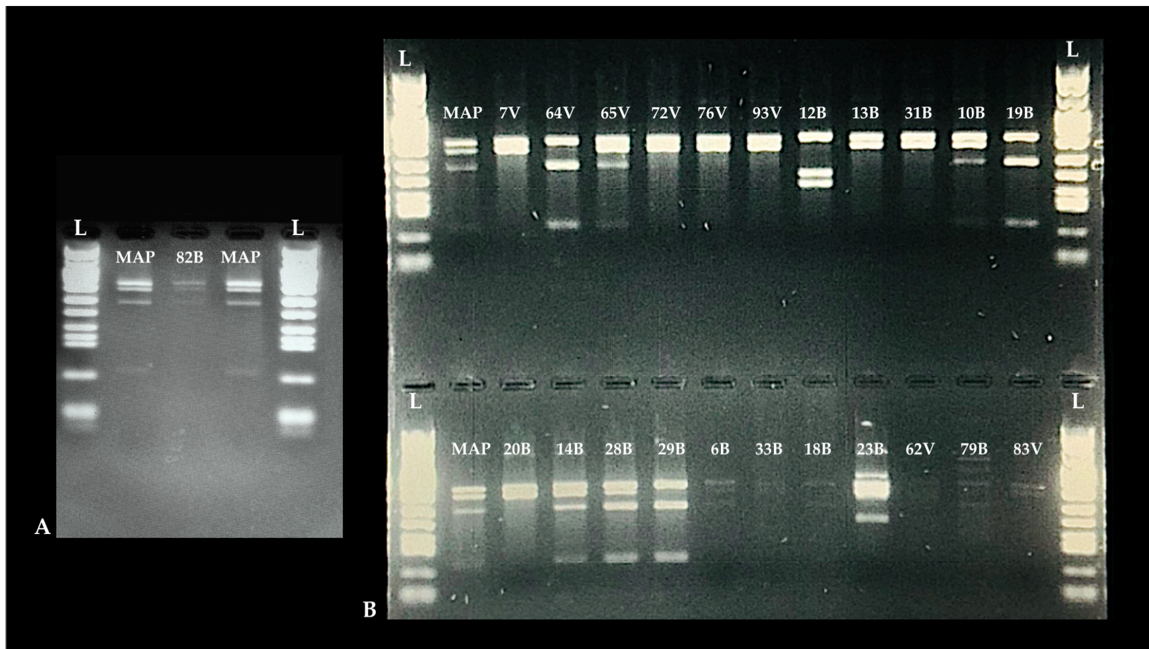

Figure 22. Restriction enzyme analysis (REA) on IS*1311*-positive PCR products obtained from sheep milk samples. Lanes in panel **A** from left to right are: 100-bp marker, MAP standard strain 1515 (C-type), sample 82B (C-type), MAP standard strain 1515 (C-type), and 100-bp marker. In panel **B**, first and last lanes are 100-bp marker (L) and second lane from the left belonged to MAP standard strain 1515. The remaining lanes contain REA analyzed milk samples. Samples "13B, 20B, 31B, and 33B" at the BTM level and "7V, 62V, 72V, 76V, 83V, and 93V" at the MIF level are S-type while samples "6B, 10B, 14B, 23B, 28B, and 79B" at BTM level and "65V" at MIF level are C-type. B-type samples "18B, 19B, and 29B" at BTM level and "64V" at MIF level were also observed. Sample 12B yielded an unusual pattern not seen before.

Table 18. Distribution of 23 IS*1311*-positive samples in BTM and MIF categories based on the type of MAP strain (S/C/Bison) and corresponding RE fragments on gel-electrophoresis.

Strain Type	Sample Type		RE[3] fragments on gel-electrophoresis based on base pair			
	BTM[1] %	MIF[2] %	67-bp	218-bp	285-bp	323-bp
S	26.67	75%			+	+
C	46.67	12.5	+	+	+	+
Bison	20	12.5	+	+		+

[1] BTM: Bulk tank milk
[2] MIF: MAP infected flock milk samples
[3] RE: Restriction Enzyme analysis

The results of strain typing on 23 (IS*900*/IS*1311*)-positive DNAs extracted from colonies or milk samples revealed that, C (46.67%) and S (75%) classes were the predominant strain types at the level of BTM and individual (MIF) respectively. Although, the overall rates of H-MELISA L3P/L5P positivity at both levels of herd and individual were in accordance with this strain-type orientation, there were some C and S-type samples that did not follow the

expected patterns in reactivity against L3P and L5P. In which, among four BTMs recognized as being S-type, sample 33B showed higher antibody reactivity against L3P, whereas samples 20B and 31B had almost similar optical densities against both L3P and L5P, and sample 13B was more responsive against L5P (Table 19). The difference between antibody reactivity of each S-type sample against L3P and L5P ranged between 0.014 ≥ OD ≥ 0.54 through H-MELISA analysis. In addition, at the same group, a weak agreement was found between antibody reactivity against L5P and being as C-type MAP strain. In brief, two out of seven BTMs that were characterized as being C-type reacted more against L5P (samples 14B and 28B; Table 19), samples 10B and 23B had similar reaction against L3P and L5P, whereas samples 6B, 79B, and 82B were almost more reactive against L3P (samples 6B, 79B, and 82B; Table 19). The difference in antibody reactivity of each C-type BTM against L3P and L5P ranged between 0.0425 ≥ OD ≥ 0.5125 through H-MELISA analysis. In contrast, a a never-before-defined correlation was found between antibody reactivity against L3P and being as Bison-type was discovered, in which samples 18B, 19B, and 29 (Table 19) recognized as Bison-type reacting more against L3P than L5P, and the difference between antibody reactivity against L3P and L5P of each Bison-type sample ranged between 0.049 ≥ OD ≥ 0.3295.

The uncertainty in stratification of MAP strains (C or S types) based on H-MELISA L3P/L5P positivity was also noticed in MIF category. 3 out of 6 S-type isolates were highly reactive against L3P (samples 7V, 72V, 83V; Table 19). Samples 62V and 93V had the same titers of antibodies directed against both L3P and L5P, whereas sample 76V had a slight rise in the titers of antibody against L5P rather than L3P. Interestingly, the only Bison-type (64V) and C-type (65V) isolates of this category reacted more against L3P. The difference between

antibody reactivity of each S-type, C-type, Bison-type sample against L3P and L5P were estimated "0.0065 ≥ OD ≥ 0.3115", "OD = 0.3085", and "OD = 0.1325" respectively.

Table 19. Distribution of 15 BTMs and 8 individual milk (MIF) samples based on the types of MAP in strain typing analysis and H-MELISA L3P/L5P positivity/negativity.

Number of Sample	Strain Type	H-MELISA L3P (Cutoff = 0.8895)[1] (Cutoff = 0.406)[2]	H-MELISA L5P (Cutoff = 0.59925)[3] (Cutoff = 0.513)[4]
6B	C-type	1.092	0.5795
10B	C-type	0.5545	0.597
12B	Unknown	0.627	0.7505
13B	S-type	0.3865	0.9265
14B	C-type	0.433	0.882
18B	Bison	0.7075	0.6585
19B	Bison	0.89	0.5605
20B	S-type	0.822	0.842
23B	C-type	0.978	0.885
28B	C-type	0.978	1.311
29B	Bison	0.865	0.729
31B	S-type	0.79	0.776
33B	S-type	0.9015	0.6215
79B	C-type	0.755	0.503
82B	C-type	1.006	0.533
7V	S-type	0.4725	0.161
62V	S-type	0.509	0.5155
64V	Bison	0.4445	0.312
65V	C-type	0.926	0.6175
72V	S-type	0.418	0.2535
76 V	S-type	0.175	0.3845
83V	S-type	1.062	0.7985
93V	S-type	0.2025	0.2145

[1 and 2] Optical densities of 0.8895 and 0.406 were adjusted as the cutoffs corresponding H-MELISA L3P positivity at BTM (B) and individual (V) levels respectively.
[3 and 4] Optical densities of 0.59925 and 0.513 were adjusted as the cutoffs corresponding H-MELISA L5P positivity at BTM (B) and individual (V) levels respectively.

4.2.5. Discussion

The level of antibodies directed against MAP could comparably be traced in milk samples as well as sera [308] through ELISA analysis if MAP-specific epitopes are selected [309] to capture the right antibodies and appropriate gold standard models are employed [224] to estimate the best cutoffs for determining positivity. Previous studies declared that MAP L5P specifically induces humoral responses in MAP-infected animals [227] and this characteristic

could be exploited in immunological detection of MAP and screening animals with JD. The efficiency of MAP lipopeptides in serological detection of MAP has previously been evaluated in other studies [219,227,228]. As in a survey on the accuracy of three different ELISAs in screening Paratuberculosis in sera of healthy, MAP and non-MAP (other mycobacteria) infected cows, L5P was employed as a capture antigen for developing an in-house ELISA assay and it detected antibodies directed against MAP in sera of studied animals with a significant specificity (98.9%) but less sensitivity (37%) [219]. Further sequence analysis along with biochemical and physico-chemical investigations of MAP lipopeptides clarified that the structures of lipopeptides varies in MAP strains that are indigenous in sheep (S-type) and cow (C-type), in which the *mps1* gene that encodes a non-ribosomal peptide synthetases contributing in production of lipopeptide in various strains (S and C types) are constituted of five and three modules in C-type and S-type MAP strains respectively [9]. This suggested that L5P and L3P might be ideal MAP-specific targets that could differentiate not only MAP from other mycobacteria, but also MAP strains of C-type and S-type from each other [9].

The present study, for the first time, used the MAP surface-exposed lipopeptide of L3P as capture antigen molecule in an in-house milk ELISA in order to screen antibodies directed against MAP in sheep milk samples. Furthermore, the functionality of L3P was compared with the other lipopeptides (L5P) performing H-MELISA L5P on the same samples. To select the best cutoffs corresponding positivity, ROC Curve analysis was performed. Cutoffs representing positivity have been selected carefully, since any miscalculations in this step may influence the specificity and sensitivity of the assay significantly [310]. The importance of using various gold standards in this study was to measure out how a reference model in isolation and association with other models could bias the positivity cutoffs for positivity.

This is on the condition that many studies have consensus on the efficiency of culture (SN: 30% and SP: 100%)[272], whereas no perfect gold standard has been created that could match all requirements of all assays in various studies [311]. The milk samples that were used in this study, were previously tested by milk qPCR and commercial milk ELISA in comparison with other MAP diagnostic techniques such as serum ELISA and fecal PCR in our recent work [224]. Accordingly, milk qPCR, commercial milk ELISA, serum ELISA, and fecal PCR were assigned as references in determining the positivity and negativity status of each milk sample. Therefore, milk samples were distributed into two categories of negative and MAP-positive controls. We noticed that the type of gold standard could influence the sensitivity and specifity of H-MELISA L3P/L5P at both levels of BTM and individual (MIF). In which, H-MELISA L3P and H-MELISA L5P represented better AUC and more specificity when, respectively, milk qPCR and commercial milk ELISA were gold standard at BTM level, whereas at MIF level, the most optimum specificity (above 70%) were induced to both H-MELISA L3P and L5P when serum ELISA was binary reference model. The recent result was in agreement with our previous study on 128 individual milk samples from a MAP infected sheep flock that indicated that serum ELISA (SP: 0.94, SN: 0.75; $p < 0.0001$) induced a significant specificity and sensitivity to milk ELISA assessments [224]. Accordingly, optical densities that conferred the specificity (SP) of equal or between 70-80% and sensitivity (SN) of above 30% with almost majority of reference models were selected as cutoffs for positivity. These specificity and sensitivity were at the same ranges as the ones (SP: 0.83-1.00 and SN: 0.29-0.61) defined by a review study on ante mortem diagnosis of Paratuberculosis in MAP infected animals [310].

To the best of our knowledge, several factors could influence the specificity and sensitivity of H-MELISA L3P/L5P including the sample size, the type of gold standard selected in ROC curve analysis, the status Johne's disease in animals participated in a survey.

Our analysis depicted that the overall rates of H-MELISA L3P/L5P positivity varied by the source of milk samples (BTM or individual). More samples were reactive against L5P and L3P at BTM and individual (MIF) levels respectively. Surprisingly, the majority of negative controls (their negativity confirmed by all following assays: milk qPCR, commercial milk ELISA, serum ELISA, fecal PCR) represented titers of antibodies directed against L5P and L3P epitopes in BTMs and individual milk samples respectively. An issue that might be discussed here is that why these negative controls should contain that much antibodies against L3P and L5P epitopes to be characterized as being MAP infected cases with various MAP strain types, while no evidence of MAP DNA was recognized in these samples. According to our analysis, MAP DNA could not be tracked down in a sample except if it presents at detectable concentration. Although target IS*900* has 16-22 copies [312] in whole MAP genome that seem sufficient for molecular diagnosis, these copies could not entirely be transferred into the qPCR reaction vessels. Specifically, we cut down the volume of milk samples required in DNA extraction to only 5 mL in order to overcome problems raised by resource limitation and this could further reduce the presence of MAP DNA in milk samples. On the other hand, the absence of MAP DNA in milk samples could not deny the presence of antibodies directed against MAP lipopeptides (L3P or L5P) circulating in milk and other body fluids of the corresponding animals. Since, MAP infected animals are characterized based on the types of immune responses that they have in different stages of JD, in which they might be just MAP shedders or just have humoral reactivity against MAP or have both responses simultaneously.

In addition, the comparison between the results of H-MELISA L3P/L5P and other antibody assessment methods depicted that H-MELISA L5P at BTM level and H-MELISA L3P at individual level (MIF) had the lowest level of agreement with commercial milk ELISA and serum ELISA/ commercial milk ELISA respectively. This may explain that H-MELISA L3P/L5P could even better function than commercial ELISA tests (milk or serum) and even detect minor titers of antibodies against MAP in milk samples. In fact, the types of capture antigen molecules used in the structure of H-MELISA L3P/L5P and commercial ELISA tests could influence the functionality of the techniques significantly. The most commercial ELISA tests are designed the way to detect antibodies against crude extract or specific epitopes of C-type MAP (as capture antigens) in milk or serum samples. Based on our interpretations, in MAP relevant infections, a noticeable proportion of antibodies against MAP are induced against its lipopeptides, since lipopeptides as well as lipids are existed with higher frequency in whole MAP cell structure rather than other epitopes. Therefore, we selected L3P and L5P as capture antigen molecules in H-MELISA test to target as much as antibodies existed against these epitopes in milk samples.

Based on the positivity patterns in H-MELISA L3P/L5P, it could be interpreted C-type and S-type MAP are dominant strains at BTM and individual (MIF) levels respectively, since previous studies confirmed that L3P and L5P are specific lipopeptides native in S and C types MAP strains [9].

The recent presumptions have been proved by PCR IS*1311*-REA hinf-1 analysis, in which all three MAP strains of C, S, and Bison types occurred among Sardinian sheep communities. In herd (BTM) group, C-type MAP was the dominant strain (46.67%) rather than S-type (26.67%), Bison-type (20%), and an unknown strain (6.6%; this strain was not reported before). In contrast, S-type was more prevalent (75%) in individual (MIF) level compared to

C-type and Bison-type that had the lowest incidences by 12.5% each. A question that might raise here is that why C-type MAP, a native strain in cow, should be a common strain among sheep animals at BTM level? While, S and C types were initially defined as the indigenous strains isolated from, respectively, sheep and bovine, further studies revealed that this host orientation couldn't inevitably predict the types of MAP strain (S or C) [313]. In fact, genotypic and phenotypic (e.g. pathogenesis and growth patterns) divergences are what could prognosticate S and C types from each other [40,313,314]. Previous group typing studies depicted that sheep and goat could be infected with both S-type and C-type MAP strains [46,315]. This is due to either an inter-species transmission or the presence of the multiple sources of infection in a farm [315]. These hypotheses seem logical enough, because BTM is a combination of several individual milk samples that might be infected with either each or both MAP strains of S and C types simultaneously. Superiorly, farmers usually keep various species of animals (specifically ruminants) together at the same farm and this could enhance the risk of inter-species transmission among animals in a herd.

Although, the distribution of MAP type strains (S/C) in both herd and individual levels was in accordant with the overall rates of H-MELISA L3P/L5P positivity, some S- or C-type MAP strains did not follow the predicted patterns in H-MELISA analysis. In which, the majority (44.44%) of S- and C-type MAP strains were both H-MELISA L3P- and L5P-positive, 22.22% were S type or C type as expected from their positivity patterns in H-MELISA L3P/L5P, and only 11.11% were positive but classified in unexpected categories. Surprisingly, the result of H-MELISA L3P/L5P on BTMs and individual milk samples (MIF) depicted that the majority of Bison-type isolates were more reactive against L3P rather than L5P, in both herd and individual levels. Previous molecular analysis unveiled that Bison type was derived from C type MAP strain that underwent a single nucleotide polymorphism in

IS*1311* sequence [313,316], but the complex growth requirements and disease manifestation patterns distinguished the Bison type from C-type [316]. Further investigation on Bison strains isolated from US and India [307,313] demonstrated that Indian strains have a TG deletion at base pairs 64 and 65 of locus 2 in IS*1311* [313,317]. To the best of our knowledge, the tendency of Bison type MAP in reactivity against L3P has never been reported in previous studies, in which more researches are needed to explain this orientation based on the characteristics of lipopeptide in this MAP strain.

At the first sight on the recent result, an ambiguity might be found in the stratification of MAP strain types (S or C) based on the result of H-MELISA L3P/L5P. We hypothesized that the antibody reactivity against L3P or L5P might be influenced by either a cross reactivity between these two the two lipopeptides or a possible co-infection of the studied animals with the two MAP strains of S and C types. Previous studies straightforwardly evidenced that MAP strains (S and C types) have various lipopeptides (L3P and L5P) [9]. While, the possibility of any cross reactivity from L5P in mycobacteria close to *Mycobacterium avium complex* (MAC) or other species such as *M. bovis* has been rejected [228], the theory of cross reactivity between L3P and L5P might not be out of imagination, since both lipopeptideds have common paratopes (e.g. amino acids of D-Phe, N-Methyl-L-Val and L-Ala) to share [9]. However, L3P has been subjected to evolutional modifications that specified its structures from L5P, in which as a result of mutations (deletions) in S-type MAP, it has no longer two amino acids of L-Ile and L-Phe in its structure [9]. This is under the condition that a study on engineered soluble-in-water L5P revealed that L5P could not differentiate sheep animals that experimentally infected with subtype I of S strain MAP from healthy animals. This may represent that S-I MAP possesses a lipopeptide that is different from L3P (specific lipopeptide in S-III MAP) and L5P (specific lipopeptide in C type MAP) [228].

On the other hand, the possibility of a mixed infection with both MAP type (S and C) strains, should be examined carefully, to which some samples (specifically BTMs) might contain enough antibodies directed against both L3P and L5P to being recognized positive by both H-MELISA L3P and H-MELISA L5P simultaneously. As the result of RE on amplified IS*1311* fragments confirmed that three different MAP strains of S, C, and Bison types circulated among animals at herd and individual levels. Our assumption about the presence of a mixed infection, specifically, in herd group (BTM) was fortified when Pearson analysis explained a moderate and low positive correlation between antibody reactivity against L3P and L5P at herd (BTM; (r (45) = 0.5, p =0.00039) and individual levels (MIF; (r (79) = 0.37, p =0.00059) respectively. This result indicated that the patterns of antibody reactivity against L3P and L5P are more similar at BTM level rather than MIF level.

MAP-derived lipopeptides of L3P and L5P could be considered as potent capture antigens in serum/milk antibody-detection analyses. Our result suggests that these lipopeptides, in the format of an in-house milk ELISA and as a complementary MAP-screening test could sensitively predict the infected animals (sheep) at BTM and individual levels. As H-MELISA L3P/L5P discovered many potential positive cases among the negative controls that were completely negative via other diagnostic assays. Accordingly, the majority of sheep milk samples were detected positive by H-MELISA L5P and H-MELISA L3P at the levels of herd (BTM) and individual (MIF) respectively. On the one hand, the overall rates of H-MELISA L3P/L5P confirmed the higher incidence of C-type and S-type classes of MAP in herd (BTM) and individual (MIF) categories respectively. On the contrary to this overall estimation, some S- or C-type MAP strains didn't show the expected reactivity against L3P and L5P, in which either they were positive by both H-MELISA L3P and L5P or they were L5P/L3P instead of being L3P/L5P. This might express the possibility of either cross reactivity between L3P and

L5P due to similarity in the overall structures of two epitopes or a within-herd mixed infection with both MAP strains of S and C types. However, the presence of various strain types of MAP (S/C/Bovine) along with a moderate correlation between antibody reactivity against L3P and L5P, that was estimated by Pearson correlation test, urged us to conclude that a co-infection with both MAP strains (S and C) happened among studied animals at the herd level (BTM). These findings suggest that the L3P and L5P antigens could be useful for improvement of the existing diagnostic tests especially considering the MAP strain diversity affecting the animals.

4.3. Detection of MAP Viability in Sheep and Goat Milk Samples Via A Novel and Conventional Phage Assay

4.3.1. Statistical Analysis

Receiver operating characteristic (ROC) and area under the curve (AUC) were carried out via R software (version 4.0.5) and the sensitivity and specificity of phage-beads qPCR (PBQ) and peptide-mediated-magnetic separation (PMS) phage assays were evaluated at different cutoffs using various binary reference models including milk qPCR, milk ELISA, and serum ELISA. The level of dependency between PBQ and other MAP diagnostic assays was computed using kappa co-efficient on GraphPad Prism while statistical significance was adjusted for a p-value of < 0.05. Additionally, McNemar's test for paired data (online GraphPad Prism software) and Venn analysis were performed in order to estimate and represent the distribution of samples based on positivity/negativity status in each binary test of PBQ/PMS-phage with milk qPCR, PBQ/PMS-phage with milk ELISA, and PBQ/PMS-phage with serum ELISA.

4.3.2. Optimization of peptide-mediated magnetic separation (PMS) phage assay using two different sources of Mycobacteriophage D29

Peptide-mediated magnetic separation (PMS) phage assay was optimized with intervention of two MAP-complementary peptideds of aMp3 and aMptD on milk samples contaminated with different concentrations of MAP (Figure 23). Two different sources of mycobacteriophage D29, named Laval and Actiphage, were used at optimization step. These strains were distinguished by various characteristics. Phage D29 Laval strain developed tiny plaques around 1 mm on Middlebrook 7H10, whereas the size of plaques produced by Actiphage was 3 mm. The numbers of lysed plaques were inconsistent at different dilutions (Table 20) via

Laval D29, in which the number of plaques reduced from 458 in 10^3 cfu/mL to 155 in 10^2 cfu/mL but it suddenly sored to 600 in 10^1 cfu/mL. qPCR analysis on DNAs extracted from plaques confirmed the presence of target IS*900* at concentrations 10^3 and 10^1 cfu/mL, therefore the limit of detection (LOD) of 10^1 cfu/mL was suggested for PMS-phage assay via Laval D29. In contrast, the result of optimization of PMS-phage assay with D29 from Actiphage kit depicted that an optimal regularity existed in the number of lysed plaques. In which, the numbers of plaques were gradually decreased from too-much-to-count (Figure 24A) to 30 (Figure 24B) at plates containing 10^4 cfu/mL to 10^2 cfu/mL MAP respectively. PCR IS*900* (primers P90 and P91) on DNAs extracted from lysed plaques developed on MB 7H10 agar confirmed the limit of detection of 10^2 cfu/mL for PMS-phage assay via Actiphage D29 (Figure 24B, Table 21).

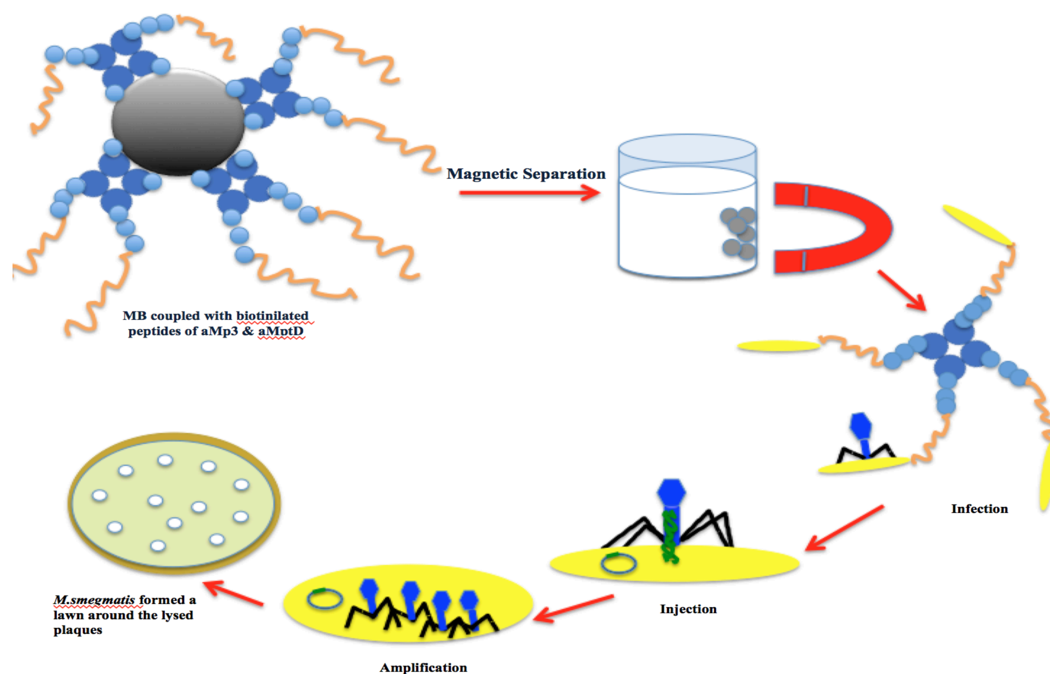

Figure 23. Procedures of peptide-mediated magnetic separation (PMS) phage assay with intervention of two MAP-complementary peptides of aMp3 and aMptD on MAP-spiked milk samples consisting: 1) magnetic separation: magnetic beads (MB) that were coupled with aMp3 and aMptD were added to samples and retrieved magnetically, 2) infection: captured MAP cells were infected by mycobacteriophage D29, 3) injection: D29 injected its DNA into the captured MAP, 4) amplification: D29 used the replication system of MAP host in order to replicate its DNA and assembled its body parts, 5) bursting and plaque formation: D29 lysed

its MAP host cells in a lawn made by *M. smegmatis* and plaques containing MAP DNA were formed on the medium.

Table 20. Optimization of PMS-phage assay via mycobacteriophage D29 from the University of Laval on aliquots of PBS and a known negative bovine milk sample contaminated with different concentrations of MAP comparing the number of lysed plaques appeared on MB 7H10 agar.

Dilutions/Concentrations	Number of Plaques in Milk	qPCR IS*900*
10^4 / 10^3	>458	Positive
10^3 / 10^2	155	Negative
10^2 / 10^1	>600	Positive
10^1 / 10^0	20	Negative

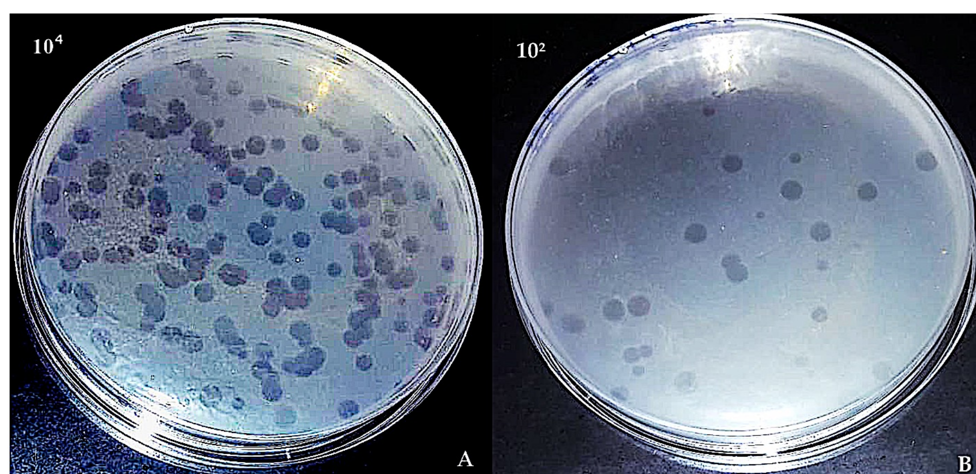

Figure 24. A schematic view of lysed plaques (3-4 nm) corresponding to MAP concentrations of 10^4 (A) and 10^2 (B) cfu/mL in an artificially contaminated milk sample (These photos were taken before ending the 18-hour incubation time considered for cell lysis).

Table 21. Optimization of PMS-phage assay on MAP-spiked PBS and milk samples representing the number of lysed plaques developed on MB 7H10 and the positivity status of DNA extracted from lysed plaques via PCR IS*900* analysis

Dilutions/Concentrations	Number of Plaques in Milk	PCR IS*900* (Primers P90-P91)
10^{-1} / 10^6	Totally Lysed	-
10^{-2} / 10^5	Totally Lysed	-
10^{-3} / 10^4	Many	Positive
10^{-4} / 10^3	31	Positive
10^{-5} / 10^2	30	Positive
10^{-6} / 10^1	0	-

4.3.2.1. Reproducibility assessment and Optimization of PMS-phage assay on 14 sheep milk samples via Laval D29

Seven out of fourteen sheep milk samples from a MAP-infected flock (MIF) produced lysed plaques in PMS-phage assay via mycobacteriophage D29 from the University of Laval (Figure 25). qPCR IS*900* analysis on plaques' DNAs confirmed the positivity of three samples (42.86%), whereas the other three samples were IS*900*-negaive. The positivity ranged between 38.76 to 42.82 cycles. Meanwhile, these 14 sheep milk samples were tested by milk qPCR and ELISA (Table 22). Although, the positivity of none of IS*900*-positive plaques were confirmed by milk qPCR, PMS-phage assay and milk qPCR were concordant by 64.29% (9 out of 14 samples). In contrast, the result of milk and serum ELISA on the same animals demonstrated that 100% of IS*900*-positive plaques were positive by milk and serum ELISA as well. Serum ELISA had the highest level of agreement with milk ELISA by 78.57%, whereas its concordance with milk qPCR was estimated 28.57%. Additionally, milk ELISA and qPCR had the minimum agreement among other tests by 21.43%.

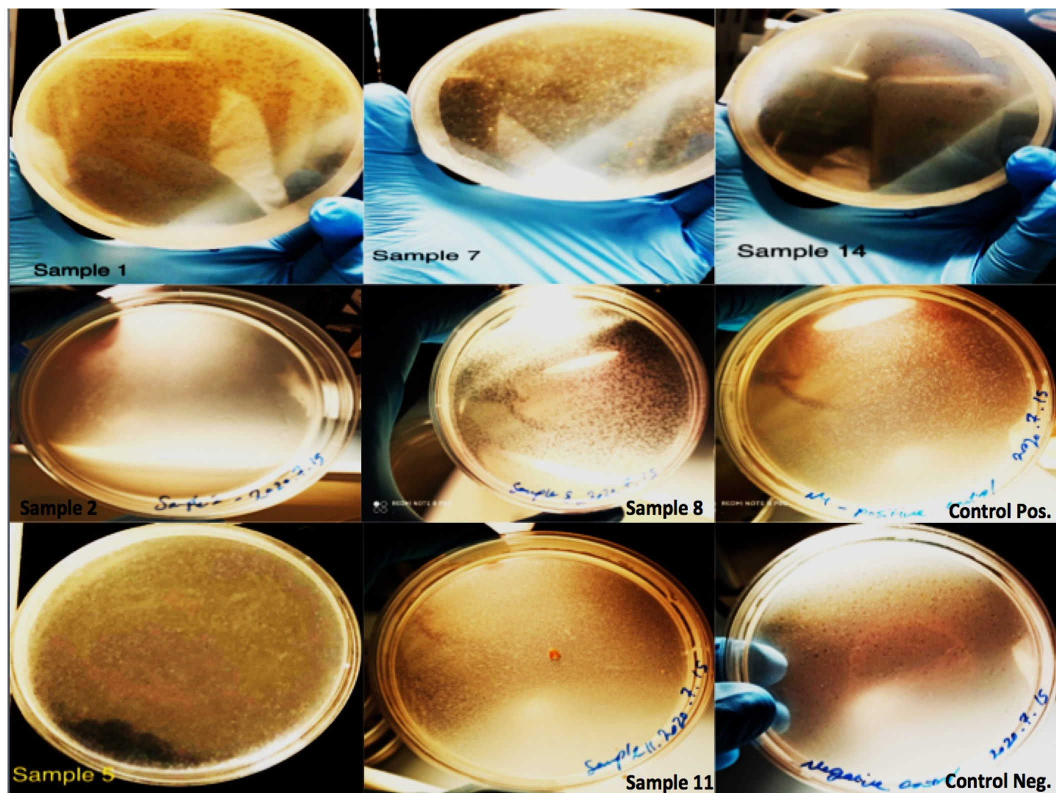

Figure 25. PMS-phage assay on 14 sheep milk samples. Seven samples developed lysed plaques that underwent further molecular (IS*900*) analysis.

Table 22. Comparison among the results of HPA and three other tests of MELISA, SELISA and MqPCR

Number of Sample	Lysed Plaques/ qPCR IS*900*	Milk ELISA (IDEXX)	Serum ELISA	Milk qPCR Status (TC/MT)
1	Yes/ Negative	Positive	Positive	0
2	Yes/ Positive [1]	Positive	Positive	0
3	No	Negative	Positive	Positive (34.8/ 91ºC)
4	No	Positive	Positive	0
5	Yes/ Negative	Positive	Positive	0
6	No	Negative	Negative	0
7	Yes/ Negative	Positive	Positive	0
8	Yes/ Positve [2]	Positive	Positive	0
9	No	Negative	Positive	0
10	No	Negative	Negative	Positive (36.97/ 91ºC)
11	Yes-Positve [3]	Positive	Positive	0
12	No	Positive	Positive	0
13	No	Negative	Negative	0
14	Yes/ Negative	Positive	Negative	0

[1, 2, 3] represented the threshold cycles (TCs) of 38.76, 41.74, and 42.87 respectively (melting temperature (MT) of 91 ºC)

4.3.2.2. Reproducibility assessment and Optimization of PMS-phage assay on 16 bovine milk samples via Actiphage D29

The PMS-phage assay was performed on 16 bovine milk samples using Actiphage as the infecting mycobacteriphage. 3 out of 16 (18.75%) milk samples collected from individuals in a cattle were plaque-positive with PMS-phage assay. qPCR IS*900* analysis on DNA extracted from these plaques revealed that only one of them was IS*900*-positive. Further ELISA analysis on the same sixteen milk samples revealed that none of these samples contain detectable concentrations of DNA against MAP (Table 23). However, a significant level of concordance was seen between PMS-phage assay and milk ELISA results by 87.5%.

Table 23. The comparison between the results of plaque qPCR IS*900* and milk ELISA on 16 bovine milk samples

Sample Number	Number of Plaques/ qPCR IS*900*	Milk ELISA
1	0	Negative
2	0	Negative
3	0	Negative
4	0	Negative
5	0	Negative
6	0	Negative
7	0	Negative
8	0	Negative
9	0	Negative
10	0	Negative
11	50*/ Positive	Negative
12	0	Negative
13	2/ Negative	Positive
14	0	Negative
15	0	Negative
16	40/ Negative	Negative

* The threshold cycle of this sample in qPCR IS*900* was 20.62 at melting temperature (MT) of 91 ºC.

Although, the limit of detection of PMS-phage assay via Laval D29 was 10 fold lower than PMS-phage assay via Actiphage D29, Actiphage D29 was used for the rest of this study. Since, the number of lysed plaques consistently changed based on the concentrations of MAP in milk samples via Actiphage D29, whereas the number of lysed plaques did not match the concentration of MAP in milk samples in PMS-phage assay via Laval D29. In addition, Laval D29 did not respond to virucide (FAS was the virucide that used for elimination of exogenous mycobacteriophages) effectively. Therefore many false MAP-negative lysed plaques appeared on various plates even negative controls.

4.3.3. PMS-phage assay on unpasteurized sheep milk samples in comparison with milk qPCR IS*900* and milk/serum ELISA

Despite the fact that some samples produced IS*900*-negative lysed plaques, no viable MAP was detected through PMS-phage assay on 29 unpasteurized milk samples collected from asymptomatic sheep animals (plaque numbers ranged from 1 to above 400 pfu/10 mL). PMS-phage assay and milk qPCR were concordant by 75.86% (kappa = 0), and only 24.14% (7 out of 29) of samples showed traces of MAP DNA corresponding dead cells at threshold cycles (TC) between 37.16 to 41.07 cycles ($C > 5.25 \times 10^{-6}$ ng/µL) via milk qPCR IS*900* analysis. On the other hand, 13.79% and 24.14% out of 29 animals were just milk and serum ELISA-positive respectively. In fact, PMS-phage dataset were strongly concordant with milk and serum ELISA (both with kappa value of zero) by 86.21% and 75.86%. McNemar's test was significant between PMS-phage and each test of milk qPCR or serum ELISA, representing that the proportion of MAP negative cases detected by each bi-test of PMS-phage and milk qPCR, PMS-phage and serum ELISA was statistically significant (both with two-tailed *p*-value of 0.0233; Venn analysis Figure 26A. and Figure 26C) rather than milk qPCR-positive and serum ELISA-positive cases. In contrast, McNemar was insignificant in comparison between PMS-phage and milk ELISA (two-tailed *p*-value = 0.1336; Figure 26B) with a higher magnitude of the cases that were detected negative by both PMS-phage and milk ELISA rather than serum ELISA positive cases. Further ROC curve analysis represented an insignificant AUC of 50% with all reference models of milk qPCR, milk ELISA, and serum ELISA (SP: 1, SN: 0).

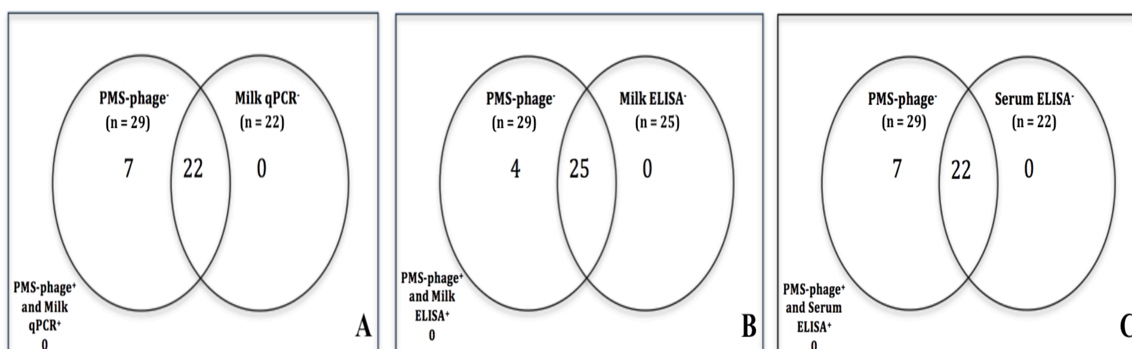

Figure 26. Venn comparison analysis between peptide mediated magnetic separation phage assay (PMS-phage) dataset and each MAP diagnostic assay of milk qPCR (**A**), milk ELISA (**B**), and serum ELISA (**C**).

4.3.4. Optimization of Phage-Bead qPCR (PBQ) in MAP-spiked PBS and known negative milk

Phage-bead qPCR (PBQ) was optimized at concentration of 10^1 cfu/mL in PBS and artificially contaminated milk samples, and this endpoint was appointed as the limit of detection (LOD) of the assay in both PBS and milk. The results of qPCR IS*900* (TaqMan) depicted a correspondent threshold cycle (TC) values of MAP concentrations between 10^4 to 10^1 cfu/mL in the paired PBS and milk samples (Table 24).

Table 24. Threshold cycles corresponding different concentrations of MAP in MAP-spiked PBS and a known negative milk sample

Concentrations (cfu/mL)	PBS (TC)	Milk (TC)
10^4	32.21	32.56
10^3	34.21	35.85
10^2	36.52	39.43
10^1	40.17	38.24

4.3.5. PBQ on unpasteurized milk samples from goat and sheep flocks in comparison with milk qPCR, milk ELISA, and serum ELISA

PBQ was assayed on 41 goats and sheep milk samples and viable MAP was detected in 48.78% of samples by qPCR IS*900* corresponding to the concentration of 5.25×10^{-3} ng/µL < C > 5.25×10^{-6} ng/µL (TC between 35.29 to 40.15 cycles). MAP-clumps captured by phage

beads were visible in some cases even with naked eyes (Figure 27A). The result of qPCR IS*900* on the same milk samples revealed that only 35% of PBQ-positive cases had detectable concentrations of MAP DNA (C >5.25×10^{-6} ng/μL, TC between 38.82 and 39.9 cycles) corresponding to both dead and viable cells in milk as well. The level of agreement between PBQ and milk qPCR was estimated fairly significant by 63.41% (kappa = 0.2581, 95% CI = 0.0083 to 0.508), whereas 31.7% and 4.8% were just PBQ-positive and milk qPCR-positive respectively. In addition, McNemar's test determined a statistically significant difference in the proportion of PBQ-positive cases rather than milk qPCR-positive subjects (two-tailed *p*-value =0.0098; Venn analysis (Figure 28A)).

Further ELISA assessments reveled that among 41 sheep and goat animals 14.63% were both milk and serum ELISA positive; 2.4% and 9.8% of cases were milk and serum ELISA-positive respectively. In fact, PBQ assay had insignificant and almost similar level of concordance with both milk and serum ELISA by 43.9% (kappa = -0.1403, 95% confidence interval (CI) = -0.3697 to 0.0892) and 41.46% (kappa = -0.1855, 95% CI = -0.1855, -0.4449 to 0.0738) respectively. McNemar between PBQ and milk qPCR or milk ELISA confirmed that the proportion of PBQ-positive animals was statistically higher than milk or serum ELISA-positive cases with two-tailed *p*-values of 0.0123 and 0.066 represented by Venn analysis (Figure 28B) and (Figure 28C) respectively.

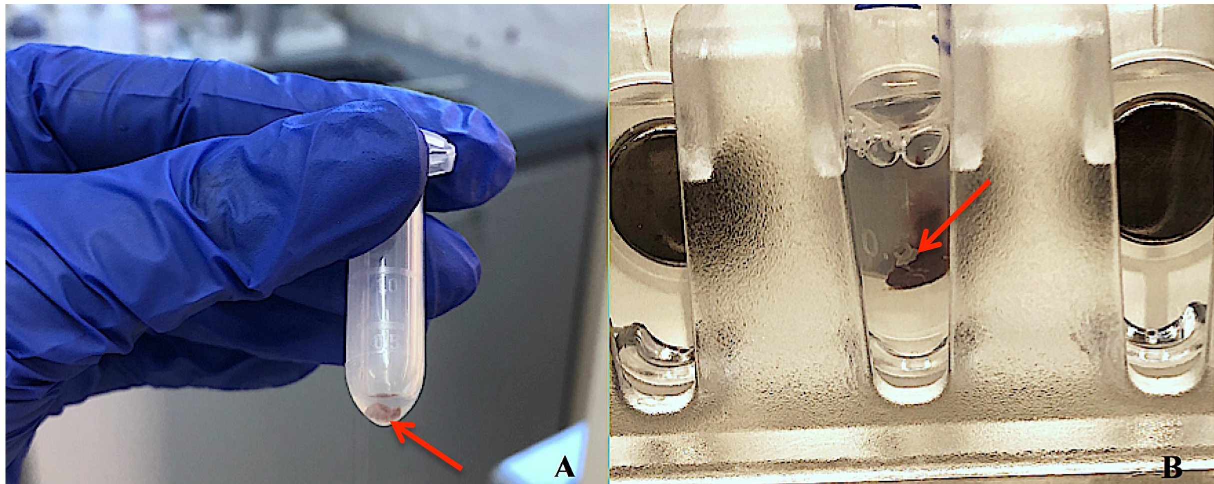

Figure 27. Schematic views of MAP clumps that are visible with naked eyes captured by phage beads in a MAP-positive goat milk sample (**A**; the last step after centrifugation that supernatant containing DNA was aspirated and subjected to qPCR IS*900* analysis) and MAP-positive control (**B**: Micro-tube containing positive control was placed in magnetic rack during washing step).

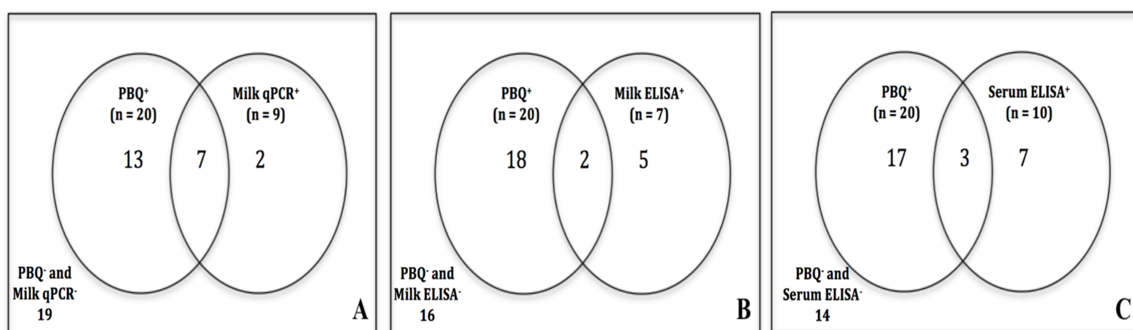

Figure 28. Venn comparison analysis between phage bead qPCR (PBQ) dataset and each MAP diagnostic assay of milk qPCR (**A**), milk ELISA (**B**), and serum ELISA (**C**).

On the other hand, ROC curve analysis depicted that milk qPCR, as a binary reference model, induced higher specificity to PBQ analysis (AUC = 72.2%, cutoff = 37.935, SP: 87.5%, SN: 55.56%; Figure 29A) compared to milk and serum ELISA that significantly elevated the sensitivity of PBQ rather than specificity (milk ELISA (AUC: 62.2%, cutoff: 35.37, SP: 50%, SN: 71.43%; Figure 29B); serum ELISA (AUC: 60.3%, cutoff: 35.37, SP: 54.84, SN: 70%; Figure 29C)).

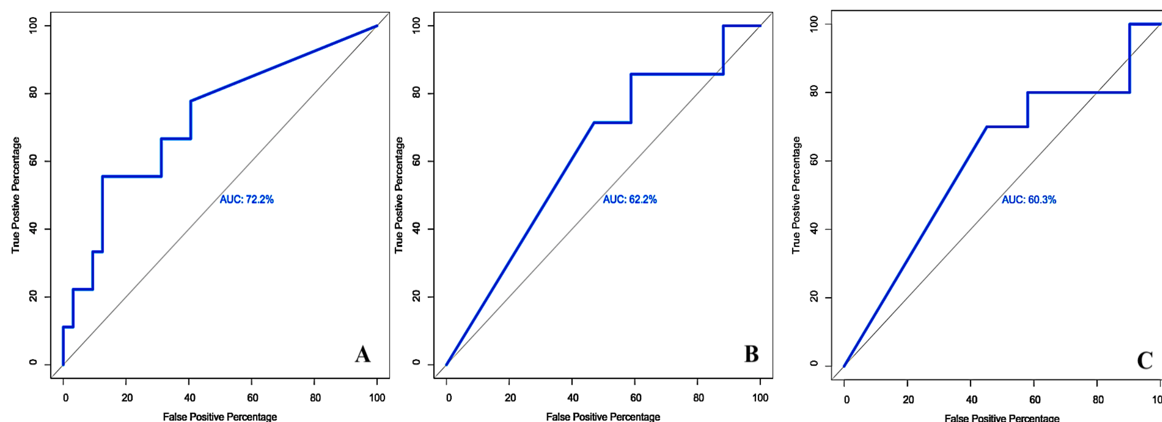

Figure 29. Receiver operating characteristic (ROC) curve analysis and corresponding area under the curve (AUC) analysis on PBQ dataset when milk qPCR (**A**), milk ELISA (**B**), serum ELISA (**C**) were binary reference models.

4.3.6. PBQ and PMS-phage assay on milk samples taken from sheep animals in two instances of sampling in comparison with other MAP diagnostic assays of milk qPCR, milk ELISA, and serum ELISA

The viability of MAP was confirmed in none of 42 sheep milk samples (21 animals) that were tested by both PBQ and PMS-phage assays. These samples were taken from the same animals with a gap time of two weeks. The result of milk qPCR IS*900* on these samples depicted that some animals intermittently shed MAP in their milk samples, in which 23.8% of samples that were milk qPCR-positive, became negative at the second time, instead 9.5% (2 samples) that were negative at the first time became positive at the second time (Figure 30A). Among 42 milk and serum samples taken in two rounds of sampling, 19.04% and 33.33% of samples were respectively milk- and serum ELISA-positive at both rounds, and only one sheep that was firstly milk ELISA-negative became positive at the second time (Figure 30B.). However the titers of antibody directed against MAP saw a gradual rise or fall by 0-18.04 degrees in sample to positivity ratio (S/P%) (Figure 30B.).

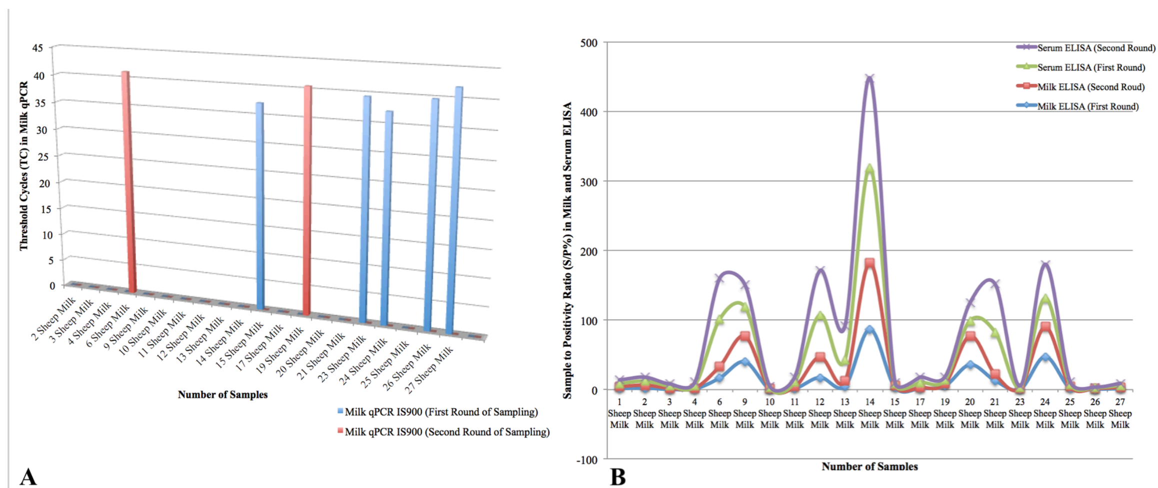

Figure 30. Comparison among the results of three diagnostic assays of milk qPCR, milk ELISA, serum ELISA at the first and second rounds of sampling. This comparison is based on threshold cycles (TC) and sample to positivity ratio (S/P%) generated in qPCR IS*900* (**A**) and milk/serum ELISA (**B**) respectively.

4.3.7. Discussion

The slow-growth characteristic of MAP imposed huge struggles on the detection of viable bacterium through culture-based analysis. Recent innovations in selective capture of target bacteria via magnetic beads speeded up the discovery of viable MAP in various samples significantly. This improvement was more noticeable when ligand peptides of aMp3/aMptD along with a phage amplification step were included to the primary version of magnetic separation (MS). In fact, aMp3 and aMptD are biotinylated MAP specific complementary peptides that were recognized through phage display biopanning against whole MAP cell and the MAP-surface exposed proton of aMptD respectively [247,252]. Furthermore, phage amplification was characterized by the introduction of mycobacteriophage D29 (a lytic phage) to the recovered MAP cells with the aim of liberating DNAs from infected cells. D29 is not a specific phage for MAP [265,318,319], however it specifically expresses its DNA only in the viable mycobacterial hosts [320]. A survey on MAP-spiked milk samples depicted that heat treatment before PMS-phage assay could not affect the MAP viability along phage functionality, in which a significant correlation was found between cfu/mL and pfu/mL in

unheated (r^2 = 0.943) and heated (r^2 = 0.971) milk samples [253]. Before, PMS-phage assay was privileged other techniques of PMS-PCR and PMS-MGIT in detection of viable MAP in individual and bulk tank milk (BTM) samples [277]. Although, the limit of detection (LOD) of PMS-phage assay via Laval D29 was 10 fold lower than PMS-phage assay via Actiphage D29, a few reasons encouraged us to use Actiphage D29 for the rest of phage-based analysis in this study. The comparison between the two sources of mycobacteriophage D29 depicted that Laval D29 functioned more sensitively than Actiphage D29, however Laval D29 lacked enough specificity in discriminating between MAP and other mycobacterial species effectively, since some samples developed MAP-negative false lysed plaques that belonged to other environmental mycobacterial species such as *M. smegmatis*. As based on the documents provided by the Laval University, *M. smegmatis* was the main host species for this D29 strain. In addition, the inconsistency in the numbers of lysed plaques produced by Laval D29 at different concentrations of MAP in milk and PBS suggested that virucide (FAS) could not eliminate the exogenous mycobacteriophages effectively. The small size (1 mm) of lysed plaques produced by Laval D29 was another imperfection of the Laval D29 facing the manipulation and extraction of DNA from the lysed plaques with difficulties.

In optimization of the two phage-based assays in this study, PBQ excelled PMS-phage assay by 10 fold in detection of the lowest quantity of MAP (10^1 cfu/10 mL) presented in an artificially MAP spiked milk sample. This functionality was previously reported by the original phage-bead qPCR study on assessment of MAP viability in bovine milk samples [259], although the 10 fold reduction in the LOD of PMS-phage assay was possibly due to the sample's final volume, to which the assay was optimized for (10 mL compared to 50 mL in other studies [277]). Up to now, PMS-phage assay was tried and tested on various matrixes such as raw milk ($LOD_{50\%}$ = 0.90 to 0.95), blood, and peripheral blood mononuclear cells

(PBMC) diagnosing MAP at concentrations between 7.3 × 10^2 pfu/mL to 10 MAP cells/50 mL [277,321,322]. To the best of our knowledge, LOD in PMS-phage assay might be affected by few factors including: 1) the final volume of sample; 2) the quality and concentration of peptides; 3) the quality of beads; 4) the quality that magnetic beads get coated; 4) the binding buffer's pH; 5) the temperature of sample before and after magnetic separation; 6) the strain of mycobacteriophage D29.

Our PBQ analysis was examined on 41 unpasteurized goat and sheep milk samples indicating that various concentrations of viable MAP existed in 48.78% of the specimens. The functionality of Phage-bead assay in sensitively detection of viable MAP has been proved in a recent study, in which viable MAP was found in 49% out of 100 BTMs collected from different farms [259]. Interestingly, PBQ result had the most level of agreement with milk qPCR by 63.41% rather than with milk and serum ELISA each by 43.9%. This consensus could even be noticed in ROC curve analysis, in which the highest specificity (SP: 87.5%) and a moderate sensitivity (SN: 55.56%) were induced to PBQ analysis when the binary reference model was adjusted to milk qPCR compared to the condition that milk ELISA (SP: 50%, SN: 71.43%) and serum ELISA (SP: 54.84, SN: 70%) were independently a gold standard and instead PBQ was more sensitive. Furthermore, no viable MAP was detected in 29 sheep milk samples that were only tested by PMS-phage assay. However, some samples developed lysed plaques that were qPCR IS*900*-negative corresponding to either disability of the FAS in deactivating all exogenous D29 mycobacteriophages or the presence of massive fat cells in the structure of sheep milk samples that could meantime bind to the surface of peptide mediated magnetic beads and D29 myco-hosts other than MAP conveying them up to the plaque formation step. PMS-phage dataset was remarkably compatible with all MAP diagnostic assays of milk qPCR (75.86%), milk ELISA (86.21%), and serum ELISA

(75.86%). Statistically, the highest proportions of samples were negative by each bi-test of "PMS phage-milk qPCR" and "PMS phage-milk ELISA" (*p*-value = 0.0233). Further ROC curve analysis on PMS-phage assay data could not privilege a reference model to other ones and influence the specificity and sensitivity of PMS-phage assay, in which PMS-phage assay had the utmost specificity (100%) but least sensitivity (0%) with the all gold standards. This is definitely due to the small sample size and the absence of milk samples containing viable MAP that could balance data analysis. Similarly, a previous comparative study on the strength of PMS-phage assay and PMS-culture for detection of viable MAP in bovine milk samples depicted that both PMS-based methods introduced a noticeable specificity (100% and 96.2% resp.) rather than sensitivity (32.5% and 25% resp.) to MAP viability assessments [323].

To be confident whether or not PBQ could only detect viable MAP in milk but not dead cells, a parallel study via the two phage assays was carried out on sheep milk samples in two different time points. In fact, we did not have access to sufficient amount of milk samples to test all of them by two protocols at the same time. The result of this comparison depicted that viable MAP was existed in none of samples tested by PBQ and PMS-phage assay. We noticed that the recent samples collected from animals that suffered from a progressive Johne's disease, since either the positivity status of some animals was changed through milk qPCR analysis or the antibody titers against MAP in milk and serum samples saw a fluctuation between 0-18.04 degree in S/P% within two times milk sampling.

PBQ and PMS-phage could be promising methods for assessment of MAP viability in milk and even other clinical samples. PBQ detected viable MAP among numbers of unpasteurized goat and sheep milk samples provided from apparently healthy animals. PBQ had a considerable level of concordance with milk qPCR by 63.41% concordance. In addition,

ROC curve analysis estimated a remarkable specificity and sensitivity for PBQ analysis when milk qPCR was the gold standard. In a comparative study on milk samples taken from the same sheep animals in two instances of sampling, we noticed that some PBQ- and PMS-negative animals were shedding the dead microorganism intermittently, in which some animals that were milk qPCR-positive at first, turned negative at the second time or vice versa. This heterogeneity might be the consequence of diversity of animals in the stages of Johne's disease. This claim has been proved through a follow-up ELISA test on milk and serum of MAP shedder animals revealing that the antibody titers against MAP in milk and serum saw fluctuations within two times sampling. Eventually, three factors privileged PBQ to PMS-phage assay in this study including: 1) low LOD: PBQ with LOD of 10 viable cells in 10 mL milk excelled PMS-phage by 10 folds; 2) rapidity and cost effectiveness: PBQ could be carried out in only 9-10 hours with least material and equipment, whereas PMS-phage assay needs at least 48 hours; 3) lack of need for FAS treatment: Based on our experience the quality of applied FAS could affect the number of lysed plaques in PMS-phage assay, therefore this inconsistent functionality could undermine the specificity of the PMS-phage assay whereas no FAS treatment is needed in PBQ.

Chapter V: Conclusion

1) The presence of MAP and antibodies against it could be tracked in milk samples as well as other specimens such as blood.
2) qPCR IS*900* analysis on milk samples collected from Bulk tank milk (BTM) could be an economic diagnostic way of MAP shedder animals at the level of herd.
3) The concentration of MAP and antibodies directed against it varied by the type of milk samples. The load of bacterium and antibodies against it are higher in BTMs, since BTM is a mix of several individual milk samples. Therefore, more infected cases might be detected through diagnostic analysis on BTMs.
4) Our BTM-relevant study revealed that MAP positivity via qPCR and milk ELISA analyses has a seasonal pattern. In which the incidence of MAP (qPCR; 45.21%) and antibodies (CMELISA; 17.81%) directed against it were higher in spring and summer respectively. The higher proportion of MAP (MqPCR +) in spring could explain that the excretion of MAP in milk via feces or semen of MAP shedder animals increases in spring due to seasonal breading and sexual transmission of MAP.
5) Our longitudinal study on 14 sheep herds over two instances of sampling confirmed that MAP shedder animals existed in some herds, in which some milk samples that were qPCR positive at first became negative at the second time and vice versa. Some samples that had lower concentration of MAP DNA at first, became highly positive at the second time (according to the lower threshold cycles through milk qPCR analysis: 16 to 34 cycles). In addition, the comparison between the result of commercial milk ELISA at the first and second rounds of sampling depicted that the titers of antibodies directed against MAP saw a remarkable rise within the course of study.

6) Milk could be an alternative sample to serum in antibody screening analysis. Since, at individual level, a remarkable level of concordance was seen between antibody titers against MAP in serum (commercial serum ELISA) and milk samples (commercial milk ELISA).
7) The type of gold standard could affect the sensitivity and specificity of a diagnostic assay in ROC curve analysis significantly.
8) MAP-derived lipopeptides (L3P and L5P) that differ by the types of MAP strain (S or C) could be potent capture antigen molecules in screening the antibodies directed against MAP in serum or milk samples. They could be used in the format of an in-house milk ELISA and as a complementary MAP diagnostic test to unveil positive cases among the samples that were potentially negative by other MAP diagnostic techniques.
9) Our in-house milk ELISA (H-MELISA) tests suggested that the pattern of H-MELISA L3P/L5P positivity varies by the type of milk samples. In which, the incidence of H-MELISA L5P positive cases were higher at BTM level rather than individual milk samples that were more H-MELISA L3P positive.
10) The overall rates of H-MELISA L3P/L5P positivity could predict which MAP strain happens with higher incidence among BTMs and individual milk samples. In which, the higher proportion of H-MELISA L5P and H-MELISA L3P positive cases at BTM and individual milk samples depicted that C-type and S-type were predominant MAP strains at BTM and individual levels respectively. The recent presumption was proved by strain typing analysis on some of the negative or positive H-MELISA L3P/L5P positive or negative cases using PCR-IS*1311* restriction enzyme analysis via *hinf*-1.

This analysis depicted that the overall percentages of S or C type MAP strains could be anticipated by H-MELISA L3P/L5P positivity status.

11) Some S or C type MAP strains were positive by both H-MELISA L3P and H-MELISA L5P positive or had reverse positivity patterns via H-MELISA L3P/L5P. This might be the consequences of either a cross reactivity between L3P and L5P due to the similarity in the overall structures of these lipopeptides or a within-herd mixed infection with both MAP strains of S and C. Further analysis through Pearson correlation test revealed that a moderate positive correlation between antibody titers against L3P and L5P at BTM level, therefore the hypothesis of presence of a mixed infection with S and C types MAP could be explainable at BTM level.

12) Phage bead qPCR (PBQ) and peptide-mediated magnetic separation (PMS) phage assay could be promising methods for detection of MAP viability in milk and even other clinical samples.

13) The result of PBQ and PMS-phage assay on samples taken from the same animals depicted that the assays function comparably.

14) However, PBQ seems to be more advantageous in comparison with PMS-phage assay, since it benefits from a lower LOD, rapidity and cost effectiveness. PBQ works without any needs to lawn-maker bacteria (*M. smegmatis)* or FAS treatment that are crucial steps in visualization of lysed plaques and deactivation of exogenous mycobacteriophages respectively.

References

1. Lefrancois, L.H.; Bodier, C.C.; Cochard, T.; Canepa, S.; Raze, D.; Lanotte, P.; Sevilla, I.A.; Stevenson, K.; Behr, M.A.; Locht, C.; et al. Novel Feature of *Mycobacterium avium* subsp. *paratuberculosis*, Highlighted by Characterization of the Heparin-Binding Hemagglutinin Adhesin. **2013**, doi:10.1128/JB.00671-13.
2. Wiszniewska-Łaszczych, A.; Liedtke, K.G.; Szteyn, J.M.; Lachowicz, T. The Effect of *Mycobacterium avium* subsp. *Paratuberculosis* Infection on the Productivity of Cows in Two Dairy Herds with a Low Seroprevalence of Paratuberculosis. **2020**, *10*, 490, doi:10.3390/ani10030490.
3. Baumgartner, W.; Khol, J.L. PARATUBERCULOSIS (JOHNE´S DISEASE) IN RUMINANTS – AN ONGOING STORY. *Vet. Med.* **2006**, *43*, 5–10.
4. Johne HJ, F.J. Ein eigentümlicher Fall von Tuberculose beim Rind. *Dtsch Z Tiermed Pathol* **1895**, *21*, 438–54.
5. Harris, N.B.; Barletta, R.G. *Mycobacterium avium* subsp. *paratuberculosis* in Veterinary Medicine. *Clin. Microbiol. Rev.* **2001**, *14*, 489–512, doi:10.1128/CMR.14.3.489-512.2001.
6. Clarke, C.J. The pathology and pathogenesis of paratuberculosis in ruminants and other species. *J. Comp. Pathol.* 1997, *116*, 217–261.
7. Chiodini, R.J.; Van Kruiningen, H.J.; Merkal, R.S. Ruminant paratuberculosis (Johne's disease): the current status and future prospects. *Cornell Vet.* **1984**, *74*, 218–262.
8. Harding, H.P. The histopathology of *Mycobacterium johnei* infection in small laboratory animals. *J. Pathol. Bacteriol.* **1959**, *78*, 157–169, doi:https://doi.org/10.1002/path.1700780117.
9. Bannantine, J.P.; Etienne, G.; Laval, F.; Stabel, J.R.; Lemassu, A.; Daffé, M.; Bayles, D.O.; Ganneau, C.; Bonhomme, F.; Branger, M.; et al. Cell wall peptidolipids of *Mycobacterium avium*: from genetic prediction to exact structure of a nonribosomal peptide. *Mol. Microbiol.* **2017**, *105*, 525–539, doi:10.1111/mmi.13717.
10. Chen, H.; Nyantakyi, S.A.; Li, M.; Gopal, P.; Aziz, D.B.; Yang, T.; Moreira, W.; Gengenbacher, M.; Dick, T.; Go, M.L. The Mycobacterial Membrane: A Novel Target Space for Anti-tubercular Drugs . *Front. Microbiol.* 2018, *9*, 1627.
11. Marrakchi, H.; Lanéelle, M.A.; Daffé, M. Mycolic acids: Structures, biosynthesis, and beyond. *Chem. Biol.* **2014**, *21*, 67–85, doi:10.1016/j.chembiol.2013.11.011.
12. Daffé, M.; Quémard, A.; Marrakchi, H. Mycolic Acids: From Chemistry to Biology. In; 2017; pp. 1–36 ISBN 978-3-319-43676-0.
13. Ripoll, F.; Deshayes, C.; Pasek, S.; Laval, F.; Beretti, J.-L.; Biet, F.; Risler, J.-L.; Daffé, M.; Etienne, G.; Gaillard, J.-L.; et al. Genomics of glycopeptidolipid biosynthesis in *Mycobacterium abscessus* and M. chelonae. *BMC Genomics* **2007**, *8*, 114, doi:10.1186/1471-2164-8-114.
14. Park, I.K.; Hsu, A.P.; Tettelin, H.; Shallom, S.J.; Drake, S.K.; Ding, L.; Wu, U.-I.; Adamo, N.; Prevots, D.R.; Olivier, K.N.; et al. Clonal Diversification and Changes in Lipid Traits and Colony Morphology in *Mycobacterium abscessus* Clinical Isolates. *J. Clin. Microbiol.* **2015**, *53*, 3438–3447, doi:10.1128/JCM.02015-15.
15. Bansal-Mutalik, R.; Nikaido, H. Mycobacterial outer membrane is a lipid bilayer and the inner membrane is unusually rich in diacyl phosphatidylinositol dimannosides. *Proc. Natl. Acad. Sci.* **2014**, *111*, 4958 LP – 4963, doi:10.1073/pnas.1403078111.
16. Chiaradia, L.; Lefebvre, C.; Parra, J.; Marcoux, J.; Burlet-Schiltz, O.; Etienne, G.;

Tropis, M.; Daffé, M. Dissecting the mycobacterial cell envelope and defining the composition of the native mycomembrane. *Sci. Rep.* **2017**, *7*, 12807, doi:10.1038/s41598-017-12718-4.
17. Percival, S.; Yates, M. V; Williams, D.; Chalmers, R.; Gray, N.F. *Microbiology of Waterborne Diseases: Microbiological Aspects and Risks: Second Edition*; 2014; ISBN 978-0-12-415846-7.
18. Adikaram CP Overview of Non Tuberculosis Mycobacterial Lung Diseases. In *Mycobacterium - Research and Development*; 2018.
19. Collins, C.H.; Grange, J.M. MYCOBACTERIA. In *Encyclopedia of Food Sciences and Nutrition*; Elsevier, 2003; pp. 4067–4072.
20. Falkinham, J.O. Nontuberculous mycobacteria in the environment. *Clin. Chest Med.* 2002, *23*, 529–551.
21. Griffith, D.E.; Aksamit, T.; Brown-Elliott, B.A.; Catanzaro, A.; Daley, C.; Gordin, F.; Holland, S.M.; Horsburgh, R.; Huitt, G.; Iademarco, M.F.; et al. An Official ATS/IDSA Statement: Diagnosis, Treatment, and Prevention of Nontuberculous Mycobacterial Diseases. *Am. J. Respir. Crit. Care Med.* **2007**, *175*, 367–416, doi:10.1164/rccm.200604-571ST.
22. Stahl, D.A.; Urbance, J.W. The division between fast- and slow-growing species corresponds to natural relationships among the mycobacteria. *J. Bacteriol.* **1990**, *172*, 116–124, doi:10.1128/jb.172.1.116-124.1990.
23. Godreuil, S.; Marchandin, H.; Michon, A.-L.; Ponsada, M.; Chyderiotis, G.; Brisou, P.; Bhat, A.; Panteix, G. *Mycobacterium riyadhense* pulmonary infection, France and Bahrain. *Emerg. Infect. Dis.* **2012**, *18*, 176–178, doi:10.3201/eid1801.110751.
24. Loebinger, M.R.; Welte, T. Current Perspectives in the Diagnosis and Treatment of Nontuberculous Mycobacterial Pulmonary Disease. *Eur. Respir. Pulm. Dis.* **2016**, *02*, doi:10.17925/ERPD.2016.02.02.54.
25. Cayrou, C.; Turenne, C.; Behr, M.A.; Drancourt, M. Genotyping of *Mycobacterium avium complex* organisms using multispacer sequence typing. *Microbiology* **2010**, *156*, doi:10.1099/mic.0.033522-0.
26. Thorel MF, K.M.L.-F.V. Numerical Taxonomy of Mycobactin-Dependent Mycobacteria, Emended Description of *Mycobacterium avium*, and Description of Mycobacterium avium subsp. avium subsp. nov. , *Mycobacterium avium* subsp. *paratuberculosis* subsp. nov. , and *Mycobacterium avium* subsp. *silvaticum* subsp. nov. *Int. J. Syst. Bacteriol.* **1990**, *40*, 254–260, doi:10.1099/00207713-40-3-254.
27. Green, E.P.; Tizard, M.L.V.; Moss, M.T.; Thompson, J.; Winterbourne, D.J.; Mcfadden, J.J.; Hermon-Taylor, J. Sequence and characteristics or IS900, an insertion element identified in a human crohn's disease isolate or *Mycobacterium paratuberculosis*. *Nucleic Acids Res.* **1989**, *17*, doi:10.1093/nar/17.22.9063.
28. Collins, D.M.; de Lisle, G.W. Restriction endonuclease analysis of various strains of *Mycobacterium paratuberculosis* isolated from cattle. *Am. J. Vet. Res.* **1986**, *47*.
29. Franco-Paredes, C.; Marcos, L.A.; Henao-Martínez, A.F.; Rodríguez-Morales, A.J.; Villamil-Gómez, W.E.; Gotuzzo, E.; Bonifaz, A. Cutaneous mycobacterial infections. *Clin. Microbiol. Rev.* 2019, *32*.
30. Grant, I.R.; Kirk, R.B.; Hitchings, E.; Rowe, M.T. Comparative evaluation of the MGIT^{TM} and BACTEC culture systems for the recovery of *Mycobacterium avium* subsp. *paratuberculosis* from milk. *J. Appl. Microbiol.* **2003**, *95*, 196–201, doi:10.1046/j.1365-2672.2003.02003.x.
31. Behr, M.A.; Collins, D.M. *Paratuberculosis: Organism, disease, control*; CABI

Publishing, 2010; ISBN 9781845936136.
32. Laurin, E.; McKenna, S.; Chaffer, M.; Keefe, G. Sensitivity of solid culture, broth culture, and real-time PCR assays for milk and colostrum samples from *Mycobacterium avium ssp. paratuberculosis*-infectious dairy cows. **2015**, doi:10.3168/jds.2014-8758.
33. Lilenbaum, W.; Marassi, C.D.; Oelemann, W.M.R. Paratuberculosis: an update. *Brazilian J. Microbiol.* **2007**, *38*, 580–590, doi:10.1590/S1517-83822007000400001.
34. Grant, I.R. *Mycobacterium avium ssp. paratuberculosis*: Its incidence, heat resistance and detection in milk and dairy products. *Int. J. Dairy Technol.* **2001**, *54*, 2–13, doi:10.1046/j.1471-0307.2001.00009.x.
35. Sung, N.; Collins, M.T. Effect of three factors in cheese production (pH, salt, and heat) on *Mycobacterium avium* subsp. *paratuberculosis* viability. *Appl. Environ. Microbiol.* **2000**, *66*, 1334–1339, doi:10.1128/AEM.66.4.1334-1339.2000.
36. Patel, A.; Shah, N. *Mycobacterium avium* subsp. *paratuberculosis*-Incidences in milk and milk products, their isolation, enumeration, characterization, and role in human health. *J. Microbiol. Immunol. Infect.* **2011**, *44*, 473–479, doi:10.1016/j.jmii.2011.04.009.
37. Grant IR, B.H.R.M. A novel staining technique for assessing clumping and viability of *Mycobacterium paratuberculosis* cells during pasteurization. In Proceedings of the Fifth International Colloquium on Paratuberculosis; Chiodini RJ, Hines ME, and C.M., Ed.; International Association for Paratuberculosis: Rehoboth, Mass, 1997; pp. 374–377.
38. Hammer, P.; Kiesner, C.; Walte, H.G.; Knappstein, K.; Teufel, P. Heat resistance of *Mycobacterium avium ssp. paratuberculosis* in raw milk tested in a pilot plant pasteurizer. *Kieler Milchwirtsch. Forschungsberichte* **2002**, *54*.
39. Grant, I.R.; Williams, A.G.; Rowe, M.T.; Muir, D.D. Efficacy of various pasteurization time-temperature conditions in combination with homogenization on inactivation of *Mycobacterium avium subsp. paratuberculosis* in milk. *Appl. Environ. Microbiol.* **2005**, *71*, doi:10.1128/AEM.71.6.2853-2861.2005.
40. Bryant, J.M.; Thibault, V.C.; Smith, D.G.E.; McLuckie, J.; Heron, I.; Sevilla, I.A.; Biet, F.; Harris, S.R.; Maskell, D.J.; Bentley, S.D.; et al. Phylogenomic exploration of the relationships between strains of *Mycobacterium avium* subspecies *paratuberculosis*. *BMC Genomics* **2016**, *17*, 79, doi:10.1186/s12864-015-2234-5.
41. Ahlstrom, C.; Barkema, H.W.; Stevenson, K.; Zadoks, R.N.; Biek, R.; Kao, R.; Trewby, H.; Haupstein, D.; Kelton, D.F.; Fecteau, G.; et al. Limitations of variable number of tandem repeat typing identified through whole genome sequencing of *Mycobacterium avium* subsp. *paratuberculosis* on a national and herd level. **2015**, *16*, 161, doi:10.1186/s12864-015-1387-6.
42. Collins, D.M.; Gabric, D.M.; de Lisle, G.W. Identification of two groups of *Mycobacterium paratuberculosis* strains by restriction endonuclease analysis and DNA hybridization. *J. Clin. Microbiol.* **1990**, *28*, 1591 LP – 1596.
43. Windsor, P.A. Paratuberculosis in sheep and goats. *Vet. Microbiol.* **2015**, *181*, 161–169, doi:10.1016/j.vetmic.2015.07.019.
44. Laurin, E.; McKenna, S.; Chaffer, M.; Keefe, G. Sensitivity of solid culture, broth culture, and real-time PCR assays for milk and colostrum samples from *Mycobacterium avium ssp. paratuberculosis*-infectious dairy cows. *J. Dairy Sci.* **2015**, *98*, 8597–8609, doi:10.3168/jds.2014-8758.
45. Stevenson, K.; Hughes, V.M.; de Juan, L.; Inglis, N.F.; Wright, F.; Sharp, J.M.

Molecular characterization of pigmented and nonpigmented isolates of *Mycobacterium avium* subsp. *paratuberculosis*. *J. Clin. Microbiol.* **2002**, *40*, 1798–1804, doi:10.1128/JCM.40.5.1798-1804.2002.
46. Stevenson, K. Genetic diversity of *Mycobacterium avium* subspecies *paratuberculosis* and the influence of strain type on infection and pathogenesis: a review. *Vet. Res.* **2015**, *46*, 64, doi:10.1186/s13567-015-0203-2.
47. Harris, S.R.; Feil, E.J.; Holden, M.T.G.; Quail, M.A.; Nickerson, E.K.; Chantratita, N.; Gardete, S.; Tavares, A.; Day, N.; Lindsay, J.A.; et al. Evolution of MRSA during hospital transmission and intercontinental spread. *Science (80-.).* **2010**, *327*, doi:10.1126/science.1182395.
48. Whittington, R.J.; Begg, D.J.; de Silva, K.; Purdie, A.C.; Dhand, N.K.; Plain, K.M. Case definition terminology for paratuberculosis (Johne's disease). *BMC Vet. Res.* 2017, *13*.
49. Arsenault, R.J.; Maattanen, P.; Daigle, J.; Potter, A.; Griebel, P.; Napper, S. From mouth to macrophage: Mechanisms of innate immune subversion by *Mycobacterium avium* subsp. *Paratuberculosis*. *Vet. Res.* **2014**, *45*, 1–15, doi:10.1186/1297-9716-45-54.
50. Payne, J.M.; Rankin, J.D. The Pathogenesis of Experimental Johne's Disease in Calves. *Res. Vet. Sci.* **1961**, *2*, doi:10.1016/s0034-5288(18)34970-1.
51. Sweeney, R.W.; Uzonna, J.; Whitlock, R.H.; Habecker, P.L.; Chilton, P.; Scott, P. Tissue predilection sites and effect of dose on *Mycobacterium avium* subsp. *paratuberculosis* organism recovery in a short-term bovine experimental oral infection model. *Res. Vet. Sci.* **2006**, *80*, doi:10.1016/j.rvsc.2005.07.007.
52. Charavaryamath, C.; Gonzalez-Cano, P.; Fries, P.; Gomis, S.; Doig, K.; Scruten, E.; Potter, A.; Napper, S.; Griebel, P.J. Host responses to persistent *Mycobacterium avium* subspecies *paratuberculosis* infection in surgically isolated bovine ileal segments. *Clin. Vaccine Immunol.* **2013**, *20*, doi:10.1128/CVI.00496-12.
53. Määttänen, P.; Trost, B.; Scruten, E.; Potter, A.; Kusalik, A.; Griebel, P.; Napper, S. Divergent immune responses to *Mycobacterium avium* subsp. *paratuberculosis* infection correlate with kinome responses at the site of intestinal infection. *Infect. Immun.* **2013**, *81*, 2861–2872, doi:10.1128/IAI.00339-13.
54. Momotani, E.; Whipple, D.L.; Thiermann, A.B.; Cheville, N.F. Role of M Cells and Macrophages in the Entrance of *Mycobacterium paratuberculosis* into Domes of Ileal Peyer's Patches in Calves. *Vet. Pathol.* **1988**, *25*, 131–137, doi:10.1177/030098588802500205.
55. Bermudez, L.E.; Petrofsky, M.; Sommer, S.; Barletta, R.G. Peyer's patch-deficient mice demonstrate that *Mycobacterium avium* subsp. *paratuberculosis* translocates across the mucosal barrier via both M cells and enterocytes but has inefficient dissemination. *Infect. Immun.* **2010**, *78*, 3570–3577, doi:10.1128/IAI.01411-09.
56. Fries, P.N.; Popowych, Y.I.; Guan, L.L.; Griebel, P.J. Age-related changes in the distribution and frequency of myeloid and T cell populations in the small intestine of calves. *Cell. Immunol.* **2011**, *271*, 428–437, doi:https://doi.org/10.1016/j.cellimm.2011.08.012.
57. Malmuthuge, N.; Li, M.; Fries, P.; Griebel, P.J.; Guan, L.L. Regional and age dependent changes in gene expression of Toll-like receptors and key antimicrobial defence molecules throughout the gastrointestinal tract of dairy calves. *Vet. Immunol. Immunopathol.* **2012**, *146*, 18–26, doi:https://doi.org/10.1016/j.vetimm.2012.01.010.
58. Bannantine, J.P.; Bermudez, L.E. No holes barred: invasion of the intestinal mucosa by

Mycobacterium avium subsp. *paratuberculosis*. *Infect. Immun.* **2013**, *81*, 3960–3965, doi:10.1128/IAI.00575-13.
59. Sigurðardóttir, Ó.G.; Valheim, M.; Press, C.M. Establishment of *Mycobacterium avium* subsp. *paratuberculosis* infection in the intestine of ruminants. *Adv. Drug Deliv. Rev.* **2004**, *56*, 819–834, doi:https://doi.org/10.1016/j.addr.2003.10.032.
60. Khare, S.; Nunes, J.S.; Figueiredo, J.F.; Lawhon, S.D.; Rossetti, C.A.; Gull, T.; Rice-Ficht, A.C.; Adams, L.G. Early Phase Morphological Lesions and Transcriptional Responses of Bovine Ileum Infected with *Mycobacterium avium* subsp. *paratuberculosis*. *Vet. Pathol.* **2009**, *46*, 717–728, doi:10.1354/vp.08-VP-0187-G-FL.
61. Guirado, E.; Schlesinger, L.S.; Kaplan, G. Macrophages in tuberculosis: friend or foe. *Semin. Immunopathol.* **2013**, *35*, 563–583, doi:10.1007/s00281-013-0388-2.
62. Premanandan, C.; Storozuk, C.A.; Clay, C.D.; Lairmore, M.D.; Schlesinger, L.S.; Phipps, A.J. Complement protein C3 binding to Bacillus anthracis spores enhances phagocytosis by human macrophages. *Microb. Pathog.* **2009**, *46*, 306–314, doi:https://doi.org/10.1016/j.micpath.2009.03.004.
63. Hostetter, J.; Kagan, R.; Steadham, E. Opsonization effects on *Mycobacterium avium* subsp. *paratuberculosis*--macrophage interactions. *Clin. Diagn. Lab. Immunol.* **2005**, *12*, 793–796, doi:10.1128/CDLI.12.6.793-796.2005.
64. Koul, A.; Herget, T.; Klebl, B.; Ullrich, A. Interplay between mycobacteria and host signalling pathways. *Nat. Rev. Microbiol.* **2004**, *2*, 189–202, doi:10.1038/nrmicro840.
65. Brumell, J.H.; Scidmore, M.A. Manipulation of rab GTPase function by intracellular bacterial pathogens. *Microbiol. Mol. Biol. Rev.* **2007**, *71*, 636–652, doi:10.1128/MMBR.00023-07.
66. Cheville, N.F.; Hostetter, J.; Thomsen, B. V; Simutis, F.; Vanloubbeeck, Y.; Steadham, E. Intracellular trafficking of *Mycobacterium avium* subsp. *paratuberculosis* in macrophages. *Dtsch. Tierarztl. Wochenschr.* **2001**, *108*, 236–243.
67. Karakousis, P.C.; Bishai, W.R.; Dorman, S.E. *Mycobacterium tuberculosis* cell envelope lipids and the host immune response. *Cell. Microbiol.* **2004**, *6*, 105–116, doi:https://doi.org/10.1046/j.1462-5822.2003.00351.x.
68. Goren, M.B.; Vatter, A.E.; Fiscus, J.; Friedrich, O.A.F. Polyanionic Agents Do Not Inhibit Phagosome-Lysosome Fusion in Cultured Macrophages. *J. Leukoc. Biol.* **1987**, *41*, 122–129, doi:https://doi.org/10.1002/jlb.41.2.122.
69. Vergne, I.; Chua, J.; Lee, H.-H.; Lucas, M.; Belisle, J.; Deretic, V. Mechanism of phagolysosome biogenesis block by viable *Mycobacterium tuberculosis*. *Proc. Natl. Acad. Sci. U. S. A.* **2005**, *102*, 4033–4038, doi:10.1073/pnas.0409716102.
70. Tsukano, H.; Kura, F.; Inoue, S.; Sato, S.; Izumiya, H.; Yasuda, T.; Watanabe, H. Yersinia pseudotuberculosis blocks the phagosomal acidification of B10.A mouse macrophages through the inhibition of vacuolar H+-ATPase activity. *Microb. Pathog.* **1999**, *27*, 253–263, doi:https://doi.org/10.1006/mpat.1999.0303.
71. Weiss, D.J.; Evanson, O.A.; Moritz, A.; Deng, M.Q.; Abrahamsen, M.S. Differential responses of bovine macrophages to *Mycobacterium avium* subsp. *paratuberculosis* and *Mycobacterium avium* subsp. *avium*. *Infect. Immun.* **2002**, *70*, 5556–5561, doi:10.1128/IAI.70.10.5556-5561.2002.
72. Murphy, J.T.; Sommer, S.; Kabara, E.A.; Verman, N.; Kuelbs, M.A.; Saama, P.; Halgren, R.; Coussens, P.M. Gene expression profiling of monocyte-derived macrophages following infection with *Mycobacterium avium* subspecies *avium* and *Mycobacterium avium* subspecies *paratuberculosis*. *Physiol. Genomics* **2006**, *28*, 67–75, doi:10.1152/physiolgenomics.00098.2006.

73. Weiss, D.; Evanson, O.; Souza, C.; Abrahamsen, M. A critical role of interleukin-10 in the response of bovine macrophages to infection by *Mycobacterium avium* subsp. *paratuberculosis*. *Am. J. Vet. Res.* **2005**, *66*, 721–726, doi:10.2460/ajvr.2005.66.721.
74. Wong, D.; Bach, H.; Sun, J.; Hmama, Z.; Av-Gay, Y. *Mycobacterium tuberculosis* protein tyrosine phosphatase (PtpA) excludes host vacuolar H+ ATPase to inhibit phagosome acidification. *Proc. Natl. Acad. Sci.* **2011**, *108*, 19371 LP – 19376, doi:10.1073/pnas.1109201108.
75. Scott, C.C.; Botelho, R.J.; Grinstein, S. Phagosome Maturation: A Few Bugs in the System. *J. Membr. Biol.* **2003**, *193*, 137–152, doi:10.1007/s00232-002-2008-2.
76. Sakurai, C.; Hashimoto, H.; Nakanishi, H.; Arai, S.; Wada, Y.; Sun-Wada, G.-H.; Wada, I.; Hatsuzawa, K. SNAP-23 regulates phagosome formation and maturation in macrophages. *Mol. Biol. Cell* **2012**, *23*, 4849–4863, doi:10.1091/mbc.E12-01-0069.
77. Chua, C.E.L.; Gan, B.Q.; Tang, B.L. Involvement of members of the Rab family and related small GTPases in autophagosome formation and maturation. *Cell. Mol. Life Sci.* **2011**, *68*, 3349, doi:10.1007/s00018-011-0748-9.
78. Fratti, R.A.; Backer, J.M.; Gruenberg, J.; Corvera, S.; Deretic, V. Role of phosphatidylinositol 3-kinase and Rab5 effectors in phagosomal biogenesis and mycobacterial phagosome maturation arrest. *J. Cell Biol.* **2001**, *154*, 631–644, doi:10.1083/jcb.200106049.
79. Ferrari, G.; Langen, H.; Naito, M.; Pieters, J. A Coat Protein on Phagosomes Involved in the Intracellular Survival of Mycobacteria. *Cell* **1999**, *97*, 435–447, doi:https://doi.org/10.1016/S0092-8674(00)80754-0.
80. Fratti, R.A.; Chua, J.; Deretic, V. Induction of p38 Mitogen-activated Protein Kinase Reduces Early Endosome Autoantigen 1 (EEA1) Recruitment to Phagosomal Membranes*. *J. Biol. Chem.* **2003**, *278*, 46961–46967, doi:https://doi.org/10.1074/jbc.M305225200.
81. Sanjuan, M.A.; Milasta, S.; Green, D.R. Toll-like receptor signaling in the lysosomal pathways. *Immunol. Rev.* **2009**, *227*, 203–220, doi:https://doi.org/10.1111/j.1600-065X.2008.00732.x.
82. Mucha, R.; Bhide, M.R.; Chakurkar, E.B.; Novak, M.; Mikula, I. Toll-like receptors TLR1, TLR2 and TLR4 gene mutations and natural resistance to *Mycobacterium avium* subsp. *paratuberculosis* infection in cattle. *Vet. Immunol. Immunopathol.* **2009**, *128*, 381–388, doi:https://doi.org/10.1016/j.vetimm.2008.12.007.
83. Bafica, A.; Scanga, C.A.; Feng, C.G.; Leifer, C.; Cheever, A.; Sher, A. TLR9 regulates Th1 responses and cooperates with TLR2 in mediating optimal resistance to *Mycobacterium tuberculosis*. *J. Exp. Med.* **2005**, *202*, 1715–1724, doi:10.1084/jem.20051782.
84. Noss, E.H.; Pai, R.K.; Sellati, T.J.; Radolf, J.D.; Belisle, J.; Golenbock, D.T.; Boom, W.H.; Harding, C. V Toll-Like Receptor 2-Dependent Inhibition of Macrophage Class II MHC Expression and Antigen Processing by 19-kDa Lipoprotein of *Mycobacterium tuberculosis*. *J. Immunol.* **2001**, *167*, 910 LP – 918, doi:10.4049/jimmunol.167.2.910.
85. Triantafilou, M.; Gamper, F.; Haston, R.; Mouratis, M.; Morath, S.; Hartung, T.; Triantafilou, K. Membrane Sorting of Toll-like Receptor (TLR)-2/6 and TLR2/1 Heterodimers at the Cell Surface Determines Heterotypic Associations with CD36 and Intracellular Targeting. *J. Biol. Chem.* **2006**, *281*, 31002–31011, doi:10.1074/jbc.M602794200.
86. Ruiz-Larrañaga, O.; Garrido, J.M.; Iriondo, M.; Manzano, C.; Molina, E.; Koets, A.P.; Rutten, V.P.M.G.; Juste, R.A.; Estonba, A. Genetic association between bovine NOD2

polymorphisms and infection by *Mycobacterium avium* subsp. *paratuberculosis* in Holstein-Friesian cattle. *Anim. Genet.* **2010**, *41*, 652–655, doi:https://doi.org/10.1111/j.1365-2052.2010.02055.x.
87. Weiss, D.J.; Souza, C.D.; Evanson, O.A.; Sanders, M.; Rutherford, M. Bovine monocyte TLR2 receptors differentially regulate the intracellular fate of *Mycobacterium avium* subsp. *paratuberculosis* and *Mycobacterium avium* subsp. *avium*. *J. Leukoc. Biol.* **2008**, *83*, 48–55, doi:https://doi.org/10.1189/jlb.0707490.
88. Knutson, K.L.; Hmama, Z.; Herrera-Velit, P.; Rochford, R.; Reiner, N.E. Lipoarabinomannan of *Mycobacterium tuberculosis* Promotes Protein Tyrosine Dephosphorylation and Inhibition of Mitogen-activated Protein Kinase in Human Mononuclear Phagocytes: ROLE OF THE Src HOMOLOGY 2 CONTAINING TYROSINE PHOSPHATASE 1*. *J. Biol. Chem.* **1998**, *273*, 645–652, doi:https://doi.org/10.1074/jbc.273.1.645.
89. Dorman, S.E.; Holland, S.M. Mutation in the signal-transducing chain of the interferon-gamma receptor and susceptibility to mycobacterial infection. *J. Clin. Invest.* **1998**, *101*, 2364–2369, doi:10.1172/JCI2901.
90. Bach, E.A.; Aguet, M.; Schreiber, R.D. THE IFNγ RECEPTOR:A Paradigm for Cytokine Receptor Signaling. *Annu. Rev. Immunol.* **1997**, *15*, 563–591, doi:10.1146/annurev.immunol.15.1.563.
91. Cooper, A.M.; Dalton, D.K.; Stewart, T.A.; Griffin, J.P.; Russell, D.G.; Orme, I.M. Disseminated tuberculosis in interferon gamma gene-disrupted mice. *J. Exp. Med.* **1993**, *178*, 2243–2247, doi:10.1084/jem.178.6.2243.
92. Dupuis, S.; Döffinger, R.; Picard, C.; Fieschi, C.; Altare, F.; Jouanguy, E.; Abel, L.; Casanova, J.-L. Human interferon-g-mediated immunity is a genetically controlled continuous trait that determines the outcome of mycobacterial invasion. *Immunol. Rev.* **2000**, *178*, 129–137, doi:https://doi.org/10.1034/j.1600-065X.2000.17810.x.
93. Sweeney, R.W.; Jones, D.E.; Habecker, P.; Scott, P. Interferon-gamma and interleukin 4 gene expression in cows infected with *Mycobacterium paratuberculosis. Am. J. Vet. Res.* **1998**, *59*, 842–847.
94. Coussens, P.M.; Verman, N.; Coussens, M.A.; Elftman, M.D.; McNulty, A.M. Cytokine gene expression in peripheral blood mononuclear cells and tissues of cattle infected with *Mycobacterium avium* subsp. *paratuberculosis*: evidence for an inherent proinflammatory gene expression pattern. *Infect. Immun.* **2004**, *72*, 1409–1422, doi:10.1128/IAI.72.3.1409-1422.2004.
95. Zurbrick, B.G.; Follett, D.M.; Czuprynski, C.J. Cytokine regulation of the intracellular growth of *Mycobacterium paratuberculosis* in bovine monocytes. *Infect. Immun.* **1988**, *56*, 1692–1697, doi:10.1128/iai.56.7.1692-1697.1988.
96. Liu, X.; Feng, Z.; Harris, N.B.; Cirillo, J.D.; Bercovier, H.; Barletta, R.G. Identification of a secreted superoxide dismutase in *Mycobacterium avium* subsp. *paratuberculosis*. *FEMS Microbiol. Lett.* **2001**, *202*, 233–238, doi:10.1111/j.1574-6968.2001.tb10809.x.
97. Arsenault, R.J.; Li, Y.; Bell, K.; Doig, K.; Potter, A.; Griebel, P.J.; Kusalik, A.; Napper, S. *Mycobacterium avium* subsp. *paratuberculosis* inhibits gamma interferon-induced signaling in bovine monocytes: insights into the cellular mechanisms of Johne's disease. *Infect. Immun.* **2012**, *80*, 3039–3048, doi:10.1128/IAI.00406-12.
98. Arsenault, R.J.; Li, Y.; Maattanen, P.; Scruten, E.; Doig, K.; Potter, A.; Griebel, P.; Kusalik, A.; Napper, S. Altered Toll-like receptor 9 signaling in *Mycobacterium avium* subsp. *paratuberculosis*-infected bovine monocytes reveals potential therapeutic

targets. *Infect. Immun.* **2013**, *81*, 226–237, doi:10.1128/IAI.00785-12.

99. Chan, J.; Xing, Y.; Magliozzo, R.S.; Bloom, B.R. Killing of virulent *Mycobacterium tuberculosis* by reactive nitrogen intermediates produced by activated murine macrophages. *J. Exp. Med.* **1992**, *175*, 1111–1122, doi:10.1084/jem.175.4.1111.
100. Adams, L.B.; Fukutomi, Y.; Krahenbuhl, J.L. Regulation of murine macrophage effector functions by lipoarabinomannan from mycobacterial strains with different degrees of virulence. *Infect. Immun.* **1993**, *61*, 4173–4181, doi:10.1128/iai.61.10.4173-4181.1993.
101. Denis, M.; Gregg, E.O.; Ghandirian, E. Cytokine modulation of *Mycobacterium tuberculosis* growth in human macrophages. *Int. J. Immunopharmacol.* **1990**, *12*, 721–727, doi:https://doi.org/10.1016/0192-0561(90)90034-K.
102. Zhao, B.; Collins, M.T.; Czuprynski, C.J. Effects of gamma interferon and nitric oxide on the interaction of *Mycobacterium avium* subsp. *paratuberculosis* with bovine monocytes. *Infect. Immun.* **1997**, *65*, 1761–1766, doi:10.1128/iai.65.5.1761-1766.1997.
103. Davis, A.; Vergne, I.; Master, S.; Kyei, G.; Chua, J.; Deretic, V. Mechanism of Inducible Nitric Oxide Synthase Exclusion from Mycobacterial Phagosomes. *PLoS Pathog.* **2008**, *3*, e186, doi:10.1371/journal.ppat.0030186.
104. Alberts, B; Johnson, A; Lewis, J; Raff, M; Roberts, K; Walter, P. *Molecular Biology of the Cell*; 4th ed.; Garland Science: New York, 2002; ISBN ISBN-10: 0-8153-3218-1 and ISBN-10: 0-8153-4072-9.
105. Molloy, A.; Laochumroonvorapong, P.; Kaplan, G. Apoptosis, but not necrosis, of infected monocytes is coupled with killing of intracellular bacillus Calmette-Guérin. *J. Exp. Med.* **1994**, *180*, 1499–1509, doi:10.1084/jem.180.4.1499.
106. Fratazzi, C.; Arbeit, R.D.; Carini, C.; Balcewicz-Sablinska, M.K.; Keane, J.; Kornfeld, H.; Remold, H.G. Macrophage apoptosis in mycobacterial infections. *J. Leukoc. Biol.* **1999**, *66*, 763–764, doi:https://doi.org/10.1002/jlb.66.5.763.
107. Allen, S.; Sotos, J.; Sylte, M.J.; Czuprynski, C.J. Use of Hoechst 33342 staining to detect apoptotic changes in bovine mononuclear phagocytes infected with *Mycobacterium avium* subsp. *paratuberculosis*. *Clin. Diagn. Lab. Immunol.* **2001**, *8*, 460–464, doi:10.1128/CDLI.8.2.460-464.2001.
108. Periasamy, S.; Tripathi, B.N.; Singh, N. Mechanisms of *Mycobacterium avium* subsp. *paratuberculosis* induced apoptosis and necrosis in bovine macrophages. *Vet. Microbiol.* **2013**, *165*, 392–401, doi:https://doi.org/10.1016/j.vetmic.2013.03.030.
109. Kabara, E.; Coussens, P. Infection of Primary Bovine Macrophages with *Mycobacterium avium* Subspecies *paratuberculosis* Suppresses Host Cell Apoptosis . *Front. Microbiol.* 2012, *3*, 215.
110. Borutaite, V.; Brown, G.C. Nitric oxide induces apoptosis via hydrogen peroxide, but necrosis via energy and thiol depletion. *Free Radic. Biol. Med.* **2003**, *35*, 1457–1468, doi:https://doi.org/10.1016/j.freeradbiomed.2003.08.003.
111. Marone, M.; Scambia, G.; Mozzetti, S.; Ferrandina, G.; Iacovella, S.; De Pasqua, A.; Benedetti-Panici, P.; Mancuso, S. bcl-2, bax, bcl-XL, and bcl-XS expression in normal and neoplastic ovarian tissues. *Clin. Cancer Res.* **1998**, *4*, 517 LP – 524.
112. Stickles B., X.; Marchion C., D.; Bicaku, E.; Al Sawah, E.; Abbasi, F.; Xiong, Y.; Bou Zgheib, N.; Boac M., B.; Orr C., B.; Judson L., P.; et al. BAD-mediated apoptotic pathway is associated with human cancer development. *Int J Mol Med* **2015**, *35*, 1081–1087, doi:10.3892/ijmm.2015.2091.
113. Donnelly, R.P.; Dickensheets, H.; Finbloom, D.S. The Interleukin-10 Signal

Transduction Pathway and Regulation of Gene Expression in Mononuclear Phagocytes. *J. Interf. Cytokine Res.* **1999**, *19*, 563–573, doi:10.1089/107999099313695.
114. Pott, J.; Basler, T.; Duerr, C.U.; Rohde, M.; Goethe, R.; Hornef, M.W. Internalization-dependent recognition of *Mycobacterium avium* subsp. *paratuberculosis* by intestinal epithelial cells. *Cell. Microbiol.* **2009**, *11*, 1802–1815, doi:https://doi.org/10.1111/j.1462-5822.2009.01372.x.
115. Yayo Ayele, W.; Macháčková, M.; Pavlík, I. The transmission and impact of paratuberculosis infection in domestic and wild ruminants. *Vet. Med. (Praha).* **2001**, *46*, 205–224, doi:10.17221/7878-vetmed.
116. Manning, E.J.B.; Collins, M.T. *Mycobacterium avium* subsp. *paratuberculosis*: Pathogen, pathogenesis and diagnosis. *OIE Rev. Sci. Tech.* **2001**, *20*, 133–150, doi:10.20506/rst.20.1.1275.
117. Kirkwood, C.D.; Wagner, J.; Boniface, K.; Vaughan, J.; Michalski, W.; Catto-Smith, A.; Cameron, D.J.S.; Bishop, R. *Mycobacterium avium supspecies paratuberculosis* in children with early-onset Crohn’s disease. *Inflamm. Bowel Dis.* **2009**, *15*, 1643–1655, doi:10.1002/ibd.20967.
118. De Lisle G.W., C.M.D. Johne’s disease in farmed deer. **1993**, *20*, 18–19.
119. Pavlik, I.; Bartl, J.; Dvorska, L.; Svastova, P.; du Maine, R.; Machackova, M.; Yayo Ayele, W.; Horvathova, A. Epidemiology of paratuberculosis in wild ruminants studied by restriction fragment length polymorphism in the Czech Republic during the period 1995–1998. *Vet. Microbiol.* **2000**, *77*, 231–251, doi:https://doi.org/10.1016/S0378-1135(00)00309-6.
120. Larsen AB, Moon HW, M.R. Susceptibility of swine to *Mycobacterium paratuberculosis*. *Am J Vet Res* **1971**, *32*, 589–95.
121. Larsen AB, Moon HW, M.R. Susceptibility of horses to *Mycobacterium paratuberculosis*. *Am J Vet Res* **1972**, *33*, 2185–9.
122. MF, T. Relationship between Mycobacterium avium, *M. paratuberculosis* and mycobacteria associated with Crohn’s disease. *Vet, Ann Rech* **1989**, *20*, 417–29.
123. McClure, H.M.; Chiodini, R.J.; Anderson, D.C.; Swenson, R.B.; Thayer, W.R.; Coutu, J.A. *Mycobacterium paratuberculosis* Infection in a Colony of Stumptail Macaques (Macaca arctoides). *J. Infect. Dis.* **1987**, *155*, 1011–1019, doi:10.1093/infdis/155.5.1011.
124. Greig, A.; Stevenson, K.; Perez, V.; Pirie, A.A.; Grant, J.M.; Sharp, J.M. Paratuberculosis in wild rabbits (Oryctolagus cuniculus). *Vet. Rec.* **1997**, *140*, 141–143, doi:https://doi.org/10.1136/vr.140.6.141.
125. Greig, A.; Stevenson, K.; Henderson, D.; Perez, V.; Hughes, V.; Pavlik, I.; Hines 2nd, M.E.; McKendrick, I.; Sharp, J.M. Epidemiological study of paratuberculosis in wild rabbits in Scotland. *J. Clin. Microbiol.* **1999**, *37*, 1746–1751, doi:10.1128/JCM.37.6.1746-1751.1999.
126. Beard, R.M.; Henderson, D.; Daniels, M.J.; Pirie, A.; Buxton, D.; Greig, A.; Hutchings, M.R.; McKendrick, I.; Rhind, S.; Stevenson, K.; et al. Evidence of paratuberculosis in fox (Vulpes vulpes) and stoat (Mustela erminea). *Vet. Rec.* **1999**, *145*, 612–613, doi:https://doi.org/10.1136/vr.145.21.612.
127. Agrawal, A.; Varshney, R.; Kirthika, P.; Gupta, R.; Sulabh, S.; Varshney, R.; Chakravarti, S.; Thankappan, S. Global scenario of paratuberculosis: a threat to livestock sector. *Biol. Rhythm Res.* **2021**, *52*, 957–972, doi:10.1080/09291016.2019.1610858.

128. Hermon-Taylor, J.; Bull, T.J.; Sheridan, J.M.; Cheng, J.; Stellakis, M.L.; Sumar, N. Causation of Crohn’s Disease by *Mycobacterium avium* Subspecies *Paratuberculosis*. *Can. J. Gastroenterol.* **2000**, *14*, 798305, doi:10.1155/2000/798305.
129. Eslami, M.; Shafiei, M.; Ghasemian, A.; Valizadeh, S.; Al-Marzoqi, A.H.; Shokouhi Mostafavi, S.K.; Nojoomi, F.; Mirforughi, S.A. *Mycobacterium avium paratuberculosis* and *Mycobacterium avium complex* and related subspecies as causative agents of zoonotic and occupational diseases. *J. Cell. Physiol.* **2019**, *234*, 12415–12421, doi:https://doi.org/10.1002/jcp.28076.
130. Berry, A.; Wu, C.; Venturino, A.J.; Talaat, A.M. Biomarkers for Early Stages of Johne’s Disease Infection and Immunization in Goats . *Front. Microbiol.* 2018, *9*, 2284.
131. Tiwari, A.; VanLeeuwen, J.A.; McKenna, S.L.B.; Keefe, G.P.; Barkema, H.W. Johne’s disease in Canada Part I: clinical symptoms, pathophysiology, diagnosis, and prevalence in dairy herds. *Can. Vet. J. = La Rev. Vet. Can.* **2006**, *47*, 874–882.
132. Lobão-Tello, E.R.; Herbach, E.P.; Navarrete-Talloni, M.J. Paratuberculosis: new histopathological findings in red deer (Cervus elaphus) and fallow deer (Dama dama) in Chile. *Pesqui. Veterinária Bras.* **2017**, *37*, 749–753, doi:10.1590/s0100-736x2017000700016.
133. Whitlock, R.H.; Buergelt, C. Preclinical and Clinical Manifestations of Paratuberculosis (Including Pathology). *Vet. Clin. North Am. Food Anim. Pract.* **1996**, *12*, 345–356, doi:https://doi.org/10.1016/S0749-0720(15)30410-2.
134. Manning, E.J.; Steinberg, H.; Rossow, K.; Ruth, G.R.; Collins, M.T. Epizootic of paratuberculosis in farmed elk. *J. Am. Vet. Med. Assoc.* **1998**, *213*, 1280-1281,1320-1322.
135. Williams, E.S.; Snyder, S.P.; Martin, K.L. Pathology of Spontaneous and Experimental Infection of North American Wild Ruminants with *Mycobacterium paratuberculosis*. *Vet. Pathol.* **1983**, *20*, 274–290, doi:10.1177/030098588302000304.
136. Valheim, M.; Sigurðardóttir, Ó.G.; Storset, A.K.; Aune, L.G.; Press, C.M. Characterization of Macrophages and Occurrence of T cells in Intestinal Lesions of Subclinical Paratuberculosis in Goats. *J. Comp. Pathol.* **2004**, *131*, 221–232, doi:https://doi.org/10.1016/j.jcpa.2004.04.004.
137. KUBO, M.; MORIWAKI, M.; WATASE, H. Electron Microscopic Observations on the Intestine of a Cow with Johne’s Disease. *Japanese J. Vet. Sci.* **1983**, *45*, 259–262, doi:10.1292/jvms1939.45.259.
138. Paliwal, O.P.; Rehbinder, C. Ultrastructural Studies of Paratuberculosis (Johne’s Disease) in Goats. *Acta Vet. Scand.* **1981**, *22*, 180–188, doi:10.1186/BF03547507.
139. Hines, M.E.; Kreeger, J.M.; Herron, A.J. Mycobacterial infections of animals: pathology and pathogenesis. *Lab. Anim. Sci.* **1995**, *45*, 334–351.
140. Clarke, C.J.; Little, D. The pathology of ovine paratuberculosis: Gross and histological changes in the intestine and other tissues. *J. Comp. Pathol.* **1996**, *114*, 419–437, doi:https://doi.org/10.1016/S0021-9975(96)80017-X.
141. SigurdardÓttir, Ó.G.; Press, C.M.; Saxegaard, F.; Evensen, Ø. Bacterial Isolation, Immunological Response, and Histopathological Lesions during the Early Subclinical Phase of Experimental Infection of Goat Kids with *Mycobacterium avium* subsp. *paratuberculosis*. *Vet. Pathol.* **1999**, *36*, 542–550, doi:10.1354/vp.36-6-542.
142. St-Jean, G.; Jernigan, A.D. Treatment of *Mycobacterium Paratuberculosis* Infection in Ruminants. *Vet. Clin. North Am. Food Anim. Pract.* **1991**, *7*, 793–804, doi:https://doi.org/10.1016/S0749-0720(15)31085-9.

143. Kopecky, K.E. Distribution of paratuberculosis in Wisconsin, by soil regions. *J. Am. Vet. Med. Assoc.* **1977**, *170*, 320–324.
144. Spickler, A.R. *Paratuberculosis*; 2007;
145. B., A.; H.P., R.; D.W., H. Diagnosis of Johne's disease (paratuberculosis) in northern California cattle and a note on its economic significance. *Calif. Vet.* 1983, *v. 37*.
146. Raizman, E.A.; Fetrow, J.P.; Wells, S.J. Loss of income from cows shedding *Mycobacterium avium* subspecies *paratuberculosis* prior to calving compared with cows not shedding the organism on two Minnesota dairy farms. *J. Dairy Sci.* **2009**, *92*, 4929–4936, doi:10.3168/jds.2009-2133.
147. MT., C. Clinical approach to control of bovine paratuberculosis. *J Am Vet Med Assoc.* **1994**, *204*, 208–10.
148. Sweeney, R.W. Transmission of Paratuberculosis. *Vet. Clin. North Am. Food Anim. Pract.* **1996**, *12*, 305–312, doi:https://doi.org/10.1016/S0749-0720(15)30408-4.
149. N.A., A.-G. Zur Frage der Pathogenese und Bazillenausscheidung bei Rinderparatuberkulose. *Infekt. Krank. Haus* **1929**, *36*, 312–317.
150. N.H., H. The diagnosis of Johne's disease. In Proceedings of the XV. International veterinary congress; 1953; pp. 173–177.
151. Pearson J.K., M.T.G. Uterine infection and congenital Johne's disease in cattle. *Vet. Rec.* **1955**, *67*, 615–616.
152. Sweeney, R.W.; Whitlock, R.H.; Rosenberger, A.E. *Mycobacterium paratuberculosis* isolated from fetuses of infected cows not manifesting signs of the disease. *Am. J. Vet. Res.* **1992**, *53*, 477–480.
153. Taylor, T.K.; Wilks, C.R.; McQueen, D.S. Isolation of *Mycobacterium paratuberculosis* from the milk of a cow with Johne's disease. *Vet. Rec.* **1981**, *109*, 532–533.
154. Streeter, R.N.; Hoffsis, G.F.; Bech-Nielsen, S.; Shulaw, W.P.; Rings, D.M. Isolation of *Mycobacterium paratuberculosis* from colostrum and milk of subclinically infected cows. *Am. J. Vet. Res.* **1995**, *56*, 1322–1324.
155. W.E., L. Congenital infection with *M. paratuberculosis* in cattle. *Vet. Rec.* **1956**, *68*, 312–314.
156. T.M., D. Foetal infection in Johne's disease. *Vet. Rec.* **1958**, *70*, 328.
157. Larsen, A.B.; Kopecky, K.E. *Mycobacterium paratuberculosis* in reproductive organs and semen of bulls. *Amer J Vet Res* 1970.
158. Larsen, A.B.; Stalheim, O.H.; Hughes, D.E.; Appell, L.H.; Richards, W.D.; Himes, E.M. *Mycobacterium paratuberculosis* in the semen and genital organs of a semen-donor bull. *J. Am. Vet. Med. Assoc.* **1981**, *179*, 169–171.
159. Toman M., Pavlík I., Faldyna M., Mátlová L., H.P. Immunological characteristics of cattle with various forms of *Mycobacterium avium* subsp. *paratuberculosis* infection. In Proceedings of the Sixth International Colloquium on Paratuberculosis; Melbourne, Victoria, Australia; pp. 616–625.
160. Larsen, A.B.; Merkal, R.S.; Cutlip, R.C. Age of cattle as related to resistance to infection with *Mycobacterium paratuberculosis*. *Am. J. Vet. Res.* **1975**, *36*, 255–257.
161. Douarre, P.E.; Cashman, W.; Buckley, J.; Coffey, A.; O'Mahony, J.M. Isolation and detection of *Mycobacterium avium* subsp. *paratuberculosis* (MAP) from cattle in Ireland using both traditional culture and molecular based methods. *Gut Pathog.* **2010**, *2*, 1–7, doi:10.1186/1757-4749-2-11.
162. Pritchard, T.C.; Coffey, M.P.; Bond, K.S.; Hutchings, M.R.; Wall, E. Phenotypic effects of subclinical paratuberculosis (Johne's disease) in dairy cattle. *J. Dairy Sci.*

2017, *100*, 679–690, doi:https://doi.org/10.3168/jds.2016-11323.
163. Sartor, R.B. Does *Mycobacterium avium* subspecies *paratuberculosis* cause Crohn's disease? *Gut* **2005**, *54*, 896 LP – 898, doi:10.1136/gut.2004.055889.
164. UZOIGWE, J.C.; KHAITSA, M.L.; GIBBS, P.S. Epidemiological evidence for *Mycobacterium avium* subspecies *paratuberculosis* as a cause of Crohn's disease. *Epidemiol. Infect.* **2007**, *135*, 1057–1068, doi:DOI: 10.1017/S0950268807008448.
165. Dalziel, T.K. Chronic Interstitial enteritis. *Br. Med. J. 2*, 1068–1070.
166. CROHN, B.B.; GINZBURG, L.; OPPENHEIMER, G.D. REGIONAL ILEITIS: A PATHOLOGIC AND CLINICAL ENTITY. *J. Am. Med. Assoc.* **1932**, *99*, 1323–1329, doi:10.1001/jama.1932.02740680019005.
167. Juste, R.A.; Elguezabal, N.; Pavón, A.; Garrido, J.M.; Geijo, M.; Sevilla, I.; Cabriada, J.L.; Tejada, A.; García-Campos, F.; Casado, R.; et al. Association between *Mycobacterium avium* subsp. *paratuberculosis* DNA in blood and cellular and humoral immune response in inflammatory bowel disease patients and controls. *Int. J. Infect. Dis.* **2009**, *13*, 247–254, doi:https://doi.org/10.1016/j.ijid.2008.06.034.
168. Lamont, E.A.; Bannantine, J.P.; Armién, A.; Ariyakumar, D.S.; Sreevatsan, S. Identification and Characterization of a Spore-Like Morphotype in Chronically Starved *Mycobacterium avium* subsp. *Paratuberculosis* Cultures. *PLoS One* **2012**, *7*, e30648.
169. Mura, M.; Bull, T.J.; Evans, H.; Sidi-Boumedine, K.; McMinn, L.; Rhodes, G.; Pickup, R.; Hermon-Taylor, J. Replication and long-term persistence of bovine and human strains of *Mycobacterium avium* subsp. *paratuberculosis* within Acanthamoeba polyphaga. *Appl. Environ. Microbiol.* **2006**, *72*, 854–859, doi:10.1128/AEM.72.1.854-859.2006.
170. Chiodini, R.J.; Chamberlin, W.M.; Sarosiek, J.; McCallum, R.W. Crohn's disease and the mycobacterioses: A quarter century later. Causation or simple association? *Crit. Rev. Microbiol.* **2012**, *38*, 52–93, doi:10.3109/1040841X.2011.638273.
171. McNees, A.L.; Markesich, D.; Zayyani, N.R.; Graham, D.Y. *Mycobacterium paratuberculosis* as a cause of Crohn's disease. *Expert Rev. Gastroenterol. Hepatol.* **2015**, *9*, 1523–1534, doi:10.1586/17474124.2015.1093931.
172. Barrington, G.M.; Gay, J.M.; Eriks, I.S.; Davis, W.C.; Evermann, J.F.; Emerson, C.; O'Rourke, J.L.; Hamilton, M.J.; Bradway, D.S. Temporal Patterns of Diagnostic Results in Serial Samples from Cattle with Advanced Paratuberculosis Infections. *J. Vet. Diagnostic Investig.* **2003**, *15*, 195–200, doi:10.1177/104063870301500219.
173. Sweeney, R.W.; Whitlock, R.H.; Rosenberger, A.E. *Mycobacterium paratuberculosis* cultured from milk and supramammary lymph nodes of infected asymptomatic cows. *J. Clin. Microbiol.* **1992**, *30*, 166–171, doi:10.1128/jcm.30.1.166-171.1992.
174. Patel, D.; Danelishvili, L.; Yamazaki, Y.; Alonso, M.; Paustian, M.L.; Bannantine, J.P.; Meunier-Goddik, L.; Bermudez, L.E. The ability of *Mycobacterium avium* subsp. *paratuberculosis* to enter bovine epithelial cells is influenced by preexposure to a hyperosmolar environment and intracellular passage in bovine mammary epithelial cells. *Infect. Immun.* **2006**, *74*, 2849–2855, doi:10.1128/iai.74.5.2849-2855.2006.
175. Chiodini, R.J.; Hermon-Taylor, J. The Thermal Resistance of *Mycobacterium Paratuberculosis* in Raw Milk under Conditions Simulating Pasteurization. *J. Vet. Diagnostic Investig.* **1993**, *5*, 629–631, doi:10.1177/104063879300500424.
176. Meylan, M.; Rings, D.M.; Shulaw, W.P.; Kowalski, J.J.; Bech-Nielsen, S.; Hoffsis, G.F. Survival of *Mycobacterium paratuberculosis* and preservation of immunoglobulin G in bovine colostrum under experimental conditions simulating pasteurization. *Am. J.*

Vet. Res. **1996**, *57*, 1580–1585.
177. Sung, N.; Collins, M.T. Thermal tolerance of *Mycobacterium paratuberculosis*. *Appl. Environ. Microbiol.* **1998**, *64*, 999–1005, doi:10.1128/AEM.64.3.999-1005.1998.
178. Grant, I.R.; Ball, H.J.; Neill, S.D.; Rowe, M.T. Inactivation of *Mycobacterium paratuberculosis* in cows' milk at pasteurization temperatures. *Appl. Environ. Microbiol.* **1996**, *62*, 631–636, doi:10.1128/aem.62.2.631-636.1996.
179. Grant; Ball; Rowe Effect of high-temperature, short-time (HTST) pasteurization on milk containing low numbers of *Mycobacterium paratuberculosis*. *Lett. Appl. Microbiol.* **1998**, *26*, 166–170, doi:https://doi.org/10.1046/j.1472-765X.1998.00309.x.
180. Hope A.F., Tulk P.A., C.R.J. Pasteurisation of *Mycobacterium paratuberculosis* in whole milk. In Proceedings of the 6th International Colloquium on Paratuberculosis (Man- ning E.J.B., Collins M.T., eds.); International Association for Paratuberculosis, Madison, W., Ed.; Melbourne; pp. 377–382.
181. Nauta, M.J.; van der Giessen, J.W.B. Human exposure to *Mycobacterium paratuberculosis* via pasteurised milk: A modelling approach. *Vet. Rec.* **1998**, *143*, 293–296, doi:https://doi.org/10.1136/vr.143.11.293.
182. Hermon-Taylor, J. Causation of Crohn's disease: the impact of clusters. *Gastroenterology* **1993**, *104*, 643–646, doi:10.1016/0016-5085(93)90438-i.
183. Mayberry, J.F.; Hitchens, R.A.N. Distribution of crohn's disease in Cardiff. *Soc. Sci. Med. Part D Med. Geogr.* **1978**, *12*, 137–138, doi:https://doi.org/10.1016/0160-8002(78)90018-7.
184. Fischer, O.; Mátlová, L.; Dvorská, L.; . Švástová, P.; Bartl, J.; Melichárek, I.; Weston, R.T.; Pavlík, I. Diptera as vectors of mycobacterial infections in cattle and pigs. *Med. Vet. Entomol.* **2001**, *15*, 208–211, doi:https://doi.org/10.1046/j.1365-2915.2001.00292.x.
185. Baptista, F.M.; Nielsen, S.S.; Toft, N. Association Between the Presence of Antibodies to *Mycobacterium avium* subspecies *paratuberculosis* and Somatic Cell Count. *J. Dairy Sci.* **2008**, *91*, 109–118, doi:https://doi.org/10.3168/jds.2007-0502.
186. Cheng, Z.; Liu, M.; Wang, P.; Liu, P.; Chen, M.; Zhang, J.; Liu, S.; Wang, F. Characteristics and Epidemiological Investigation of Paratuberculosis in Dairy Cattle in Tai'an, China. *Biomed Res. Int.* **2020**, *2020*, 3896754, doi:10.1155/2020/3896754.
187. Phil Scott DVM, S DipECBHM, CertCHP, DSHP, F. Johne's disease, Bovine Virus Diarrhoea Virus (BVDV), Salmonellosis, Bovine Tuberculosis, Leptospirosis, and Infectious Bovine Rhinotracheitis (IBR) are just some examples of infectious diseases that can be introduced onto your cattle farm and severely af.
188. Kirkeby, C.; Græsbøll, K.; Nielsen, S.S.; Christiansen, L.E.; Toft, N.; Halasa, T. Adaptive Test Schemes for Control of Paratuberculosis in Dairy Cows. *PLoS One* **2016**, *11*, e0167219.
189. Gupta, S.; Singh, S.V.; Singh, M.; Chaubey, K.K.; Karthik, K.; Bhatia, A.K.; Kumar, N.; Dhama, K. Vaccine approaches for the "therapeutic management" of *Mycobacterium avium* subspecies *paratuberculosis* infection in domestic livestock. *Vet. Q.* **2019**, *39*, 143–152, doi:10.1080/01652176.2019.1667042.
190. Whittington, R.; Donat, K.; Weber, M.F.; Kelton, D.; Nielsen, S.S.; Eisenberg, S.; Arrigoni, N.; Juste, R.; Sáez, J.L.; Dhand, N.; et al. Control of paratuberculosis: who, why and how. A review of 48 countries. *BMC Vet. Res.* **2019**, *15*, 198, doi:10.1186/s12917-019-1943-4.
191. Whitlock R., Sweeney R., Fyock T., and S.J. MAP super-shedders: another factor in the control of Johne's disease. In Proceedings of the 8th International Colloquium on

Paratuberculosis; Manning E, N.S., Ed.; International Association for Paratuberculosis: Madison, 2005; p. 164.
192. Munir M.T., Munir A.R., Hassan M., and A.M. Epidemiology, diagnosis and control options of Johne's disease in endemic situations. *Res J Vet Pr.* **2014**, 84–90.
193. Konboon, M.; Bani-Yaghoub, M.; Pithua, P.O.; Rhee, N.; Aly, S.S. A nested compartmental model to assess the efficacy of paratuberculosis control measures on U.S. dairy farms. *PLoS One* **2018**, *13*, e0203190–e0203190, doi:10.1371/journal.pone.0203190.
194. Singh, S.; Singh, P.; Kumar, N.; Gupta, S.; Chaubey, K.; Singh, B.; Yadav, S.; Dhama, K. Evaluation of goat based 'Indigenous vaccine' against Bovine Johne's Disease in endemically infected native cattle herds. *Indian J. Exp. Biol.* **2015**, *52*, 16–24.
195. Bastida, F.; Juste, R.A. Paratuberculosis control: a review with a focus on vaccination. *J. Immune Based Ther. Vaccines* **2011**, *9*, 8, doi:10.1186/1476-8518-9-8.
196. Coad, M.; Clifford, D.J.; Vordermeier, H.M.; Whelan, A.O. The consequences of vaccination with the Johne's disease vaccine, Gudair, on diagnosis of bovine tuberculosis. *Vet. Rec.* **2013**, *172*, 266, doi:https://doi.org/10.1136/vr.101201.
197. Serrano, M.; Elguezabal, N.; Sevilla, I.A.; Geijo, M. V; Molina, E.; Arrazuria, R.; Urkitza, A.; Jones, G.J.; Vordermeier, M.; Garrido, J.M.; et al. Tuberculosis Detection in Paratuberculosis Vaccinated Calves: New Alternatives against Interference. *PLoS One* **2017**, *12*, e0169735.
198. Singh, S.; Gupta, S.; Chaubey, K.; Bhushan, S.; Rawa, K.; Kumar, N.; Tiwar, H.; Chaturvedi, V.; Soha, J.; Dhama, K.; et al. "Therapeutic Management" of Incurable Paratuberculosis Using "Indigenous Vaccine" in Goatherds, Endemically Infected with Johne's Disease. *Int. J. Pharmacol.* **2017**, *13*, 145–155, doi:10.3923/ijp.2017.145.155.
199. Chaubey, K.K.; Singh, S.V.; Bhatia, A.K. Evaluation of 'recombinant secretary antigens' based 'cocktail ELISA' for the diagnosis of Johne's disease and to differentiate non-infected, infected and vaccinated goats in combination with indigenous ELISA test. *Small Rumin. Res.* **2018**, *165*, 24–29, doi:https://doi.org/10.1016/j.smallrumres.2018.06.005.
200. Faisal, S.M.; Yan, F.; Chen, T.-T.; Useh, N.M.; Guo, S.; Yan, W.; Wang, S.-J.; Glaser, A.L.; McDonough, S.P.; Singh, B.; et al. Evaluation of a Salmonella vectored vaccine expressing *Mycobacterium avium* subsp. *paratuberculosis* antigens against challenge in a goat model. *PLoS One* **2013**, *8*, e70171–e70171, doi:10.1371/journal.pone.0070171.
201. Gupta S., Singh S.V., and B.A.K. Immuno-reactivity pattern of secretory proteins of *Mycobacterium avium* subspecies *paratuberculosis* vaccine strain 'S 5' with potential for diagnosis of Johne's disease in early infection. *Indian J Biotech* **2016**, 306–312.
202. Park, H.-T.; Yoo, H.S. Development of vaccines to *Mycobacterium avium* subsp. *paratuberculosis* infection. *Clin. Exp. Vaccine Res.* **2016**, *5*, 108–116, doi:10.7774/cevr.2016.5.2.108.
203. Windsor, P. Research into vaccination against ovine Johne's disease in Australia. *Small Rumin. Res.* 2006, *v. 62 iss*.
204. Patton, E.A. Paratuberculosis Vaccination. *Vet. Clin. North Am. Food Anim. Pract.* **2011**, *27*, 573–580, doi:https://doi.org/10.1016/j.cvfa.2011.07.004.
205. Singh, S. V; Singh, P.K.; Singh, A. V; Sohal, J.S.; Gupta, V.K.; Vihan, V.S. Comparative efficacy of an indigenous 'inactivated vaccine' using highly pathogenic field strain of *Mycobacterium avium* subspecies *paratuberculosis* 'Bison type' with a commercial vaccine for the control of Capri-paratuberculosis in India. *Vaccine* **2007**,

25, 7102–7110, doi:https://doi.org/10.1016/j.vaccine.2007.07.054.
206. Körmendy B. Diagnostic value of mammalian, avian, and johnin PPD tuberculins in cattle herds infected by Myco- bacterium paratuberculosis. *Acta Vet. Hung.* **1988**, *36*, 177–183.
207. Wood P.R., Kopsidas K., Milner A.R., Hill J., Gill I., Webb R., Mack W.N., C.K. The development of an in vitro cellular assay for Johne's disease in cattle. In Proceedings of the Johne's Disease. Current Trends in Research, Diagnosis and Management.; Milner A.R., W.P.R., Ed.; CSRIO: Melbourne, Australia, 1989; pp. 164–167.
208. Cocito, C.; Gilot, P.; Coene, M.; de Kesel, M.; Poupart, P.; Vannuffel, P. Paratuberculosis. *Clin. Microbiol. Rev.* **1994**, *7*, 328–345, doi:10.1128/CMR.7.3.328.
209. M.T., C. Diagnosis of paratuberculosis. In *Paratuberculosis (Johne's Disease)*; R.W., S., Ed.; Vet. North Am. Food Anim. Pract., 1996; pp. 357–371.
210. S.R., H. Testing for Johne's. *Angus J.* **1998**, *3*, 194– 202.
211. Bhat, P.; Leggatt, G.; Waterhouse, N.; Frazer, I.H. Interferon-γ derived from cytotoxic lymphocytes directly enhances their motility and cytotoxicity. *Cell Death Dis.* **2017**, *8*, e2836–e2836, doi:10.1038/cddis.2017.67.
212. ROTHEL, J.S.; JONES, S.L.; CORNER, L.A.; COX, J.C.; WOOD, P.R. A sandwich enzyme immunoassay for bovine interferon-γ and its use for the detection of tuberculosis in cattle. *Aust. Vet. J.* **1990**, *67*, 134–137, doi:https://doi.org/10.1111/j.1751-0813.1990.tb07730.x.
213. Collins M.T., Z.B.Y. Comparison of the commer- cial serum antibody ELISA, δ-interferon test kit, and radiometric faecal culture for early diagnosis of paratuberculosis in experimentally infected Holstein calves. In Proceedings of the 4th Interna- tional Colloquium on Paratuberculosis; Chiodini R.J., Collins M.T., B.E.O.E., Ed.; Assoc. for Paratuberculosis: Rehoboth, MA, USA, 1995; pp. 67–76.
214. McDONALD, W.L.; RIDGE, S.E.; HOPE, A.F.; CONDRON, R.J. Evaluation of diagnostic tests for Johne's disease in young cattle. *Aust. Vet. J.* **1999**, *77*, 113–119, doi:https://doi.org/10.1111/j.1751-0813.1999.tb11679.x.
215. Nielsen S.S., Nielsen K.K., Huda A., Condron R., C.M.T. Diagnostic techniques for paratuberculosis. In: Bulletin of the international dairy federation. In Proceedings of the Bulletin of the international dairy federation- International animal health code: mammals, birds, and bees. 9th ed. OIE; IDF Office International des Epizooties – OIE: Paris, 2001; pp. 5–17.
216. Clark, D.L.; Koziczkowski, J.J.; Radcliff, R.P.; Carlson, R.A.; Ellingson, J.L.E. Detection of *Mycobacterium avium* subspecies *paratuberculosis*: Comparing Fecal Culture Versus Serum Enzyme-Linked Immunosorbent Assay and Direct Fecal Polymerase Chain Reaction. *J. Dairy Sci.* **2008**, *91*, 2620–2627, doi:10.3168/jds.2007-0902.
217. Cazer, C.L.; Mitchell, R.M.; Cicconi-Hogan, K.M.; Gamroth, M.; Richert, R.M.; Ruegg, P.L.; Schukken, Y.H. Associations between *Mycobacterium avium* subsp. *paratuberculosis* antibodies in bulk tank milk, season of sampling and protocols for managing infected cows. *BMC Vet. Res.* **2013**, *9*, doi:10.1186/1746-6148-9-234.
218. Lombard, J.E.; Byrem, T.M.; Wagner, B.A.; McCluskey, B.J. Comparison of milk and serum enzyme-linked immunosorbent assays for diagnosis of *Mycobacterium avium* subspecies *paratuberculosis* infection in dairy cattle. *J. Vet. Diagnostic Investig.* **2006**, *18*, 448–458, doi:10.1177/104063870601800504.
219. Costanzo, G.; Pinedo, F.A.; Mon, M.L.; Viale, M.; Gil, A.; Illia, M.C.; Gioffré, A.; Arese, A.; Travería, G.; Romano, M.I. Accuracy assessment and screening of a dairy

herd with paratuberculosis by three different ELISAs. *Vet. Microbiol.* **2012**, *156*, 183–188, doi:10.1016/j.vetmic.2011.10.029.

220. Collins, M.T.; Wells, S.J.; Petrini, K.R.; Collins, J.E.; Schultz, R.D.; Whitlock, R.H. Evaluation of Five Antibody Detection Tests for Diagnosis of Bovine Paratuberculosis. *Clin. Diagn. Lab. Immunol.* **2005**, *12*, 685–692, doi:10.1128/CDLI.12.6.685-692.2005.
221. Lavers, C.J.; Barkema, H.W.; Dohoo, I.R.; McKenna, S.L.B.; Keefe, G.P. Evaluation of milk ELISA fordetection of *Mycobacterium avium* subspecies *paratuberculosis* indairy herds and association with within-herd prevalence. *J. Dairy Sci.* **2014**, *97*, 299–309, doi:10.3168/jds.2013-7101.
222. Logar, K.; Kopinč, R.; Bandelj, P.; Starič, J.; Lapanje, A.; Ocepek, M. Evaluation of combined high-efficiency DNA extraction and real-time PCR for detection of *Mycobacterium avium* subsp. *paratuberculosis* in subclinically infected dairy cattle: Comparison with faecal culture, milk real-time PCR and milk ELISA. *BMC Vet. Res.* **2012**, *8*, 1–10, doi:10.1186/1746-6148-8-49.
223. Fry, M.P.; Kruze, J.; Collins, M.T. Evaluation of four commercial enzyme-linked immunosorbent assays for the diagnosis of bovine paratuberculosis in Chilean dairy herds. *J Vet Diagn Invest* **2008**, *20*, 329–332.
224. Hosseiniporgham, S.; Cubeddu, T.; Rocca, S.; Sechi, L.A. Identification of *Mycobacterium avium* subsp. *paratuberculosis* (map) in sheep milk, a zoonotic problem. *Microorganisms* **2020**, *8*, 1–20, doi:10.3390/microorganisms8091264.
225. Sugden, E.A.; Stilwell, K.; Michaelides, A. A Comparison of Lipoarabinomannan with other Antigens used in Absorbed Enzyme Immunoassays for the Serological Detection of Cattle Infected with *Mycobacterium paratuberculosis*. *J. Vet. Diagnostic Investig.* **1997**, *9*, 413–417, doi:10.1177/104063879700900413.
226. Bannantine, J.P.; Paustian, M.L.; Waters, W.R.; Stabel, J.R.; Palmer, M. V; Li, L.; Kapur, V. Profiling Bovine Antibody Responses to *Mycobacterium avium* subsp. *paratuberculosis* Infection by Using Protein Arrays †. *Infect. Immun.* **2008**, *76*, 739–749, doi:10.1128/IAI.00915-07.
227. Biet, F.; Bay, S.; Thibault, V.C.; Euphrasie, D.; Grayon, M.; Ganneau, C.; Lanotte, P.; Daffé, M.; Gokhale, R.; Etienne, G.; et al. Lipopentapeptide induces a strong host humoral response and distinguishes *Mycobacterium avium* subsp. *paratuberculosis* from *M. avium* subsp. *avium*. *Vaccine* **2008**, *26*, 257–268, doi:10.1016/j.vaccine.2007.10.059.
228. Bay S, Begg D, Ganneau C, Branger M, Cochard T, Bannantine JP, Köhler H, Moyen JL, Whittington RJ, B.F. Engineering Synthetic Lipopeptide Antigen for Specific Detection of *Mycobacterium avium* subsp. *paratuberculosis* Infection | Enhanced Reader. *Front. Vet. Sci.* **2021**, *8*, 637841, doi:10.3389/fvets.2021.637841.
229. Whittington, R. Cultivation of *Mycobacterium avium* subsp. *paratuberculosis*. In *Paratuberculosis: Organism, Disease, Control*; Behr D. M.A. and Collins D. M., E.C., Ed.; Cambridge, MA 02139, UK, 2010; pp. 244–266.
230. Whitlock, R.H.; Wells, S.J.; Sweeney, R.W.; Van Tiem, J. ELISA and fecal culture for paratuberculosis (Johne's disease): Sensitivity and specificity of each method. *Vet. Microbiol.* **2000**, *77*, 387–398, doi:10.1016/S0378-1135(00)00324-2.
231. Whipple, D.L.; Callihan, D.R.; Jarnagin, J.L. Cultivation of *Mycobacterium paratuberculosis* from bovine fecal specimens and a suggested standardized procedure. *J. Vet. Diagn. Invest.* **1991**, *3*, 368–373, doi:10.1177/104063879100300424.
232. Collins, M.T.; Kenefick, K.B.; Sockett, D.C.; Lambrecht, R.S.; McDonald, J.;

Jorgensen, J.B. Enhanced radiometric detection of *Mycobacterium paratuberculosis* by using filter-concentrated bovine fecal specimens. *J. Clin. Microbiol.* **1990**, *28*, 2514–2519, doi:10.1128/jcm.28.11.2514-2519.1990.

233. Sockett, D.C.; Carr, D.J.; Collins, M.T. Evaluation of conventional and radiometric fecal culture and a commercial DNA probe for diagnosis of *Mycobacterium paratuberculosis* infections in cattle. *Can. J. Vet. Res.* **1992**, *56*, 148–153.
234. Slana, I.; Kralik, P.; Kralova, A.; Pavlik, I. On-farm spread of *Mycobacterium avium* subsp. *paratuberculosis* in raw milk studied by IS900 and F57 competitive real time quantitative PCR and culture examination. *Int. J. Food Microbiol.* **2008**, *128*, 250–257, doi:https://doi.org/10.1016/j.ijfoodmicro.2008.08.013.
235. Vansnick, E.; De Rijk, P.; Vercammen, F.; Geysen, D.; Rigouts, L.; Portaels, F. Newly developed primers for the detection of *Mycobacterium avium* subspecies *paratuberculosis*. *Vet. Microbiol.* **2004**, *100*, 197–204, doi:10.1016/j.vetmic.2004.02.006.
236. Albuquerque, P.P.F. de; Santos, A. de S.; Souza Neto, O.L. de; Kim, P. de C.P.; Cavalcanti, E.F.T.S.F.; Oliveira, J.M.B. de; Mota, R.A.; Júnior, J.W.P. Detection of *Mycobacterium avium* subsp. *paratuberculosis* in bovine milk from the state of Pernambuco, Brazil. *Brazilian J. Microbiol.* **2017**, *48*, 113–117, doi:10.1016/j.bjm.2016.10.010.
237. Yao, L.; Zheng, L.; Cai, G.; Wang, S.; Wang, L.; Lin, J. A rapid and sensitive salmonella biosensor based on viscoelastic inertial microfluidics. *Sensors (Switzerland)* **2020**, *20*, doi:10.3390/s20092738.
238. Foddai, A.; Elliott, C.T.; Grant, I.R. Maximizing capture efficiency and specificity of magnetic separation for *Mycobacterium avium* subsp. *paratuberculosis* cells. *Appl. Environ. Microbiol.* **2010**, *76*, 7550–7558, doi:10.1128/AEM.01432-10.
239. Husakova, M.; Dziedzinska, R.; Slana, I. Magnetic Separation Methods for the Detection of *Mycobacterium avium* subsp. *Paratuberculosis* in Various Types of Matrices: A Review. *Biomed Res. Int.* **2017**, *2017*, doi:10.1155/2017/5869854.
240. Possé, B.; De Zutter, L.; Heyndrickx, M.; Herman, L. Quantitative isolation efficiency of O26, O103, O111, O145 and O157 STEC serotypes from artificially contaminated food and cattle faeces samples using a new isolation protocol. *J. Appl. Microbiol.* **2008**, *105*, 227–235, doi:https://doi.org/10.1111/j.1365-2672.2008.03739.x.
241. HSIH, H.-Y.; TSEN, H.-Y. Combination of Immunomagnetic Separation and Polymerase Chain Reaction for the Simultaneous Detection of Listeria monocytogenes and Salmonella spp. in Food Samples. *J. Food Prot.* **2001**, *64*, 1744–1750, doi:10.4315/0362-028X-64.11.1744.
242. Uyttendaele, M.; Van Hoorde, I.; Debevere, J. The use of immuno-magnetic separation (IMS) as a tool in a sample preparation method for direct detection of L. monocytogenes in cheese. *Int. J. Food Microbiol.* **2000**, *54*, 205–212, doi:https://doi.org/10.1016/S0168-1605(99)00196-8.
243. Rijpens, N.; Herman, L.; Vereecken, F.; Jannes, G.; De Smedt, J.; De Zutter, L. Rapid detection of stressed Salmonella spp. in dairy and egg products using immunomagnetic separation and PCR. *Int. J. Food Microbiol.* **1999**, *46*, 37–44, doi:https://doi.org/10.1016/S0168-1605(98)00171-8.
244. Španová, A.; Rittich, B.; Karpíšková, R.; Čechová, L.; Škapová, D. PCR identification of Salmonella cells in food and stool samples after immunomagnetic separation. *Bioseparation* **2000**, *9*, 379–384, doi:10.1023/A:1011125014586.
245. Karch, H.; Janetzki-Mittmann, C.; Aleksic, S.; Datz, M. Isolation of

enterohemorrhagic Escherichia coli O157 strains from patients with hemolytic-uremic syndrome by using immunomagnetic separation, DNA-based methods, and direct culture. *J. Clin. Microbiol.* **1996**, *34*, 516–519, doi:10.1128/jcm.34.3.516-519.1996.
246. Grant, I.R.; Ball, H.J.; Rowe, M.T. Isolation of *Mycobacterium paratuberculosis* from milk by immunomagnetic separation. *Appl. Environ. Microbiol.* **1998**, *64*, 3153–3158, doi:10.1128/aem.64.9.3153-3158.1998.
247. O'Brien, L.M.; Stewart, L.D.; Strain, S.A.J.; Grant, I.R. Novel monoclonal antibody and peptide binders for *Mycobacterium avium* subsp. *paratuberculosis* and their application for magnetic separation. *PLoS One* **2016**, *11*, 1–19, doi:10.1371/journal.pone.0147870.
248. Metzger-Boddien, C.; Khaschabi, D.; Schönbauer, M.; Boddien, S.; Schlederer, T.; Kehle, J. Automated high-throughput immunomagnetic separation-PCR for detection of *Mycobacterium avium* subsp. *paratuberculosis* in bovine milk. *Int. J. Food Microbiol.* **2006**, *110*, 201–208, doi:10.1016/j.ijfoodmicro.2006.01.042.
249. Grant, I.R.; Pope, C.M.; O'Riordan, L.M.; Ball, H.J.; Rowe, M.T. Improved detection of *Mycobacterium avium* subsp. *paratuberculosis* in milk by immunomagnetic PCR. *Vet. Microbiol.* **2000**, *77*, 369–378, doi:10.1016/S0378-1135(00)00322-9.
250. Foddai, A.; Strain, S.; Whitlock, R.H.; Elliott, C.T.; Grant, I.R. Application of a peptide-mediated magnetic separation-phage assay for detection of viable *Mycobacterium avium* subsp. *paratuberculosis* to bovine bulk tank milk and feces samples. *J. Clin. Microbiol.* **2011**, *49*, 2017–2019, doi:10.1128/JCM.00429-11.
251. Stratmann, J.; Strommenger, B.; Stevenson, K.; Gerlach, G.F. Development of a peptide-mediated capture PCR for detection of *Mycobacterium avium* subsp. *paratuberculosis* in milk. *J. Clin. Microbiol.* **2002**, *40*, 4244–4250, doi:10.1128/JCM.40.11.4244-4250.2002.
252. Stratmann, J.; Dohmann, K.; Heinzmann, J.; Gerlach, G.F. Peptide aMptD-mediated capture PCR for detection of *Mycobacterium avium* subsp. *paratuberculosis* in bulk milk samples. *Appl. Environ. Microbiol.* **2006**, *72*, 5150–5158, doi:10.1128/AEM.00590-06.
253. Foddai, A.; Elliott, C.T.; Grant, I.R. Rapid assessment of the viability of *Mycobacterium avium* subsp. *paratuberculosis* cells after heat treatment, using an optimized phage amplification assay. *Appl. Environ. Microbiol.* **2010**, *76*, 1777–1782, doi:10.1128/AEM.02625-09.
254. Twort, F.W. AN INVESTIGATION ON THE NATURE OF ULTRA-MICROSCOPIC VIRUSES. *Lancet* **1915**, *186*, 1241–1243, doi:10.1016/S0140-6736(01)20383-3.
255. d'Herelle F. Sur un microbe invisible antagoniste des bacilles dysentériques. *C R Acad Sci* **1917**, *165*, 373–5, doi:https://doi.org/10.1016/j.resmic.2007.07.005.
256. Kropinski, A.M. *Phage therapy-Everything old is new again*; 2006; Vol. 17;.
257. Stewart, L.D.; Foddai, A.; Elliott, C.T.; Grant, I.R. Development of a novel phage-mediated immunoassay for the rapid detection of viable *Mycobacterium avium* subsp. *paratuberculosis*. *J. Appl. Microbiol.* **2013**, *115*, 808–817, doi:https://doi.org/10.1111/jam.12275.
258. Botsaris, G.; Liapi, M.; Kakogiannis, C.; Dodd, C.E.R.; Rees, C.E.D. Detection of *Mycobacterium avium* subsp. *paratuberculosis* in bulk tank milk by combined phage-PCR assay: Evidence that plaque number is a good predictor of MAP. *Int. J. Food Microbiol.* **2013**, *164*, 76–80, doi:https://doi.org/10.1016/j.ijfoodmicro.2013.03.023.
259. Foddai, A.C.G.; Grant, I.R. A novel one-day phage-based test for rapid detection and

enumeration of viable *Mycobacterium avium* subsp. *paratuberculosis* in cows' milk. *Appl. Microbiol. Biotechnol.* **2020**, *104*, 9399–9412, doi:10.1007/s00253-020-10909-0.
260. Ujihara, T.; Uchiyama, J.; Nasukawa, T.; Ando, H.; Murakami, H.; Ohara, N.; Ogawa, M.; Yamazaki, T.; Daibata, M.; Sakaguchi, M.; et al. Recovery of mycobacteriophages from archival stocks stored for approximately 50 years in Japan. *Arch. Virol.* **2018**, *163*, 1915–1919, doi:10.1007/s00705-018-3788-8.
261. Uchiyama, J.; Mizukami, K.; Yahara, K.; Kato, S.-I.; Murakami, H.; Nasukawa, T.; Ohara, N.; Ogawa, M.; Yamazaki, T.; Matsuzaki, S.; et al. Genome Sequences of 12 Mycobacteriophages Recovered from Archival Stocks in Japan. **2018**, doi:10.1128/genomeA.
262. Ford, M.E.; Sarkis, G.J.; Belanger, A.E.; Hendrix, R.W.; Hatfull, G.F. Genome structure of mycobacteriophage D29: implications for phage evolution11Edited by J. Karn. *J. Mol. Biol.* **1998**, *279*, 143–164, doi:https://doi.org/10.1006/jmbi.1997.1610.
263. FROMAN, S.; WILL, D.W.; BOGEN, E. Bacteriophage active against virulent *Mycobacterium tuberculosis*. I. Isolation and activity. *Am. J. Public Health Nations. Health* **1954**, *44*, 1326–33, doi:10.2105/ajph.44.10.1326.
264. Dedrick, R.M.; Mavrich, T.N.; Ng, W.L.; Hatfull, G.F. Expression and evolutionary patterns of mycobacteriophage D29 and its temperate close relatives. *BMC Microbiol.* **2017**, *17*, 225, doi:10.1186/s12866-017-1131-2.
265. Rybniker, J.; Kramme, S.; Small, P.L. Host range of 14 mycobacteriophages in Mycobacterium ulcerans and seven other mycobacteria including *Mycobacterium tuberculosis*-application for identification and susceptibility testing., doi:10.1099/jmm.0.46238-0.
266. David, H.L.; Clement, F.; Clavel-Seres, S.; Rastog, N. Abortive infection of Mycobacterium leprae by the Mycobacteriophage D29. *Int. J. Lepr.* **1984**, *52*, 515–523.
267. Lindberg, A.A. Bacteriophage Receptors. *Annu. Rev. Microbiol.* **1973**, *27*, 205–241, doi:10.1146/annurev.mi.27.100173.001225.
268. Gao, A.; Mutharia, L.; Raymond, M.; Odumeru, J. Improved template DNA preparation procedure for detection of *Mycobacterium avium* subsp. *paratuberculosis* in milk by PCR. *J. Microbiol. Methods* **2007**, *69*, 417–420, doi:https://doi.org/10.1016/j.mimet.2006.10.019.
269. Bradner, L.; Robbe-Austerman, S.; Beitz, D.C.; Stabel, J.R. Optimization of hexadecylpyridinium chloride decontamination for culture of *Mycobacterium avium* subsp. *paratuberculosis* from milk. *J. Clin. Microbiol.* **2013**, *51*, 1575–1577, doi:10.1128/JCM.00333-13.
270. Albenzio, M.; Caroprese, M. Differential leucocyte count for ewe milk with low and high somatic cell count. *J. Dairy Res.* **2011**, *78*, 43–48, doi:DOI: 10.1017/S0022029910000798.
271. Patharkar, R. *Freeze and Squeeze Gel Extraction*;
272. Gamberale, F.; Pietrella, G.; Sala, M.; Scaramella, P.; Puccica, S.; Antognetti, V.; Arrigoni, N.; Ricchi, M.; Cersini, A. Management of *Mycobacterium avium* subsp. *paratuberculosis* in dairy farms: Selection and evaluation of different DNA extraction methods from bovine and buffaloes milk and colostrum for the establishment of a safe colostrum farm bank. *Microbiologyopen* **2019**, *8*, 1–11, doi:10.1002/mbo3.875.
273. Okuni, J.B.; Dovas, C.I.; Loukopoulos, P.; Bouzalas, I.G.; Kateete, D.P.; Joloba, M.L.; Ojok, L. Isolation of *Mycobacterium avium* subspecies *paratuberculosis* from

Ugandan cattle and strain differentiation using optimised DNA typing techniques. *BMC Vet. Res.* **2012**, *8*, 99, doi:10.1186/1746-6148-8-99.
274. Chaitanya, R.K.; Reddy, Y.K.M.; Thangavelu, A. Strain Typing of *Mycobacterium avium* subsp. *paratuberculosis* from Tamil Nadu, India based on Polymorphisms in MAP 1506 Locus and IS 1311 PCR-REA. *Adv. Anim. Vet. Sci.* **2015**, *3*, 289–294, doi:http://dx.doi.org/10.14737/journal.aavs/2015/3.5.289.294 ISSN.
275. Unknown serum, plasma or whole blood collection available online: https://www.questdiagnostics.com/home/physicians/testing-services/specialists/hospitals-lab-staff/specimen-handling/serum-plasma-whole-blood/#:~:text=For serum%2C allow the blood,tube five to ten times.
276. Biet, F.; Bay, S.; Thibault, V.C.; Euphrasie, D.; Grayon, M.; Ganneau, C.; Lanotte, P.; Daffé, M.; Gokhale, R.; Etienne, G.; et al. Lipopentapeptide induces a strong host humoral response and distinguishes *Mycobacterium avium* subsp. *paratuberculosis* from M. avium subsp. avium. *Vaccine* **2008**, *26*, 257–268, doi:10.1016/j.vaccine.2007.10.059.
277. Foddai, A.C.G.; Grant, I.R. Sensitive and specific detection of viable *Mycobacterium avium* subsp. *paratuberculosis* in raw milk by the peptide-mediated magnetic separation-phage assay. **2017**, doi:10.1111/jam.13425.
278. Butot, S.; Ricchi, M.; Sevilla, I.A.; Michot, L.; Molina, E.; Tello, M.; Russo, S.; Arrigoni, N.; Garrido, J.M.; Tomas, D. Estimation of Performance Characteristics of Analytical Methods for *Mycobacterium avium* subsp. *paratuberculosis* Detection in Dairy Products . *Front. Microbiol.* 2019, *10*, 509.
279. Wilson, D.J.; Rood, K.; Biswas, P.; Byrem, T.M. Herd-level prevalence of Johne's disease in Utah and adjacent areas of the intermountain west as detected by a bulk-tank milk surveillance project. *J. Dairy Sci.* **2010**, *93*, 5792–5797, doi:https://doi.org/10.3168/jds.2010-3481.
280. Bates, A.; O'Brien, R.; Liggett, S.; Griffin, F. The effect of sub-clinical infection with *Mycobacterium avium* subsp. *paratuberculosis* on milk production in a New Zealand dairy herd. *BMC Vet. Res.* **2018**, *14*, 93, doi:10.1186/s12917-018-1421-4.
281. Bauman, C.A.; Jones-Bitton, A.; Jansen, J.; Kelton, D.; Menzies, P. Evaluation of bulk tank milk PCR and bulk tank milk modified ELISA tests for the detection of paratuberculosis at the herd level in goat and sheep dairies in Ontario, Canada. *J. Dairy Sci.* **2019**, *102*, 511–520, doi:https://doi.org/10.3168/jds.2018-15020.
282. Faruk, M.S.; Jung, Y.; Hur, T.; Lee, S.; Cho, Y. Longitudinal Study of *Mycobacterium avium* subsp. *paratuberculosis* Antibody Kinetics in Dairy Cattle Using Sera and Milk throughout the Lactation Period. *Vet. Sci.* 2020, *7*.
283. Li, L.; Wagner, B.; Freer, H.; Schilling, M.; Bannantine, J.P.; Campo, J.J.; Katani, R.; Grohn, Y.T.; Radzio-Basu, J.; Kapur, V. Early detection of *Mycobacterium avium* subsp. *paratuberculosis* infection in cattle with multiplex-bead based immunoassays. *PLoS One* **2017**, *12*, e0189783, doi:10.1371/journal.pone.0189783.
284. Corti, S.; Stephan, R. Detection of *Mycobacterium avium* subspecies *paratuberculosis* specific IS900 insertion sequences in bulk-tank milk samples obtained from different regions throughout Switzerland. *BMC Microbiol.* **2002**, *2*, 15, doi:10.1186/1471-2180-2-15.
285. Stärk, K.D.; Frei-Stäheli, C.; Frei, P.P.; Pfeiffer, D.U.; Danuser, J.; Audigé, L.; Nicolet, J.; Strasser, M.; Gottstein, B.; Kihm, U. Frequency and cost of health problems in Swiss dairy cows and their calves (1993-1994). *Schweiz. Arch. Tierheilkd.* **1997**, *139*, 343–53.

286. Grant, I.R.; O'Riordan, L.M.; Ball, H.J.; Rowe, M.T. Incidence of *Mycobacterium paratuberculosis* in raw sheep and goats' milk in England, Wales and Northern Ireland. *Vet. Microbiol.* **2001**, *79*, 123–131, doi:https://doi.org/10.1016/S0378-1135(00)00344-8.
287. Beaver, A.; Cazer, C.L.; Ruegg, P.L.; Gröhn, Y.T.; Schukken, Y.H. Implications of PCR and ELISA results on the routes of bulk-tank contamination with *Mycobacterium avium ssp. paratuberculosis*. *J. Dairy Sci.* **2016**, *99*, 1391–1405, doi:https://doi.org/10.3168/jds.2015-9855.
288. Gonda, M.G.; Chang, Y.M.; Shook, G.E.; Collins, M.T.; Kirkpatrick, B.W. Effect of *Mycobacterium paratuberculosis* infection on production, reproduction, and health traits in US Holsteins. *Prev. Vet. Med.* **2007**, *80*, 103–119, doi:https://doi.org/10.1016/j.prevetmed.2007.01.011.
289. Mortier, R.A.R.; Barkema, H.W.; De Buck, J. Susceptibility to and diagnosis of *Mycobacterium avium* subspecies *paratuberculosis* infection in dairy calves: A review. *Prev. Vet. Med.* **2015**, *121*, 189–198, doi:https://doi.org/10.1016/j.prevetmed.2015.08.011.
290. Velázquez-Morales, J.V.; Santillán-Flores, M.A.; Gallegos-Sánchez, J.; Cuca-García, J.M.; Navarro-Maldonado, M. del C.; Rojas-Martínez, R.I.; Cortez-Romero, C. Detection of *Mycobacterium avium* subsp. *paratuberculosis* in reproductive tissue and semen of naturally infected rams. *Anim. Reprod.* **2019**, *16*, 930–937, doi:10.21451/1984-3143-AR2018-0147.
291. Buergelt, C.D.; Donovan, G.A.; Williams, J.E. Identification of *Mycobacterium avium* subspecies *paratuberculosis* by Polymeerase Chain Reaction in Blood and Semen of a Bull with Clinical Paratuberculosis. *Int. J. Appl. Res. Vet. Med.* **2004**, *2*, 130–134.
292. Ayele, W.Y.; Bartos, M.; Svastova, P.; Pavlik, I. Distribution of *Mycobacterium avium* subsp. *paratuberculosis* in organs of naturally infected bull-calves and breeding bulls. *Vet. Microbiol.* **2004**, *103*, 209–217, doi:https://doi.org/10.1016/j.vetmic.2004.07.011.
293. KHOL, J.L.; KRALIK, P.; SLANA, I.; BERAN, V.; AURICH, C.; BAUMGARTNER, W.; PAVLIK, I. Consecutive Excretion of *Mycobacterium avium* subspecies *paratuberculosis* in Semen of a Breeding Bull Compared to the Distribution in Feces, Tissue and Blood by IS*900* and *F57* Quantitative Real-Time PCR and Culture Examinations. *J. Vet. Med. Sci.* **2010**, *72*, 1283–1288, doi:10.1292/jvms.10-0052.
294. Anna Rita, A.; Victor, N.N.; Silvia, P.; Luciana, P.; Anastasia, D.; Vincenzo, C. Ovine Paratuberculosis: A Seroprevalence Study in Dairy Flocks Reared in the Marche Region, Italy. *Vet. Med. Int.* **2011**, *2011*, 782875, doi:10.4061/2011/782875.
295. Dow, C.T.; Sechi, L.A. Cows Get Crohn's Disease and They're Giving Us Diabetes. *Microorg.* 2019, *7*.
296. Sechi, L.A.; Dow, C.T. *Mycobacterium avium ss. paratuberculosis* Zoonosis – The Hundred Year War – Beyond Crohn's Disease. *Front. Immunol.* **2015**, *6*, 96, doi:10.3389/fimmu.2015.00096.
297. Bo, M.; Erre, G.L.; Bach, E.H.; Slavin, Y.N.; Manchia, P.A.; Passiu, G.; Sechi, L.A. PtpA and PknG proteins secreted by *Mycobacterium avium* subsp. *Paratuberculosis* are recognized by sera from patients with rheumatoid arthritis: A case– Control study. *J. Inflamm. Res.* **2019**, *12*, 301–308, doi:10.2147/JIR.S220960.
298. Davide, C.; Yokoyama, K.; Nobutaka, H.; A Sechi, L. From Sardinia to Japan: update on the role of MAP in multiple sclerosis. *Future Microbiol.* **2019**, *14*, 643–646, doi:10.2217/fmb-2019-0102.

299. Cossu, D.; Otsubo, S.; Otsubo, Y.; Eda, S.; Suzuki, T.; Iwao, Y.; Kuribayashi, T.; Yamamoto, S.; Sechi, L.A.; Momotani, E. *Mycobacterium avium* subsp. *paratuberculosis* Induces Specific IgE Production in Japanese People with Allergies. *Int. J. Inflam.* **2017**, *2017*, 7959154, doi:10.1155/2017/7959154.
300. Frau, J.; Cossu, D.; Sardu, C.; Mameli, G.; Coghe, G.; Lorefice, L.; Fenu, G.; Tranquilli, S.; Sechi, L.A.; Marrosu, M.G.; et al. Combining HLA-DRB1-DQB1 and *Mycobacterium avium* subspecies *Paratubercolosis* (MAP) antibodies in Sardinian multiple sclerosis patients: associated or independent risk factors? *BMC Neurol.* **2016**, *16*, 148, doi:10.1186/s12883-016-0669-1.
301. Cossu, D.; Yokoyama, K.; Sechi, L.A.; Otsubo, S.; Tomizawa, Y.; Momotani, E.; Hattori, N. Humoral response against host-mimetic homologous epitopes of *Mycobacterium avium* subsp. *paratuberculosis* in Japanese multiple sclerosis patients. *Sci. Rep.* **2016**, *6*, 29227, doi:10.1038/srep29227.
302. Mameli, G.; Cocco, E.; Frau, J.; Marrosu, M.G.; Sechi, L.A. Epstein Barr Virus and *Mycobacterium avium* subsp. *paratuberculosis* peptides are recognized in sera and cerebrospinal fluid of MS patients. *Sci. Rep.* **2016**, *6*, 22401, doi:10.1038/srep22401.
303. Mameli, G.; Madeddu, G.; Cossu, D.; Galleri, G.; Manetti, R.; Babudieri, S.; Mura, M.S.; Sechi, L.A. Immune response induced by Epstein–Barr virus and *Mycobacterium avium* subsp. *paratuberculosis* peptides in current and past infectious mononucleosis: a risk for multiple sclerosis? *Eur. J. Neurol.* **2016**, *23*, 140–147, doi:https://doi.org/10.1111/ene.12821.
304. Otsubo, S.; Cossu, D.; Eda, S.; Otsubo, Y.; Sechi, L.A.; Suzuki, T.; Iwao, Y.; Yamamoto, S.; Kuribayashi, T.; Momotani, E. Seroprevalence of IgG1 and IgG4 Class Antibodies Against *Mycobacterium avium* subsp. *paratuberculosis* in Japanese Population. *Foodborne Pathog. Dis.* **2015**, *12*, 851–856, doi:10.1089/fpd.2015.1956.
305. Masala, S.; Cossu, D.; Piccinini, S.; Rapini, N.; Mameli, G.; Manca Bitti, M.L.; Sechi, L.A. Proinsulin and MAP3865c homologous epitopes are a target of antibody response in new-onset type 1 diabetes children from continental Italy. *Pediatr. Diabetes* **2015**, *16*, 189–195, doi:https://doi.org/10.1111/pedi.12269.
306. Frau, J.; Cossu, D.; Coghe, G.; Lorefice, L.; Fenu, G.; Porcu, G.; Sardu, C.; Murru, M.R.; Tranquilli, S.; Marrosu, M.G.; et al. Role of interferon-beta in *Mycobacterium avium* subspecies *paratuberculosis* antibody response in Sardinian MS patients. *J. Neurol. Sci.* **2015**, *349*, 249–250, doi:https://doi.org/10.1016/j.jns.2015.01.004.
307. Whittington, R.J.; Marsh, I.B.; Whitlock, R.H. Typing of IS1311 polymorphisms confirms that bison (Bison bison) with paratuberculosis in Montana are infected with a strain of *Mycobacterium avium* subsp. *paratuberculosis* distinct from that occurring in cattle and other domesticated livestock. *Mol. Cell. Probes* **2001**, *15*, 139–145, doi:10.1006/mcpr.2001.0346.
308. Angelidou, E.; Kostoulas, P.; Leontides, L. Bayesian validation of a serum and milk ELISA for antibodies against *Mycobacterium avium* subspecies *paratuberculosis* in Greek dairy goats across lactation. *J. Dairy Sci.* **2014**, *97*, 819–828, doi:10.3168/jds.2013-7218.
309. Cox KL, Devanarayan V, Kriauciunas A, et al. Immunoassay Methods. In *Assay Guidance Manual [Internet]*; Markossian S, Sittampalam GS, Grossman A, et al., Ed.; Eli Lilly & Company and the National Center for Advancing Translational Sciences: Bethesda (MD).
310. Nielsen, S.S.; Toft, N. Ante mortem diagnosis of paratuberculosis: A review of accuracies of ELISA, interferon-γ assay and faecal culture techniques. *Vet. Microbiol.*

2008, *129*, 217–235.
311. Gardner, I.A.; Nielsen, S.S.; Whittington, R.J.; Collins, M.T.; Bakker, D.; Harris, B.; Sreevatsan, S.; Lombard, J.E.; Sweeney, R.; Smith, D.R.; et al. Consensus-based reporting standards for diagnostic test accuracy studies for paratuberculosis in ruminants. *Prev. Vet. Med.* **2011**, *101*, 18–34, doi:10.1016/j.prevetmed.2011.04.002.
312. Conde, C.; Price-Carter, M.; Cochard, T.; Branger, M.; Stevenson, K.; Whittington, R.; Bannantine, J.P.; Biet, F. Whole-Genome Analysis of *Mycobacterium avium* subsp. *paratuberculosis* IS900Insertions Reveals Strain Type-Specific Modalities . *Front. Microbiol.* 2021, *12*, 1012.
313. Castellanos, E.; Aranaz, A.; Romero, B.; Juan, L. de; Alvarez, J.; Bezos, J.; Rodríguez, S.; Stevenson, K.; Mateos, A.; Domínguez, L. Polymorphisms in gyrA and gyrB Genes among *Mycobacterium avium* subsp. *paratuberculosis* Type I, II, and III Isolates. *J. Clin. Microbiol.* **2007**, *45*, 3439–3442, doi:10.1128/JCM.01411-07.
314. Stevenson, K. Comparative differences between strains of *Mycobacterium avium* subsp. *paratuberculosis*. In *Paratuberculosis: Organism, Disease, Control*; Behr, M. A., Collins, D.M., Ed.; CABI Publishing, 2010; p. 126 ISBN 9781845936136.
315. Sohal, J.S.; Arsenault, J.; Leboeuf, A.; Hélie, P.; Buczinski, S.; Robinson, Y.; Labrecque, O.; Lachapelle, V.; Fecteau, G.; L'Homme, Y. Molecular characterization of *Mycobacterium avium* subspecies *paratuberculosis* C-type and S-type isolated from sheep and goats by using a combination of MIRU-VNTR loci. *Can. J. Vet. Res.* **2019**, *83*, 160–167.
316. Biet, F.; Sevilla, I.A.; Cochard, T.; Lefrançois, L.H.; Garrido, J.M.; Heron, I.; Juste, R.A.; McLuckie, J.; Thibault, V.C.; Supply, P.; et al. Inter- and Intra-subtype genotypic differences that differentiate *Mycobacterium avium* subspecies *paratuberculosis* strains. *BMC Microbiol.* **2012**, *12*, 264, doi:10.1186/1471-2180-12-264.
317. Sevilla, I.; Singh, S.; Garrido, J.; Aduriz, G.; Rodríguez, S.; Geijo, M.; Whittington, R.; Saunders, V.; Whitlock, R.; Juste, R. Molecular typing of *Mycobacterium avium* subspecies *paratuberculosis* strains from different hosts and regions. *Rev. Sci. Tech.* **2006**, *24*, 1061–1066.
318. David, H.L.; Clavel, S.; Clement, F. Adsorption and growth of the bacteriophage D29 in selected mycobacteria. *Ann. l'Institut Pasteur / Virol.* **1980**, *131*, 167–184, doi:https://doi.org/10.1016/0769-2617(80)90031-3.
319. Foley-Thomas, E.M.; Whipple, D.L.; Bermudez, L.E.; Barletta, R.G. Phage infection, transfection and transformation of *Mycobacterium avium complex* and *Mycobacterium paratuberculosis*. *Microbiology* **1995**, *141*, 1173–1181, doi:10.1099/13500872-141-5-1173.
320. Grant, I.R. Bacteriophage-Based Methods for Detection of Viable *Mycobacterium avium* subsp. *paratuberculosis* and Their Potential for Diagnosis of Johne's Disease . *Front. Vet. Sci.* 2021, *8*, 205.
321. Swift, B.M.C.; Denton, E.J.; Mahendran, S.A.; Huxley, J.N.; Rees, C.E.D. Development of a rapid phage-based method for the detection of viable *Mycobacterium avium* subsp. *paratuberculosis* in blood within 48 h. *J. Microbiol. Methods* **2013**, *94*, 175–179, doi:10.1016/j.mimet.2013.06.015.
322. Swift, B.M.C.; Huxley, J.N.; Plain, K.M.; Begg, D.J.; de Silva, K.; Purdie, A.C.; Whittington, R.J.; Rees, C.E.D. Evaluation of the limitations and methods to improve rapid phage-based detection of viable *Mycobacterium avium* subsp. *paratuberculosis* in the blood of experimentally infected cattle. *BMC Vet. Res.* **2016**, *12*, 115,

doi:10.1186/s12917-016-0728-2.
323. O’Brien, L.M.; McAloon, C.G.; Stewart, L.D.; Strain, S.A.J.; Grant, I.R. Diagnostic potential of the peptide-mediated magnetic separation (PMS)-phage assay and PMS-culture to detect *Mycobacterium avium* subsp. *paratuberculosis* in bovine milk samples. *Transbound. Emerg. Dis.* **2018**, *65*, 719–726, doi:https://doi.org/10.1111/tbed.12794.

The list of published papers, submitted manuscript, and presented posters during the PhD studies

1. Caggiu, E.; Arru, G.; **Hosseini, S.**; Niegowska, M.; Sechi, G.; Zarbo, I.R.; Sechi, L.A. Inflammation, Infectious Triggers, and Parkinson's Disease. *Frontiers in Neurology*. 2019, 10,122. https://www.frontiersin.org/article/10.3389/fneur.2019.00122

2. **Hosseiniporgham, S.**; Cubeddu, T.; Rocca, S.; Sechi, L.A. Identification of *Mycobacterium avium* subsp. *paratuberculosis* (MAP) in Sheep Milk, a Zoonotic Problem. *Microorganisms* 2020, 8, 1264. https://doi.org/10.3390/microorganisms8091264

3. Scarpa, F.; Sanna, D.; Azzena, I.; Mugetti, D.; Cerruti, F.; **Hosseini, S.**; Cossu, P.; Pinna, S.; Grech, D.; Cabana, D.; Pasquini, V.; Esposito, G.; Cadoni, N.; Atzori, F.; Antuofermo, E.; Addis, P.; Sechi, L.A.; Prearo, M.; Peletto, S.; Mossa, M.A.; Saba, T.; Gazale, V.; Casu, M. Multiple Non-Species-Specific Pathogens Possibly Triggered the Mass Mortality in Pinna nobilis. *Life* 2020, 10, 238. https://doi.org/10.3390/life10100238

4. **Hosseiniporgham, S.**; Biet, F.; Ganneau, C.; Bannantine, J.P.; Bay, S.; Sechi, L.A. A Comparative Study on the Efficiency of Two Mycobacterium avium subsp. paratuberculosis (MAP)-Derived Lipopeptides of L3P and L5P as Capture Antigens in an In-House Milk ELISA Test. *Vaccines* 2021, 9, 997. https://doi.org/10.3390/vaccines9090997

5. **Hosseinporgham, S.**; Rebechesu, L.; Pintore, P.; Lollai, S.; Dattena, M.; Russo, S.; Ruiu, A.; Sechi, L.A. Detection of *Mycobacterium avium* subsp. *paratuberculosis* (MAP) Viability in Sheep and Goat Milk Samples Via A Novel and Conventional Phage Assay. Submitted in *Scientific Reports*, *Nature*, 2021.

6. **Hosseiniporgham S.** and Sechi L.A. Evaluation of different methods, qPCR and different ELISAs, to detect MAP in milk of Sarda sheep. Poster Presentation, International Congress of Paratuberculosis (ICP), Dublin, **2020.**

7. **Hosseiniporgham S.** and Sechi L.A. Il rilevamento di MAP nei campioni di latte di pecora mediante un nuovo approccio nano-tecnologico. National Poster, "Municipl Activity of the Doctoral School (PON)"-Uniss, Italy, **2020**.

La borsa di dottorato è stata cofinanziata con risorse del
Programma Operativo Nazionale Ricerca e Innovazione 2014-2020 (CCI 2014IT16M2OP005),
Fondo Sociale Europeo, Azione I.1 "Dottorati Innovativi con caratterizzazione Industriale"

UNIONE EUROPEA
Fondo Sociale Europeo

Ministero dell'Università
e della Ricerca